Universidad del País Vasco
Euskal Herriko Unibertsitatea

Nanostructured lipid carriers for nose-to-brain delivery in neurodegenerative diseases therapy

Oihane Gartziandia Lopez de Goikoetxea

Vitoria- Gasteiz, 2016

Laboratory of Pharmaceutics,
NanoBioCel Group

Faculty of Pharmacy,
University of The Basque Country (UPV/EHU)

Eskerrak
Agradecimientos
Aknowledgements

Lerro hauen bitartez eskerrak eman nahi dizkizuet Tesiaren abentura hontan murgildu nintzenetik nire ondoan egon zareten pertsona guztiei, bai eguneroko lanean jasotako laguntzagatik baita lanetik kanpo edukitako babesagatik ere.

En primer lugar querría agradecer a Jose Luis Pedraz por haberme dado la oportunidad de formar parte del grupo de investigación NanoBioCel. Y a mis directoras de Tesis, Rosa y Manoli, muchas gracias por guiarme y ayudarme durante estos años, y por estar siempre dispuestas a aclarar todas mis dudas.

Me gustaría también dar las gracias a toda la gente del Departamento, tanto a los profesores Jon, Amaia, Gorka, Marian, Alicia, Ana, Begoña….como a los compañeros de Tecnalia, Fer, Zuri, Leire, Aitziber, Amanda, Sergio, Sonia…por estar siempre disponibles para ayudar, sobre todo cuando he tenido algún problemilla con el HPLC.

También me gustaría agradecer al Departamento de Farmacología de Leioa dirigido por Luisa Ugedo por haberme acogido como una más durante el tiempo que pasé con ellos. En especial a Jose Angel y a Cristina por las horas que pasamos en el estabulario y por vuestra disponibilidad para ayudarme cuando lo he necesitado.

Y como no, quisiera dar las gracias a tod@s mis compañer@s del "labo": Itxaso, Claudia, Aiala, Marta, Garazi, Tatiana, Ane, Argia, Edi, Edorta, Susana, Jesus, Laura, Gustavo, Haritz, Ainhoa, Ilia….por hacer que el día a día sea más fácil, por las risas y cotilleos de las comidas y cafés, los pintxo-potes, cenas, Sagardotegi, Donosti…porque además de trabajar, lo hemos pasado muy bien juntos! Dentro de este grupo me gustaría destacar a Mireia, Tania y Pello, porque comenzamos esta aventura a la vez y hemos compartido muchas dudas y alegrías juntos. Y a María, mi compi de ordenador estos últimos meses, por todas esas compras que nos servían como terapia para desconectar, las charlas sobre nuestro futuro, y en general por haber estado ahí compartiendo esta experiencia. Eta bukatzeko Enarari eman nahi dizkiot eskerrak, niretzako eredu bat izan zara laborategian, ikerkuntzaren inguruan dakidan gehiena zuregandik ikasi dut eta asko eskertzen dizut nirekin izandako pazientzia, beti laguntzeko prest egon izana eta bajoi momentuetan emandako animo guztiak, eskerrik asko denagatik wapi!

I would like to thank to Véronique Préat for giving me the opportunity to be a member of her lab during my stay in Brussels. En especial me gustaría agradecer a Ana por haberme ayudado desde el principio con todo el papeleo, y una vez allí por haberme acogido como a

una más en el labo y por todo el tiempo que dedicaste a enseñarme. Tengo que decir que ha sido un verdadero placer conocerte, creo que conseguimos hacer un buen equipo tanto dentro como fuera del labo, y sin duda has sido de lo mejor que me llevo de Bruselas… después de la Tongerlo, claro! I also would like to thank to all the members of the lab, Bernard, Kevin, Anne, John, Aurellie, Murielle, Lungile, Kiran…for all your help in the lab, and specially to the Italian team: Chiara, Dario, Alessandra and Ana (y también incluyo en este grupo a Alex y Mathew) for introducing me to the wonderful world of nutella and coffee breaks, and in general for all the time we shared in the lab and outside the lab: Namur, Dinant, Leuven, the Electro night, Ramen, panini avec poulet pané, birthday dinners...such a good memories. Torino is waiting for us guys!

Bruselan egon nintzen bitartean egindako gainerako lagunei ere eskerrak eman nahi nizkieke. Esther, Miren eta Leire, eskerrik asko elkarrekin pasatako momentu guztiengatik, nire egonaldia experientzia ahaztezina izatearen arrazoietariko bat izan zinetelako. Agurtzerakoan esan bezela, ikusten garen hurrengoan Bruselako zerbezak Euskal Herriko poteengatik ordezkatuko ditugu!

Eta nola ez nire kuadrilla maitiari, nire Poxpolinak: Garazi, Irati, Arrate, Andrea, Miren eta Ekaine. Eskerrik asko bihotz-bihotzez urte hauetan zehar zuengandik jasotako indar, laguntza eta berotasunagatik. Zuekin egun txarrak on bihurtzen direlako eta zuei esker enaizelako inoiz bakarrik sentitu. Egiten dudana oso ongi ulertu ez arren, eskerrik asko nire arratoi eta zelulatxoez hainbeste kezkatzeagtik, eta mila mila esker Andriu portada egiten laguntzeagatik. Oihana, zuri ere eskerrak eman nahi dizkizut Gasteizen elkarrekin pasatako urte guztiengatik, izan nezakeen pixukiderik onena izan zara. Hasieratik ondo ulertu ginen eta benetako lagun bat zara niretzako. Besterik gabe, eskerrik asko guztiei nire bizitzaren parte garrantzitsu bat izateagatik!

Txomin, asko eskertzen dizut Tesiaren amaieran eman dizkidazun animo guztiak. Abentura honen amaieran ezagutu garen arren, zure babesa ezinbestekoa izan da niretzako azkeneko txanpa hontan. Eskerrik asko zaren bezalakoa izateagatik!

Eta bukatzeko nire familiari, nire ezinbesteko euskarriari….Ama eta Aita, eskerrik asko beti hor egoteagatik, nigan sinisteagatik, nire humore aldaketak aguantatzeagatik, nirekin izandako pazientziagatik, gaizki egon naizen momentu guztietan entzuteko eta animatzeko prest egoteagatik….Zuen babesik gabe hau guztia ezinezkoa litzateke. Eneko, besterik gabe, eskerrik asko zaren bezalakoa izateagatik, beti hain alai, hain saltsero, eta hain bihotz oneko… nitaz harro zaudela esaten duzu, baina ni bai nagoela harro zu bezalako anai bat edukitzeaz! Ainara, eskerrik asko zuri ere hor egoteagatik, ni entzuteko prest egoteagatik eta zure aholkuengatik…koñata bat baino askoz gehiago zara niretzako. Eta nola ez, etxeko sorgintxoei, etxeko bizipoza, nire bi ilobatxoei, Anuk eta Xune…Anuk, Tesi honen hasieran iritsi zinen eta zalantzarik gabe zure maitasun, alaitasun eta bizipoza nire bitamina nagusia izan dira urte hauetan zehar, eskerrik asko hain berezia eta potxola izateagatik. Eta Xune, etxeko txikitxoa, bi hilabete baino ez dituzu, baina mila esker zurekin egote hutsak, zure xamurtasunak, arazo guztiak ahaztarazten dizkidalako. Eta azkenik Amiña Matilde eta Aittuna Paco, eskerrik asko nigan hainbeste sinisteagatik eta egiten nuena ulertu ez arren beti nitaz hainbeste arduratzegatik. ESKERRIK ASKO BIHOTZ-BIHOTZEZ FAMILY!! IZUGARRI MAITE ZAITUZTEZ!!

ESKERRIK ASKO DENOI!!!!

Oihane

ACKNOWLEDGEMENTS FOR FINANCIAL SUPPORT

This thesis has been partially supported by the "Ministerio de Economía y Competitividad" (SAF2013-42347-R), the Basque Government (Consolidated Groups, IT-407-07), the University of The Basque Country (UPV/EHU) (UFI 11/32), and FEDER founds. Oihane Gartziandia gratefully acknowledges the support provided by the University of The Basque Country (UPV/EHU) for the fellowship grant.

ACKNOWLEDGEMENTS TO THE EDITORIALS

Authors would like to thank the editorials for granting permission to reuse their previously published articles in this thesis:

The links to the final published versions are the following:

Book Chapter:

Gartziandia et al. Nanobiomaterials in Drug Delivery. Vol 9, Ch 11, 371-402 (2016)
http://dx.doi.org/10.1016/B978-0-323-42866-8.00011-3

Research articles:

Gartziandia et al. Colloids Surf B Biointerfaces 134, 304–313 (2015).
http://www.sciencedirect.com/science/article/pii/S0927776515300163

Gartziandia et al. Int J Pharm 499, 81-89 (2016).
http://www.sciencedirect.com/science/article/pii/S0378517315304440

Nire gurasoei, Mariaje eta Juanito,

eta nire anaia Enekori

“Si no escalas la montaña

jamás podrás disfrutar el paisaje”

Pablo Neruda

GLOSSARY

AAV: adeno-associated viruses

AD: Alzheimer's disease

ALS: amyotrophic lateral sclerosis

Aβ: amyloid beta

BBB: blood-brain barrier

BDNF: Brain-derived Neurotrophic Factor

bFGF: basic fibroblast growth factor

BSA: bovine serum albumin

CCK-8: Cell Counting Kit-8

CDs: cyclodextrines

CLSM: confocal laser scanning microscopy

CNS: central nervous system

CNTF: Ciliary Neurotrophic Factor

CPP: cell penetrating peptide

CS: chitosan

CSF: cerebrospinal fluid

DAB: 3,30'-diaminobenzidine

DAPI: 4',6-diamidino-2-phenylindole

DCM: dichloromethane

DDS: drug delivery systems

DiR: DiIC18 (7) (1,1'-Dioctadecyl-3,3,3',3'-Tetramethylindotricarbocyanine Iodide)

DLS: Dynamic Light Scattering

DMEM-F12: Dulbecco´s Modified Eagle Medium/Nutrient Mixture F-12

DMSO: Dimethyl sulfoxide

DPBS: Dulbecco's phosphate-buffered saline

EDC: 1-ethyl-3-(-3-dimethylaminopropyl) carbodiimide hydrochloride

EE: encapsulation efficiency

FBS: fetal bovine serum

FCS: fibronectin coating solution

FLI: fluorescence imaging

GDNF: Glial-derived Neurotrophic Factor

GFs: growth factors

GNL: gelatin nanostructured lipid carriers

HBSS: Hank's Balanced Salt Solution

HD: Huntington`s disease

hIGF-I: human insulin-like growth factor-I

HTT: huntingtin protein

ICC: immunocytochemistry

ICV: intracerebroventricular

IGF-1: Insulin-like Growth Factor –I

i.n.: intranasal

IOD: integrated optical density

IT: intrathecal

KPBS: potassium phosphate buffered saline

Lf: lactoferrin

LPS: lipopolysaccharide

MPP: 1-methyl-4-phenylpyridinium

MPTP: 1-Methyl-4-phenyl-1,2,3,6-tetrahydropyridine

MS: microspheres

MTT: 3-[4,5-dimethylthiazol-2-yl]-2,5- diphenyltetrazolium bromide; thiazolyl blue

NDs: neurodegenerative diseases

NGF: Nerve Growth Factor

NGS: Normal Goat Serum

NHS: N-hydroxysuccinimide

NLC: nanostructured lipid nanocarriers

NP: nanoparticles

NS: nanospheres

NT-3: Neurotrophin

NTFs: neurotrophic factors

NTN: Neurturin

PANAM: polyamidoamine

PBCA: poly (butyl cyanoacrylate)

PBS: phosphate-buffered saline

PD: Parkinson's disease

PDI: polydispersity index

PEG: polyethylenglicol

PEI: polyethyleneimine

Pen: Penetratin

PFA: paraformaldehyde

PGA: poly (L-glutamic acid)

PLA: poly lactic acid

PLGA: poly (lactide-co-glycolide)

P/S: Penicillin-streptomycin

PVA: poly(vinyl alcohol)

RT: room temperature

SAP: surface-associated protein

SLN: solid lipid nanoparticles

SN: substantia nigra

SOD1: superoxide dismutase 1

ST: striatum

TEER: trans-epithelial electrical resistance

TEM: transmission electron microscopy

TH: tyrosine hydroxylase

TTC: tetanus toxin fragment C

T80: Tween 80

VEGF: Vascular Endothelial Growth Factor

16HBE14o-: human bronchial epithelial cell line

6-OHDA: 6-hydroxidopamine

INDEX

Introduction

Nanotechnology-based drug delivery systems releasing growth factors to the CNS: focusing on neurodegenerative disorders

Aplications of NanoBioMaterials (I-XI) Multi-Volume SET
Nanobiomaterials in Drug Delivery, vol 9, Ch 11, 371-402 (2016)

Nanotechnology-based drug delivery systems releasing growth factors to the CNS: focusing on neurodegenerative disorders

Oihane Gartziandia[1,2,•], Enara Herran[1,2,•], Jose Luis Pedraz[1,2], Manoli Igartua[1,2], Rosa Maria Hernandez[1,2,*]

[•]These two authors contributed equally to this work.

[1]NanoBioCel Group, Laboratory of Pharmaceutics, University of the Basque Country (UPV/EHU), School of Pharmacy, Vitoria-Gasteiz, Spain.
[2] Biomedical Research Networking Center in Bioengineering, Biomaterials and Nanomedicine (CIBER-BBN), Vitoria-Gasteiz, Spain.

ABSTRACT

Over the past years there has been a remarkable increase in the prevalence of neurodegenerative diseases (NDs). Clinically, NDs include chronically progressive dementias, ataxias and disorders of movement. The most common age-related NDs are Alzheimer's and Parkinson's diseases, but there are other less frequent disorders, such as Huntington`s disease and amyotrophic lateral sclerosis. Current therapies for these conditions are only able to treat their clinical symptoms, with a temporary effect and without halting the neurodegenerative process. Due to the low effectiveness of these treatments, promising and interesting therapies, such as growth factors (GFs), have been investigated. Nevertheless, the success of these new treatment options not only depends on the application of the specific neurotrophin, but also on a suitable approach for delivering these proteins to the brain. The development of appropriate drug delivery systems (DDS) may allow an enhancement of the GFs concentration in the brain, reaching therapeutic levels. In this sense, nanotechnologies could offer novel opportunities to formulate GFs using a wide variety of biodegradable nanocarriers, including polymeric nanospheres, lipidic nanocarriers, liposomes, and gene therapy, as possible treatments for the different neurodegenerative disorders.

*Corresponding author: R.M. Hernández

Keywords: Alzheimer's disease, Amyoptrophic lateral sclerosis, Central nervous system, Drug delivery systems, GDNF, Huntington´s disease, Neurotrophic factors, Parkinson's disease, VEGF

This chapter is part of the book entitled Nanobiomaterials in Drug Delivery, from *Aplications of NanoBioMaterials (I-XI) Multi-Volume SET*, edited by Alexandru Mihai Grumezescu.

1. Introduction

The inconvenience that most drugs present to access the brain due to the presence of the blood-brain barrier (BBB) makes very complicated the design of effective therapies for central nervous system (CNS) disorders. Thus, the search of adequate brain targeting technologies has become an important challenge for CNS drug development. In this regard, in the last years, the interest in nanotechnology has grown since it offers promising solutions to address this challenge. Different techniques enable the formulation of therapeutic agents in biocompatible nanocarriers, allowing the delivery of these drugs into the brain. Moreover, these biocompatible nanocomposites can be modified with specific brain targeting moieties to achieve a higher CNS selectivity. Commonly used nanocarriers include different delivery systems such as polymeric and lipidic nanoparticles, liposomes, or gene therapy (Wong, Wu & Bendayan 2012).

To date, the scientific community has made enormous efforts to find new treatments to address CNS disorders. In this line, selective growth factors (GFs) have become an interesting therapy since they are able to provide neuroprotective, neurorestorative and stimulating effects on diseased neurons. Significant attempts have already been made to design different and promising drug delivery systems (DDS) to release the neurotrophins ino the brain in a control manner, thereby, dealing with the limitations that these factors present to access to the brain.

Regarding the CNS disorders and specifically neurodegenerative diseases (NDs), the main characteristic that they present is a progressive loss of neuronal structure and function in the brain and spinal cord, leading to alterations in different motor, cognitive, sensory and emotional functions of the patients. NDs include different unusual disorders such as Huntington`s disease (HD) and amyotrophic lateral sclerosis (ALS), while Alzheimer's disease (AD) and Parkinson's disease (PD) are among the most common age-related NDs (Foster ER 2014). The last ones are becoming a serious public health problem due to the high treatment costs, being the care of these patients abundant and growing.

Therefore, the aim of this book chapter is to summarize the up to date advances made on brain-targeting nanotechnology-based drug delivery systems for treating CNS diseases, focusing on GFs therapies for AD, PD, HD and ALS.

2. Alzheimer's disease, Parkinson's disease, Huntington´s disease and Amyotrophic lateral sclerosis

As mentioned above, depending on the disease, CNS disorders can affect different motor, cognitive, sensory and emotional functions of the patients. In this section some of the most important neurodegenerative diseases are briefly described (Table 1).

Alzheimer's Disease

AD is the most common progressive neurodegenerative disorder with an estimated prevalence of 1 percent for people of 65-69 years old, increasing to a 40-50 percent of prevalence in older population aged 95 years and over. This disease is caused by an irreversible loss of neurons and vascular toxicity due to the extracellular deposition of amyloid beta (Aβ) peptide in senile plaques and neurofibrillary tangles of phosphorylated tau protein. The clinical symptoms of AD are the progressive loss of memory and deterioration of judgment decision, orientation to physical surroundings and language (Alan E. Guttmacher, M.D. and Francis S. Collins 2003)(Desai AK1 2005, Citron M 2010, Hardy J 2006). Nowadays, the approved and most commonly used treatments for AD are acetilcolinesterase inhibitors (tacrine, donepezil, rivastigmin, galantamin) and N-metil-D-aspartate receptor antagonist (memantine). However, it is important to mention that these drugs have a temporary effect, without showing improvements in the disease progression (Citron M 2010).

Parkinson's disease

PD is the second most frequent neurodegenerative disorder after AD. For people aged 65 to 69 years, the prevalence of this disease is about 0.5-1 percent, and it is increased with age, rising to 3 percent in population aged 80 years and over. Pathologically it is characterized by the degeneration of midbrain dopaminergic neurons in the substantia nigra (SN), with the subsequent reduction of dopamine in the striatum (ST). These pathological hallmarks lead to characteristic symptoms such as bradykinesia, resting tremor, rigidity and

postural instability. Current pharmacological therapies are based on dopamimetic drugs, but they are only able to treat the clinical symptoms without interrupting the neurodegenerative process (Alan E. Guttmacher, M.D. and Francis S. Collins 2003)(Linazasoro 2009).

Huntington disease

Among the less common NDs, HD is a hereditary neurodegenerative disorder originated by the expansion of polyglutamine stretch within the first exon of huntingtin protein (HTT) (Gusella JF et al. 1993), and clinically characterized by motor dysfunction, cognitive decline and emotional and psychiatric disorder. These neurological symptoms are caused by a neurodegeneration that affects mainly the basal ganglia and cerebral cortex (Zielonka et al. 2014). HD has a low prevalence of 5–10 per 100,000 individuals in Western Europe and North America and, although the genetic mutation was identified 20 years ago, there are not effective therapies to cure or even modify the curse of this disease (Mochly-Rosen, Disatnik & Qi 2014). The current treatments available for HD are only symptomatic and their potential therapeutic benefit must be balanced with the risks. Tetrabenazine is the only drug that has been approved by the US FDA for HD, indicated for the treatment of chorea, but its use has limitations, leaving multipurpose antipsychotics as the treatment of choice for chorea (Killoran, Biglan 2014).

Amyotrophic lateral sclerosis

Lastly, ALS, described for first time in 1874 by Jean-Martin Charcot, is a fatal inherited neurodegenerative disease characterized by a progressive loss of motor neurons in the spinal cord and brain stem (Rowland LP 2001). Despite the progress made, familial ALS is the only ALS type with a known etiology, associated with 5 to 10% of all ALS cases. Around 20% of familial ALS cases are caused by mutations in the gene encoding superoxide dismutase 1 (SOD1), remaining 80% of the cases caused by defects in other genes (Rosen DR et al. 1993). As to the treatment to address ALS, the glutamate antagonist Riluzole is the only drug approved by the FDA, increasing the survival of patients by 3 months (Lacomblez L et al. 1996), (Bensimon G, Lacomblez L, Meininger V 1994), while other glutamate antagonists have not showed beneficial effects in clinical trials (Blasco H et

al. 2014). The remaining therapies are just symptomatic, without altering the disease course, but they are able to improve the quality of life of patients (Gordon 2013).

Table 1. Description of pathological characteristics, clinical symptoms and current therapies of AD, PD, HD and ALS.

ND disorder	Pathological Characteristics	Clinical symptoms	Current treatments
AD	Irreversible loss of neurons; extracellular deposition of Aβ peptide in senile plaques and neurofibrillary tangles of phosphorylated tau protein	Progressive memory loss; deterioration of judgment decision, orientation to physical surroundings and language	Acetilcolinesterasa inhibitors: tacrine, donepezil, rivastigmin, galantamin; N-metil-D-aspartate receptor antagonist: memantine
PD	Degeneration of midbrain dopaminergic neurons in the substantia nigra (SN) and the subsequent reduction of dopamine in the striatum	Bradykinesia, resting tremor, rigidity and postural instability	Levodopa/Carvidopa, Dopamimetic drugs
HD	Expansion of polyglutamine stretch within the first exon of huntingtin protein (HTT)	Motor dysfunction, cognitive decline, and emotional and psychiatric disorder	Tetrabenazine; multipurpose antipsychotics
ALS	Progressive loss of motor neurons in the spinal cord and brain stem	Progressive muscle weakness, loss of coordination, muscle cramps, language disorder	Glutamate antagonist: Riluzole

Although the treatments of AD and PD are the main priority for the neurologist community, to date, there is no cure for these two diseases, neither for HD nor ALS. Thus, current therapies are focused on modifying the disease progression and symptoms, with insufficient or null effect on the improvement of the disease (Deierborg et al. 2008).

Moreover, due to the high economic burden of these treatments, the patient care is abundant and growing. In this sense, recent advances in the research on these diseases treatment have been intensified to search of new therapies able to overcome the neurodegenerative process and to provide neuroprotection to the surviving cells.

3. Growth factors as a novel therapy to treat neurodegenerative diseases

An interesting and promising approach to address the challenge of CNS disorders is by the use of GFs, which are a group of different molecular families and individual proteins with the ability to enhance cellular growth, proliferation and differentiation. Furthermore, they are also well known for playing important roles in tissue morphogenesis, angiogenesis, cell differentiation and neurite outgrowth (Ciesler, Sari 2013, Levy YS et al. 2005, Poon VY, Choi S, Park M 2013). Bearing in mind the enormous amount of molecules that belong to the different families of GFs, this chapter is focused on those proteins that are currently used to develop new therapies against AD, PD, HD and ALS. This group of proteins, named neurotrophic factors (NTFs), encompasses those molecules that play critical roles in a number of biological processes including the induction, specification, survival and maturation of neural development (Table 2).

Among all the NTFs described, the following have special interest as promising approaches to deal neurodegenerative processes. GDNF is a neurotrophic factor that presents a high specificity towards dopaminergic neurons, being a potent candidate for the treatment of PD. In addition, GDNF exhibits trophic and protective effects on noradrenergic neurons located in the locus coeruleus (Lapchak et al. 1997, Allen et al. 2013). Another prosiming neurotrophic factor is NGF, which promotes the survival, differentiation and maintenance of sensory and sympathetic neurons, displaying neuroprotective and repair functions (Sofroniew, Howe & Mobley 2001). Moreover, BDNF has important functions in the normal development of the peripheral and central nervous systems, and it is essential to promote the survival of neurons and synaptic plasticity in the adult brain (Ventriglia et al. 2013). With regards to CNTF, this neurotrophic factor helps in the survival and differentiation of different neurons, such as sensory, sympathetic and

motoneurons (Sendtner M1, Carroll P, Holtmann B, Hughes RA, Thoenen H 1994). Furthermore, IGF-I promotes neuronal survival and it has the ability to rescue neurons from neurotoxocity, as well as the capacity to stimulate neurogenesis and synaptogenesis (Liu et al. 2001). As to NT-3, this factor promotes neuronal survival, differentiation and neurite growth (Coppola et al. 2001). Finally, VEGF is a growth factor that fosters all steps of angiogenesis and endothelial cell development, and it enhances the growth and survival of neurons as well as the axonal outgrowth (Storkebaum, Lambrechts & Carmeliet 2004, Carmeliet, Storkebaum 2002).

Table 2. Summary of different GFs released from nanotechnology-based drug delivery systems, their main functions in the CNS and their applications for the treatment of various NDs.

Growth Factor	Main functions	Application	Ref.
Glial-derived Neurotrophic Factor (GDNF)	High specificity for dopaminergic neurons Trophic and protective effects on noradrenergic neurons in the locus coeruleus	PD, ALS, HD	(Lapchak et al. 1997, Allen et al. 2013)
Nerve Growth Factor (NGF)	Promotes the survival, differentiation and maintenance of sensory and sympathetic neurons Neuroprotective and repair functions	AD	(Sofroniew, Howe & Mobley 2001)
Brain-derived Neurotrophic Factor (BDNF)	Essential for the normal development of the peripheral and the central nervous system Key role in neuronal survival and synaptic plasticity in the adult brain	ALS, HD	(Ventriglia et al. 2013)
Ciliary Neurotrophic Factor (CNTF)	Supports survival and / or differentiation of a variety of neuronal cell types including sensory, sympathetic and motoneurons	HD	(Sendtner M et al. 1994)

Insulin-like Growth Factor –I (IGF-1)	Ability to potently promote neuronal survival and rescue from neurotoxicity Stimulates neurogenesis and synaptogenesis	ALS	(Liu et al. 2001)
Neurotrophin (NT-3)	Positive functions in fostering neuronal survival, differentiation and neurite growth	PD	(Coppola et al. 2001)
Vascular Endothelial Growth Factor (VEGF)	Promotes every angiogenesis step and endothelial cell development Improves growth and survival of neurons as well as axonal outgrowth	AD, ALS	(Storkebaum, Lambrechts & Carmeliet 2004, Carmeliet, Storkebaum 2002)

4. *In vivo* administration routes of GFs to reach the brain

In order to evaluate the effectiveness of these neurotrophic proteins in the treatment of CNS diseases, GFs have been *in vivo* administered through different administration routes (Figure 1). The main objective is, in all cases, to achieve a successful access to the brain, being some administration routes more efficient than others to address this challenge. Nevertheless, to choose the most adequate administration route to attain this purpose, it is necessary to consider the safety, effectiveness and other difficult aspects related with the route of administration.

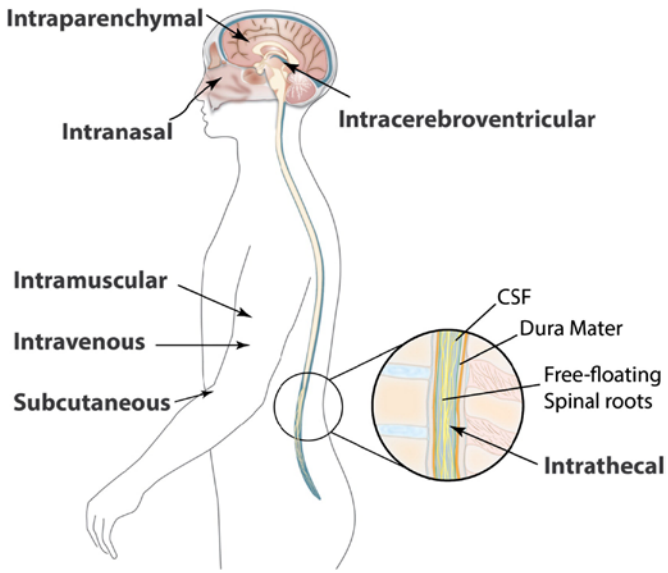

Figure 1. Different administration routes of therapeutic proteins for CNS delivery. Reprinted from (Yi et al. 2014), Copyright (2014), with permission from Elsevier.

4.1. Invasive administration routes: Intracerebroventricular and intraparenchymal routes.

In the case of intracerebroventricular (ICV) or intraparenchymal administration routes, GFs are administered directly in the lateral ventricle of the brain or into the brain parenchyma, respectively, obtaining high drug concentrations in the target site and avoiding the blood-brain barrier (BBB). However, both are invasive methods, and drug diffusion from the injection site is difficult, because the extracellular fluid space of the brain is extremely tortuous. According to this, despite having high concentration gradients in the CNS following ICV or intraparenchymal administration of GFs, the amount of drug available at brain targets located at a significant distance from the injection site could not be high enough to induce the de effect (Cook AM et al. 2009), (Kuo, Smith 2014).

4.2. Intrathecal administration.

Other less invasive administration route to access the brain avoiding the BBB is the intrathecal (IT) administration, where GFs are injected into the subarachnoid space of the

spinal cord. Nevertheless, this administration route presents some disadvantages that limit the IT delivery of drugs: on one hand the effectiveness of the drug could be reduced by the development of antibodies, and on the other hand the difficulty to predict the amount of the administered dose that will reach the brain due to variations in the cerebrospinal fluid (CSF) drug levels (Calias et al. 2014).

4.3. Parenteral administration.

Less invasive and easier to administer routes frequently used are the intravenous, intraperitoneal or subcutaneous. When using a traditional parenteral administration, the hepatic first-pass metabolism is avoided thanks to the direct access to the systemic circulation, obtaining a distribution of the GFs in the whole body, including the brain (Yi et al. 2014). However, following a parenteral administration, GFs present limitations to cross the BBB due to their inappropriate lipophilicity, molecular weight or charge (Begley 2004). Thus, high doses are required to obtain therapeutics levels of the GFs in the brain, fact that may lead to undesirable systemic effects (Mathias, Hussain 2010).

4.4. Intranasal administration.

Intranasal route is an easy and non-invasive administration way to overcome the BBB´s inherent limitations, enabling the rapid delivery of GFs to the CNS, avoiding the first-pass metabolism. Following intranasal administration, drugs are transported directly to the brain by the systemic, olfactory and trigeminal nerve pathways. In the case of the systemic pathway, drugs are absorbed immediately into the systemic veins through the nasal cavity, and then cross the BBB to reach the brain. As to the olfactory pathway, drugs first enter into the olfactory bulb and afterwards into the brain or cerebrospinal fluid (CSF) across the olfactory epithelium. Finally, by the trigeminal pathway drugs are delivered to the brain through this nerve system. Moreover, intranasal route offers some advantages that make it a promising choice for brain delivery without causing any distress in the patients, such as the large surface area and minimum peripheral size effects due to the low absorption of GFs in the systemic circulation. However, the limited drug absorption through the nasal epithelium after intranasal administration is an obstacle that still needs to be solved (Mittal et al. 2014)(Lochhead, Thorne 2012, Dhuria, Hanson & Frey 2010).

Although the previously mentioned routes could be very efficient for brain delivery of drugs, GFs are hydrophilic molecules with crucial shortcomings that limit their use, like a short circulation half-life and a rapid degradation rate after their *in vivo* administration. Therefore, with the aim of achieving a successful GFs delivery to the brain tissue, in the last years a wide variety of drug delivery systems (DDS) designed with GFs have been developed.

5. Nanotechnology-based DDS releasing growth factors for the treatment of CNS diseases

In the following section, different nanotechnology DDS that have been used for the delivery of neurotrophic factors to treat different NDs will be described, including polymeric nanoparticles, liposomes, lipidic nanocarriers, and gene therapy (Figure 2).

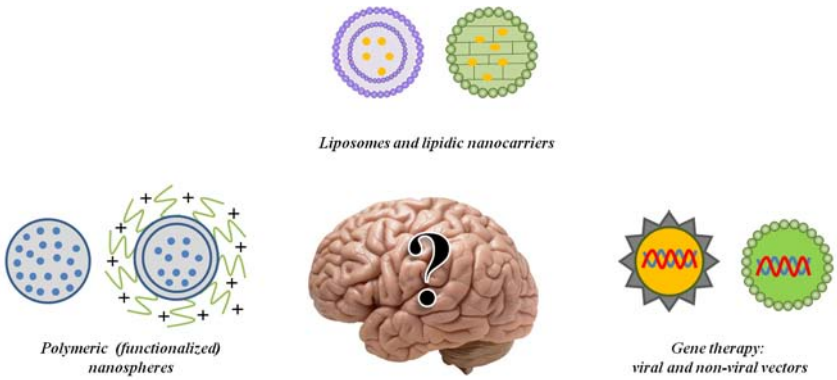

Figure 2. Schematic illustration of different nanometric drug delivery systems used for the treatment of NDs.

In the first clinical trials carried out with GFs for the treatment of neurodegenerative diseases, these were injected directly into the brain, although no promising results were obtained due to the short *in vivo* half-life of these proteins (Nutt et al. 2003, Kordower et al. 1999). Later, minipump systems were used to infuse these neurotrophins with the aim of finding an adequate method able to provide a controlled and continued administration of GFs (Slevin et al. 2006, Lang et al. 2006). However, their suitability as sustained release

delivery systems has raised many questions due to the different side effects and tissue damage caused by their use.

The previously mentioned drawbacks that GFs present have brought to light the necessity of developing suitable DDS to adequately deliver these proteins to the CNS, increasing their *in vivo* circulation half-life and protecting them from degradation. Several research groups have designed different DDS to address this challenge and achieve an appropriate delivery of GFs into the brain, either using invasive or non-invasive administration routes, besides favoring their transport across the BBB (Stockwell et al. 2014, Kabanov, Batrakova 2004). Accordingly, nanotechnology could offer new approaches by the development of DDS, due to the possibility to prepare different biodegradable or non biodegradable nanocarriers to deliver different growth and neurotrophic factors to the brain tissue.

In order to achieve a successful release of the therapeutic proteins it is essential to design carrier systems capable to avoid the GFs capture by the reticuloendothelial system, their aggregation in other tissues, the fast protein elimination from the cerebral circulation caused by enzymatic degradation, and systemic adverse effects. Furthermore, these DDS should be able to offer a continuous and controlled release of the entrapped neurotrophin over the time at their desired site of action, allowing a reduction of the administration frequency (Wong, Wu & Bendayan 2012, Angelova et al. 2013).

Taking all this into account, in this book chapter we will focus on the most frequently used nanotechnology-based DDS for the treatment of the aforementioned NDs (Table 3).

5.1. Polymeric nanospheres

Nanospheres are colloidal systems that entrap therapeutic agents within a colloidal matrix, or are attached to the particle surface by adsorption or conjugation processes. Different synthetic and natural materials are used to prepare these particles, such as poly (butyl cyanoacrylate) (PBCA), poly lactic acid (PLA) or its copolymer poly (lactide-co-glycolide) (PLGA), alginate, chitosan and other polymer combinations (Wohlfart, Gelperina & Kreuter 2012, Kreuter 2014). The previously mentioned polymers are

biodegradable, being degraded *in vivo* and eliminated by physiological metabolic pathways; therefore, they could be considered a useful strategy for human applications.

Moreover, these polymeric particles have attractive advantages, for instance a sustained and controlled drug release over the time can be obtained and, in some cases, they are able to favor the transport of different GFs across the BBB. Furthermore, the polymeric nanospheres surface can be modified using different compounds or proteins to improve their selectivity to the target site and enhance the pass across the BBB by specific mechanisms after being administered through different routes. Several targeting ligands have been used to interact with CNS receptors and transport molecules across the BBB, thus, achieving a specific delivery to the CNS. Among others, transferrin and insulin receptors have been widely used for this purpose (Kreuter 2014, Jain 2000, Mahapatro, Singh 2011).

In this sense, PLGA nanospheres (PLGA-NS) have been extensively studied by our research group. VEGF-loaded PLGA-NS demonstrated to be a potential therapeutic strategy to achieve behavioral improvements in an APP/Ps1 mouse model of AD, by performing different tests such as, T-maze, Open field test or object recognition test. Moreover, after the administration of VEGF-NS through minimally invasive craniotomy, Aβ deposits were significantly decreased in whole brain, including cerebral cortex, striatum and hippocampus (Figure 3A). VEGF-NS were also able to promote angiogenesis and protect neuronal cultures from neuroinflammation induced by lypopolysacharide (Figure 3B and 3C), in comparison with empty-NS (Herrán et al. 2013a).

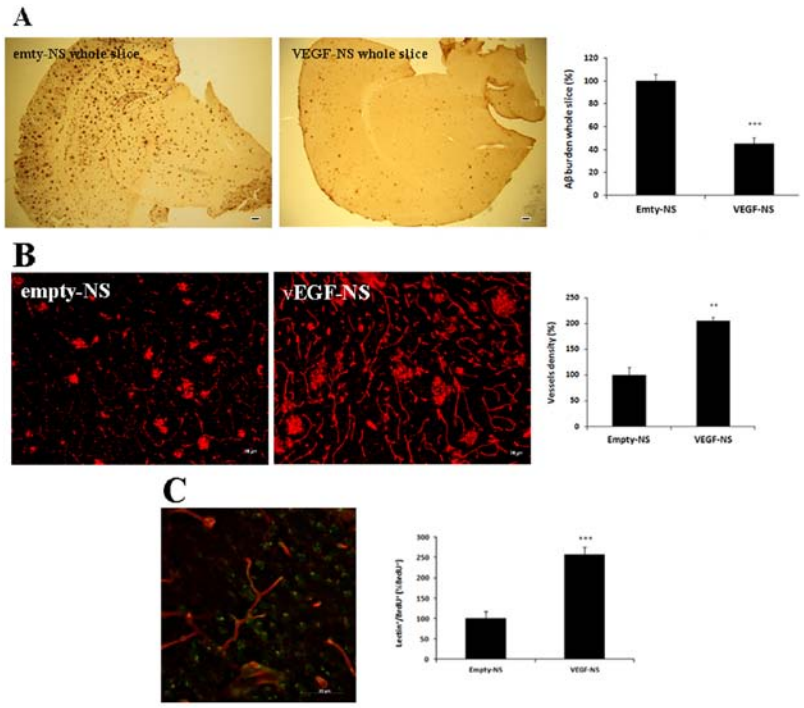

Figure 3. Brain Aβ plaques and angiogenesis after implantation of empty-NS (left) and VEGF-NS (right) in APP/Ps1 mice. Representative Aβ deposit microphotographs and histograms represent percentage of brain area covered by Aβ immunoreactivity in (A) whole slice; ***p< 0.001. Data are expressed as mean ± SEM. Scale bar= 50 μm. (B) Cerebral cortex (Cx) brain vessels marked with tomato lectin (red) in empty-NS (left) and VEGF-NS (right) treated groups. The histogram indicates vessel density in the cerebral cortex; **p< 0.01, empty-NS vs. VEGF-NS. Scale bar= 40 μm. (C) Fluorescent microphotograph showing proliferation of vessels endothelial cells in the Cx. $BrdU^+$ nuclei (green) co-labeled with tomato lectin (red) indicate newly-formed blood vessels. The histogram on the right side shows the percentage of $BrdU^+$ cells/$lectin^+$ cells; ***p< 0.001, empty-NS vs. VEGF-NS. Scale bar= 20 μm. Data are expressed as mean ± SEM. Scale bar= 20 μm.

As mentioned above, the use of biorecognitive ligands modifying the surface of these nanoparticles could enhance the drug transport to the CNS by non invasive administration routes, such as intranasal administration. In a study published by *Zhang et al.*, lectin modified bFGF-loaded PEG-PLGA nanospheres were designed to achieve a successful delivery of bFGF to the brain. The bFGF released from PEG-PLGA-NS stimulated the

survival and neurite growth of brain neurons, improving the spatial learning and memory in AD rats (Zhang et al. 2014).

The utilization of nanospheres elaborated with acrylic polymers has also been widely investigated for CNS drug delivery, particularly poly (butyl cyanoacrylate) (PBCA). In a study performed by *Kurakhmaeva et al.*, NGF adsorbed onto PBCA nanospheres delayed the progression of PD, halting the degeneration of dopaminergic neurons after being intravenously administered in a 1-Methyl-4-phenyl-1,2,3,6-tetrahydropyridine (MPTP) lesioned mouse model. Moreover, the surface modification of these nanospheres with polysorbate 80 encouraged the adsorption of apolipoproteins from the blood plasma onto the nanospheres surface, promoting the contact of the nanospheres with the brain capillary endothelial cells, with the resulting improvement of the pass across the BBB (Kurakhmaeva et al. 2009, Kurakhmaeva KB et al. 2008).

Due to the relevance of PD, our research group has developed VEGF and GDNF-loaded PLGA nanospheres to study the synergistic effect of these two GFs in a 6-OHDA rat model of PD. Following the striatal implantation of both formulations, a synergistic effect was observed, in the group which received the combined therapy, where the number of amphetamine-induced rotations decreased more significantly compared to the groups that received just one formulation. Moreover, tyrosine hydroxylase (TH) immunohistochemical analysis in the striatum and external substantia nigra (SN) confirmed a notable enhancement of neurons in the group treated with VEGF and GDNF-loaded NS (Herrán et al. 2014).

Finally, *Tan et al*. have also prepared poly (L-glutamic acid) (PGA) nanospheres loaded with BDNF. Due to the porosity of these polymeric nanocarriers, an exceptional protein adsorption capacity was appreciated, and the released BDNF was able to rescue auditory neurons in an animal model of neurodegeneration (Tan J et al. 2012).

5.2. Liposomes and lipidic nanocarriers

Lipidic nanoparticulate systems used for drug delivery and targeting to the CNS have not been widely employed for neurotrophin delivery yet. Therefore, the use of liposomes or

lipidic nanocarriers for a controlled release of GFs and neurotrophins to improve AD, PD, HD or ALS, still needs further investigation. In the following paragraphs this type of DDS and the few research studies carried out in this area, will be described.

Liposomes are synthetic small micelles formed by one or more concentric phospholipid bilayers. The structure of the lipids that form liposomes is very similar to the cell membrane structure, where cholesterol is also used, and providing similar fluidity to the cell membrane. Thus, liposomes have ability to cross any cell membrane, however, the addition of other components to their surface to enhance their effectiveness is also interesting (Barry, Vertegel 2013). In such way, liposomes can include multiple brain cell membrane targeting agents on their surface, enabling a specific interaction with target cells by molecular recognition mechanisms, and hence, improving the transport of the encapsulated GFs through the BBB (Ramos-Cabrer, Campos 2013, Huwyler, Wu & Pardridge 1996). Regarding the delivery of NTFs to address CNS disorders, *Xie et al.* designed a NGF-releasing liposome conjugated to RMP-7, a molecule with the ability to increase the permeability of the BBB, obtaining positive *in vitro* permeability results and demonstrating a rapid transport of liposomes containing NGF to the brain in *in vivo* studies, enabling the delivery of therapeutic GFs to the CNS (Xie et al. 2005).

The second lipidic nanoparticulate systems are the lipidic nanocarriers, which constitute nanometric colloidal drug carrier systems usually composed of fatty acids or mono-, di-, and try- glycerides. These nanocarriers are highly stable systems, able to cross easily the BBB due to their lipophilic nature, without producing toxic degradation compounds (Kaur et al. 2008). Among these lipidic nanocarriers, solid lipid nanoparticles (SLNs) have been studied as potential DDS for brain targeting. SLNs are nanospheres with a solid lipid matrix formed by glycerides, fatty acids, or waxes solid at room temperature, and stabilized by physiologically compatible emulsifiers. SLNs offer some advantages as DDS to be used to target therapeutic agents to the CNS, including good biocompatibility, high drug loading capacity, the avoidance of organic solvents for their production, the possibility of selective targeting to enhance their effectiveness by coating them with certain ligands, or a long stability, among others (Gastaldi et al. 2014). Other kind of lipidic

nanocarriers are the nanostructured lipid nanocarriers (NLCs), the second improved generation derived from SLNs, formed by a mixture of solid and liquid lipids. In addition to the advantages that SLNs present, NLCs have improved drug encapsulation efficiencies and release properties (Muller, Radtke & Wissing 2002).

To date, a wide range of lipidic nanocarriers have been efficiently designed and administered to transport different biological, pharmaceutical and/or magnetic active agents to the brain tissue, providing therapeutic alternatives to treat neurodegenerative diseases (Gobbi et al. 2010, Yusuf M et al. 2012). However, so far not many research works on lipidic nanocarriers delivering GFs/NTFs to treat AD, PD, HD or ALS have been published. In a recent study, *Gerald et al*. demonstrated the *in vitro* neuroprotection activity of BDNF after treating human neuroblastoma SH-SY5Y cell line with BDNF-loaded cubosome type lipid nanocarriers (containing an omega-3 polyunsaturated fatty acid) (Géral et al. 2012). As to HD, Koening's research group developed different manufacturing strategies to prepare BDNF-loaded lipid implants, confirming the biocompatibility of this system *in vivo* (Koennings et al. 2007). In another study, *Zhao Y.Z.* et al. proposed a promising therapeutic alternative to treat PD by the development of lipid-based gelatin nanoparticles loaded with basic fibroblast growth factor (bFGF). After the intranasal administration of these bFGF-loaded gelatin nanostructured lipid carriers (GNLs), important levels of the encapsulated bFGF were found in olfactory bulb and striatum, although not in the prefrontal cortex or hippocampus, compared to free bFGF (Figure 4). Thus, they could demonstrate the capacity of these nanoparticles to reach the brain. In addition, according to the obtained results, *Zhao Y.Z.* et al. demonstrated that the efficiently released bFGF reached therapeutic effects in hemiparkinsonian rats, since only the rats treated with bFGFGNLs/IN exhibited a significant decrease on apomorphine-induced rotation ($p< 0,05$) (Zhao et al. 2014).

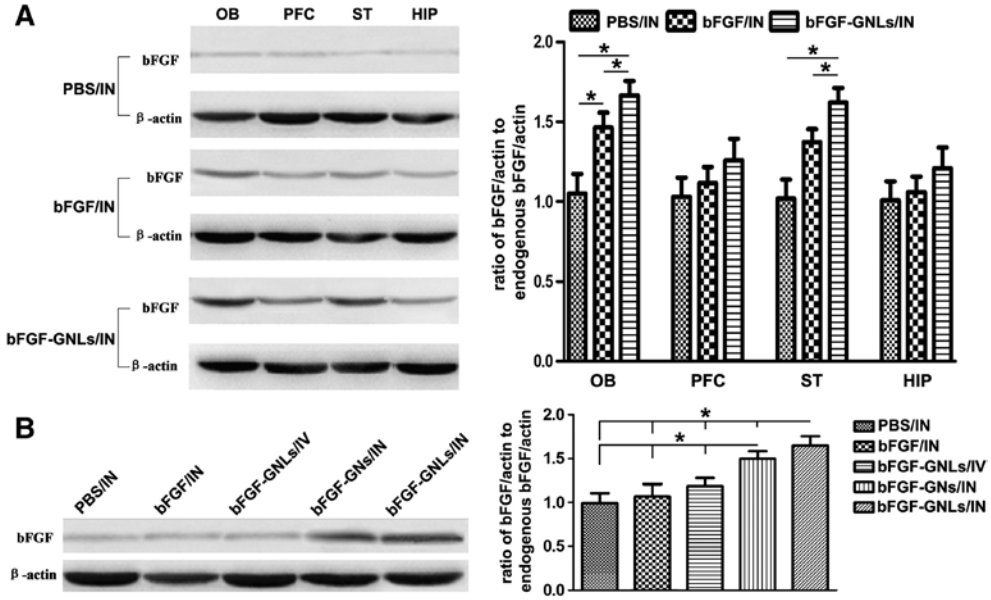

Figure 4. Protein level of bFGF in different regions of the rat brain after the administration with exogenous bFGF. (A) The presence of bFGF in olfactory bulb (OB), prefrontal cortex (PFC), striatum (ST) and hippocampus (HIP) after intranasal (IN) administration with PBS, bFGF, or bFGF-GNLs by Western blot analysis. (B) The presence of bFGF in striatum after the administration with PBS/IN, bFGF/IN, bFGF-GNs/IN, bFGF-GNLs/ IN or bFGF-GNLs/IV. Error bar: standard deviation. * represents $P < 0.05$ ($n = 3$). Reprinted from (Zhao et al. 2014), Copyright (2014), with permission from Elsevier.

5.3. Gene therapy

Current research on nanomedicine to manage AD, PD, HD and ALS is essentially focused on gene therapy as a possible approach to treat the etiology of the neurodegenerative diseases. Gene therapy consists on delivering specific genes, in this case to the CNS, which express certain molecules, such GFs, to address neurodegenerative diseases. Concretely, adeno-associated viruses (AAV) used as viral recombinant vectors to transfer genes, are considered promising tools for the treatment of CNS diseases. A series of required steps are needed to achieve a successful transduction by AAV (Figure 5): firstly, the vector has to effectively bind to the cell surface receptor, this step is followed by an endocytic uptake, and the endosomal escape; subsequently the entrance into the nucleus

takes place, followed by the capsid uncoating, genome release, second strand synthesis, and finally, the transcription of the gene (Murlidharan, Samulski & Asokan 2014).

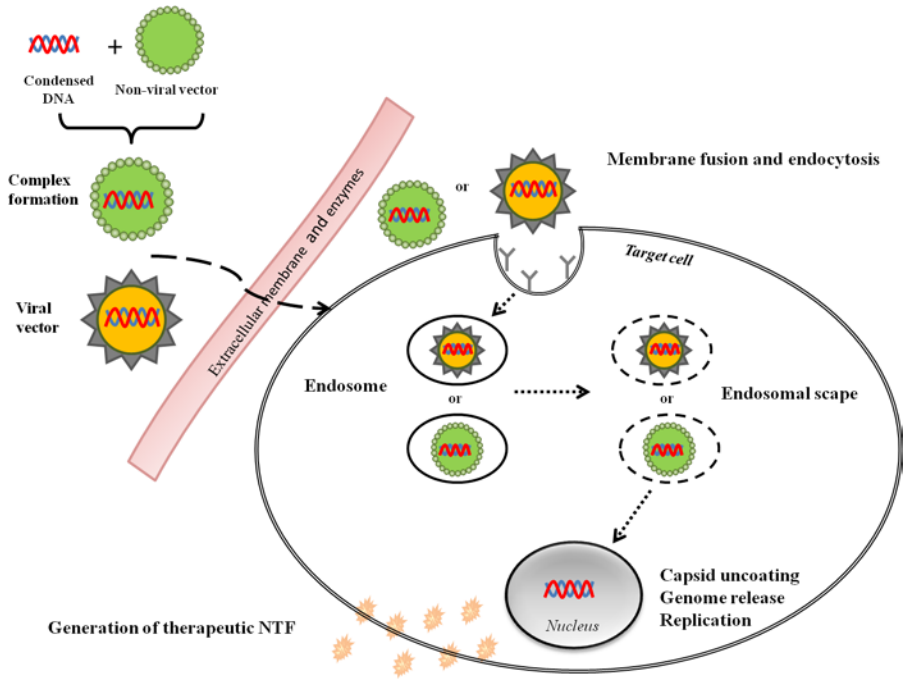

Figure 5. Schematic illustration of the transcription process of viral and non-viral gene therapy.

In order to attain this purpose, these recombinant AAVs have been used for transfecting neurons of different PD animal models (Stoessl AJ. 2014). For instance, *Eberling et al.* and *Eslamboli et al.* administered an AAV containing GDNF cDNA in a MPTP and 6-OHDA primate model of PD, respectively, with the aim of studying the safety and neuroregenerative potential of this viral vector *in vivo*. The obtained results demonstrated an increase in the dopaminergic activity in the nigroestriatal pathways with a behavioral improvement, as well as a protection from nigral dopaminergic neurons and their projections to the striatum in the lesioned hemisphere (Eberling JL et al. 2009, Eslamboli et al. 2005)(Dharmala, Yoo & Lee 2008, Pardridge 2005). In addition, *Kordower et al.* carried out an experimental assay where Neurturin was released from AVV- mediated

gene transfer, providing structural and functional neuroprotection and neurorestoration in a MPTP monkey model of PD (Kordower et al. 2006).

In the case of other neurodegenerative diseases, different *in vivo* tests have been addressed in HD and ALS mice and rat models transfected with AAV or lentivirus that express a wide variety of GFs (GDNF, IGF-I, VEGF, CNTF, BDNF and Neurturin). As to ALS, many of the viral vectors used proved a significant rescue of motor neurons, together with a prolonged animal survival (Lu et al. 2003),(Hottinger et al. 2000),(Guillot et al. 2004),(Foust KD et al. 2008),(Acsadi G et al. 2002),(Moreno-Igoa M et al. 2012),(Keir SD et al. 2001),(Wang LJ et al. 2002),(Larsen et al. 2006),(Kaspar BK et al. 2003),(Dodge et al. 2010),(Azzouz et al. 2004), while most HD animal models achieved a behavioral improvement after the GF viral gene therapy (Mittoux V et al. 2002),(Popovic et al. 2005),(McBride et al. 2003),(McBride JL et al. 2006),(Kells AP et al. 2004),(Ramaswamy et al. 2009),(Benraiss et al. 2012),(Ellison SM et al. 2013). As an example, *Guillot et al.* used lentiviral vectors to express GDNF (LV-GDNF) in a SOD1G93A transgenic ALS mouse model. In this study, a lentiviral vector expressing GDNF was administered by intraspinal or facial nucleus injection, and after 3 months mice were sacrificed for histological evaluation. The results obtained by *Guillot et al.* showed that, compared to uninjected SOD1G93A transgenic mice, LV-GDNF induced a slight but notable rescue of motoneurons in the facial nucleus, avoiding the atrophy of these neurons (Figure 6) (Guillot et al. 2004).

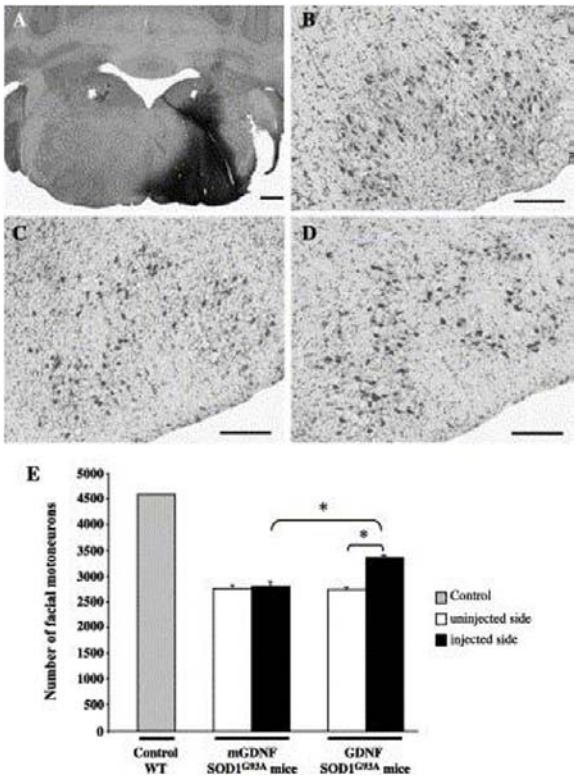

Figure 6. GDNF expression in the brainstem of a $SOD1^{G93A}$ transgenic mouse after 3 months of administration of an unilateral lentiviral vector injection. (A) Immunostaining showing extensive diffusion of GDNF in the facial nucleus. Scale bar: 600 μm. Nissl staining photomicrographs: (B) uninjected facial nucleus of a wild-type B6SJL control mouse, (C) uninjected side and (D) LV-GDNF-injected contralateral side of facial nucleus of the same $SOD1^{G93A}$ transgenic mouse. Scale bars: 200 μm. (E) Number of motoneurons in the facial nucleus of each group. * $P < 0.001$. Reprinted from (Guillot et al. 2004), Copyright (2004), with permission from Elsevier.

In another experiment carried out by *Ramaswamy et al*. in 2009, N171-82Q transgenic mice were used as an HD model to administer AAV expressing Neurturin (NTN) through an intrastriatal injection. To assess behavioral improvements, three different behavioral tests were carried out: an accelerating speed rotarod test to evaluate the locomotor coordination, hind-limb clasping to estimate the behavioral phenotype, and stride length

analysis as an index of basal ganglia dysfunction. In addition, mice brain slices were immunohistochemically labelled to obtain the neuronal density of striatum. The results obtained demonstrated the ability of this vector to delay motor deficits (Figure 7) and to protect striatal and cortical neurons (Figure 8). Figure 7 shows the results obtained by the rotarod and clasping tests. In the first test, NTN treatment appeared to delay decline, with no impairments observed in NTN-Tg mice until week 14 compared to GFP-Tg and Veh-Tg mice; that decayed on weeks 11 and 12, respectively (Figure 7A). In the clasping test, transgenic mice of all groups began clasping at similar time-points (Veh-Tg: week 11; GFPTg and NTN-Tg: week 12), although by week 16 only 40% of NTN-Tg mice exhibited clasping behavior compared to 71.4% and 75% of GFP-Tg and Veh-Tg-treated mice, respectively (Figure 7B). In Figure 8 striatal cell counts and volume are showed, confirming that NTN-Tg mice have relative normal densities of NeuN-ir neurons in the striatum, making evident a significant neuroprotection compared to both the GFP-Tg and Veh-Tg groups (Figure 8B and 8E) (Ramaswamy et al. 2009).

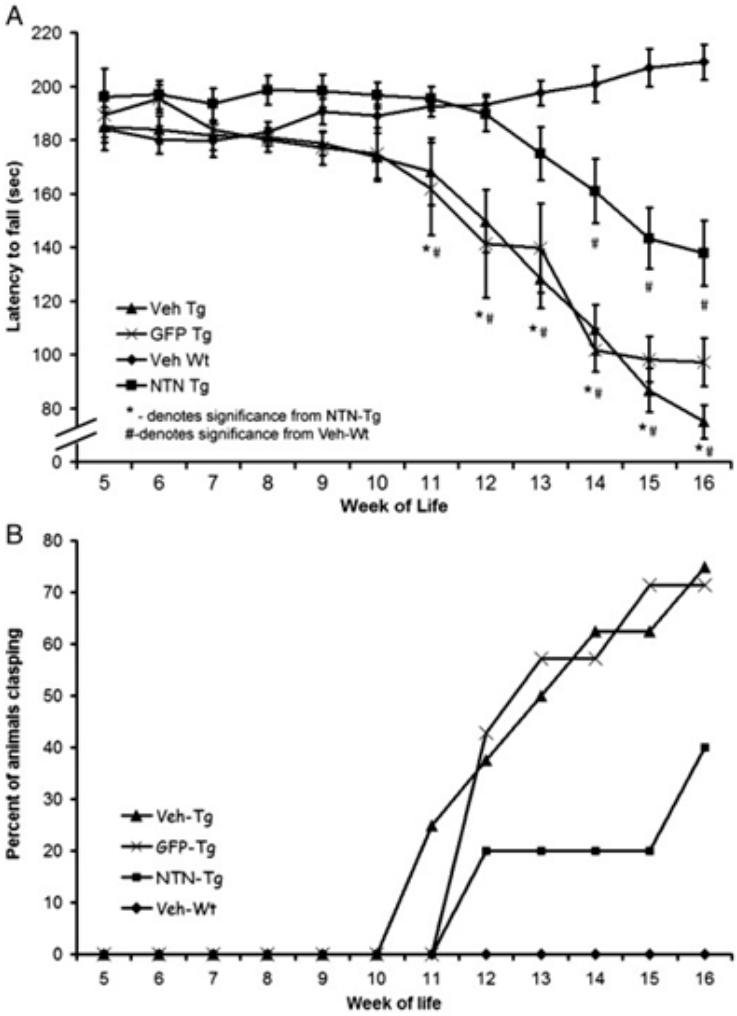

Figure 7. (A) Rotorod: tests balance and coordination using an accelerating paradigm, by recording the animals latency to fall. (B) Clasping: a phenotype only exhibited by transgenic mice. The number of mice in each group that exhibit clasping behavior each week is noted and percentages are compared between groups. Veh Tg: Transgenic mice treated with the vector vehicle, GFP Tg: Transgenic mice treated with AAV-Green Fluorescent Protein, Veh WT: Wild type mice treated with vehicle, NTN Tg: Transgenic mice treated with AAV-NTN. Reprinted from (Ramaswamy et al. 2009), Copyright (2009), with permission from Elsevier.

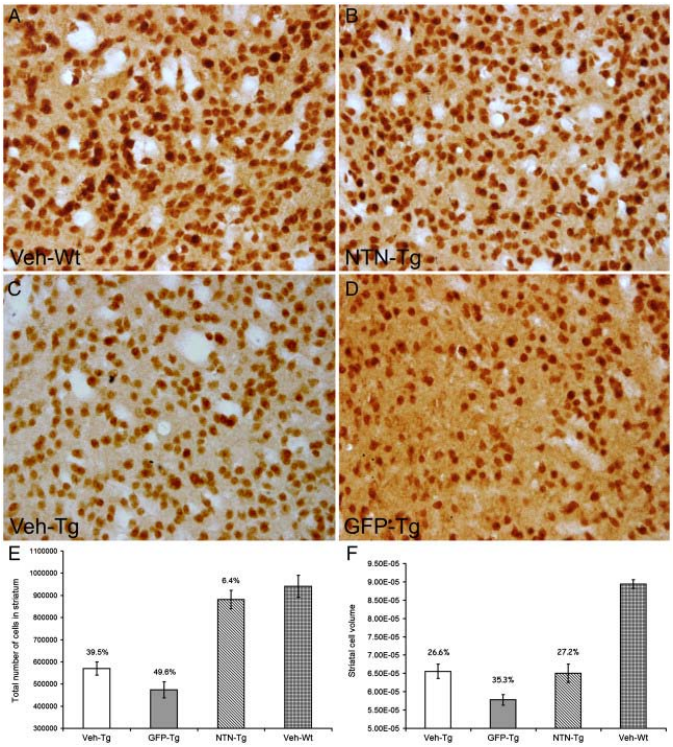

Figure 8. Striatal cell counts and volume. (A): Image (20X) of normal cell density in the Veh-Wt group. (C, D): The striatum of Veh and GFP transgenic mice. (B) The striatum of NTN-Tg mice. (E) Total numbers of cells in striatum (mean ± SEM). (F) Estimation of NeuN-ir striatal cell volume using the nucleator method. Reprinted from (Ramaswamy et al. 2009), Copyright (2009), with permission from Elsevier.

These viral vectors have also been investigated in clinical trials, mainly in Phase I studies analyzing the safety of such compounds. In this regard, a randomized placebo-controlled clinical trial was performed by *Zavalishin et al.* in ALS patients to evaluate the neurotrophic effect of VEGF expressed in AAV. This viral vector demonstrated to be safe and had the ability to increase the life span of patients (Zavalishin IA et al. 2008). Furthermore, in the case of PD, Neurturin administered by AAV vectors has been studied in clinical trials. In all the Phase I studies accomplished, all the treatments analyzed were well tolerated by patients (Bartus et al. 2013),(Marks Jr et al. 2008), while during Phase II/III

studies, not significant clinical benefits were appreciated. Besides, a double-blind, randomised, controlled trial was carried out by *Marks et al*. in 2010 to evaluate AAV expressing Neurturin in 58 patients with advanced stage of PD, however, after being bilaterally injected into the putamen, no significant differences were found in patients treated with AAV2-neurturin compared to controls, and serious adverse events appeared in 13 of 38 patients treated with this viral vector (Marks Jr et al. 2010).

It is interesting to mention that the clinical application of viral vectors is confronted due to the risks that they present, associated with immunogenicity and safety. To solve this issue, safer and effective non viral gene delivery vectors have been developed for their application in CNS diseases. These non viral vectors can transport condensed DNA to target cells and tissues, reaching the cells and entering into the nucleus to complete the gene expression (Figure 5) (Schlachetzki et al. 2004). Commonly used non-viral delivery vectors consist of cationic molecules and negatively charged nucleic acids that assemble through electrostatic interactions. Some non-viral delivery vectors may include cationic lipids, dendrimers, polymers, cyclodextrines (CDs), or nanoparticles entrapping nucleic acids (O'Mahony et al. 2013).

Taking all this into account, *Huang et al.* designed a potent non viral vector composed of polyamidoamine (PANAM) conjugated with lactoferrin (Lf) through a bifunctional polyethylenglicol (PEG), encapsulating human GDNF gene. The nanoparticles were intravenously administered and the brains were analyzed to determine GDNF expression using an ELISA kit. According to the results obtained, high GDNF levels were observed in the brains of rats treated with a single injection of Lf-modified nanoparticles (Figure 9A). Furthermore, when multiple injections of Lf-modified nanoparticles were administered, higher GDNF expression was detected compared to a single administration of the nanoparticles (Figure 9B). Moreover, the multiple Lf-modified-nanoparticles intravenously administered resulted in a significant improvement of the locomotor activity, dopaminergic neuronal number and monoamine neurotransmitter levels on rotenone-induced PD rats (Huang et al. 2010).

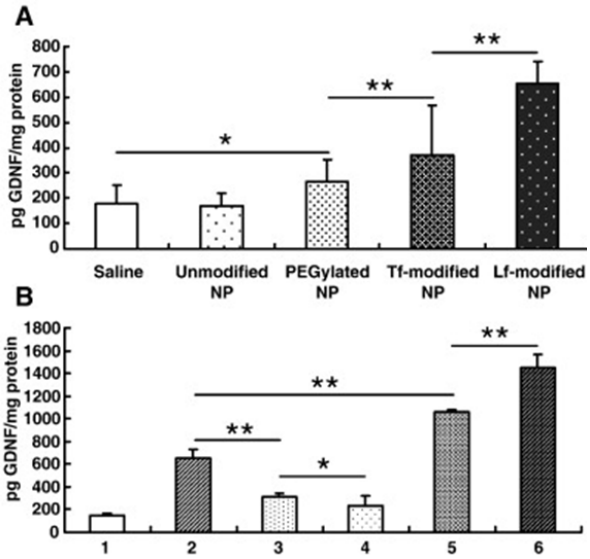

Figure 9. Detection of GDNF content in rat brains by ELISA. A: Rats receiving a unique injection of different nanoparticles loaded with hGDNF, with saline as controls. B: Rats receiving a regimen of Lf-modified nanoparticles loaded with hGDNF, with saline as controls. 1: GDNF expression two days after a unique injection of saline; 2: GDNF expression two days after a unique injection of Lf-modified nanoparticles; 3: GDNF expression six days after a unique injection of Lf-modified nanoparticles; 4: GDNF expression ten days after a unique injection of Lf-modified nanoparticles; 5: GDNF expression two days after triple injections of Lf-modified nanoparticles, one injection every other day; 6: GDNF expression two days after five injections of Lf-modified nanoparticles, one injection every other day. Data are expressed as mean ± S.E.M (n = 6). Significance: *$p < 0.05$; **$p < 0.01$. Reprinted from (Huang et al. 2010), Copyright (2010), with permission from Elsevier.

Additionally, another study accomplished by *Gonzalez Barrios et al.* to address PD with GDNF revealed the ability of neurotensin polyplexes as nanoparticulate carrier systems to target reporter genes to nigral dopaminergic neurons of hemiparkinsonian rats. After the transfection of SN with this non viral vector, hGDNF was expressed and was able to decrease the parkinsonism signs, suggesting this neurotensin polyplexes as potent and useful tools for the screening of therapeutic genes in animal models of PD. Nevertheless, their safety still needs to be proved before their clinical use (Gonzalez-Barrios et al. 2006).

In the case of ALS, experimental assays have been carried out with the tetanus toxin fragment C (TTC) as a non viral vehicle to deliver GDNF (Moreno-Igoa M et al. 2012),(Larsen et al. 2006),(Ciriza J et al. 2008) or BDNF (Calvo et al. 2011), obtaining promising results in neuroprotection and improving the survival of the treated animals. Accordingly, *Calvo et al.* used BDNF expressing TTC vectors in a SOD1G93A transgenic ALS mouse model, detecting behavioral and electrophysiological improvements, motoneuron survival and antiapoptotic/survival-activated pathways.

Table 3. Summary of different nanotechnology-based drug delivery systems releasing neurotrophins.

DDS	Growth Factor	Application	Model	Main results	Refs.
PLGA-NS	VEGF (nanoencapsulated)	AD	APP/Ps1, mouse	Improves behavioral deficits; decreases Aβ deposits; promotes angiogenesis	(Herrán et al. 2013a)
Lectin modified PEG-PLGA-NS	bFGF (nanoencapsulated)	AD	AD model induced by Aβ25-35 and IBO; rats	Improves memory; promotes the survival and neurite outgrowth	(Zhang et al. 2014)
PBCA-NS coated with polysorbate 80	NGF (adsorbed on the surface)	PD	MPTP; mouse	Increases locomotor activity; decreases rigidity	(Kurakhmaeva et al. 2009, Kurakhmaeva KB et al. 2008)

PLGA-NS	GDNF, VEGF (nanoencapsulated)	PD	6-OHDA; rats	Decreases the number of amphetamine-induced rotations; enhances TH+ neurons in SN and striatum	(Herrán et al. 2014)
Liposome conjugated with RPM-7	NGF (encapsulated)	CNS	in vitro; in vivo	Successful permeability and transport studies	(Xie et al. 2005)
Phospholipid-based gelatin-NS	bFGF (nanoencapsulated)	PD	Hemiparkinsonian rats	Increases DA levels; improves retention of nigral DA neurons; attenuates rotational behavior	(Zhao et al. 2014)
Cubosome type lipid nanocarriers	BDNF (nanoencapsulated)	CNS	in vitro; SH-SY5Y cell line	Neuroprotective effects	(Géral et al. 2012)
Protein-loaded lipid matrices	BDNF	HD	rats	Biocompatible matrices	(Koennings et al. 2007)
Transfected recombinant AAVs	GDNF, NT-3 (AAV2 vector)	PD	Primate model of PD	Structural and functional neuroprotection and neurorestoration, behavioural recovery	(Eberling JL et al. 2009, Eslamboli et al. 2005, Kordower et al. 2006)

PANAM-Lf-PEG	hGDNF (therapeutic gene hGDNF linked with PANAM)	PD	Rotenone; rats	Improved locomotor activity; reduces DA neuronal loss; enhances monoamine neurotransmitter levels	(Huang et al. 2010)
Neurotensin polyplex	GDNF(therapeutic gene hGDNF linked with neurotensin)	PD	PD animal model-6-OHDA; rats	Biochemical, anatomical and functional recovery	(Gonzalez-Barrios et al. 2006)
TTC vector	BDNF (BDNF-TTC vector)	ALS	SOD1G93A transgenic mice	Improves behavioral and electrophysiological results, motoneuron survival, antiapoptotic/survival-activated pathways	(Calvo et al. 2011)
AAV	GDNF (AAV vector)	ALS	C57BL/6J mice	Retrograde axonal transportation of the transgenic GDNF	(Lu et al. 2003)
Lentiviral-mediated expression of GDNF	GDNF (Lentiviral vector)	ALS	Facial nerve lesion; Balb/C mice	Complete and Long-Term Rescue of Lesioned Adult Motoneurons	(Hottinger et al. 2000)
Lentiviral-mediated expression of GDNF	GDNF (Lentiviral vector)	ALS	SOD1G93A transgenic mice	Induces significant rescue of motoneurons in the facial nucleus, preventes motoneuron atrophy	(Guillot et al. 2004)

AAV	GDNF (AAV vector)	ALS	Normal rats	Rubrospinal tract GDNF transport to the spinal cord	(Foust KD et al. 2008)
AVR	GDNF (AVR vector)	ALS	SOD1 mice	Increases survival and motor function	(Acsadi G et al. 2002)
Naked DNA encoding GDNF-TTC	GDNF (DNA vector)	ALS	SOD G93A mice	Delays the onset of symptoms and functional deficits	(Moreno-Igoa M et al. 2012)
AAV	GDNF (AAV vector)	ALS	Motor neuron-like cells	Protects cells from apoptosis	(Keir SD et al. 2001)
AAV	GDNF (AAV vector)	ALS	SOD G93A mice	Delays the progression of the motor dysfunction, and prolongs the life span in the treated ALS mice	(Wang LJ et al. 2002)
TTC vector	GDNF (GDNF-TTC vector)	ALS	Sciatic nerve transection model; rats	Neuroprotection	(Larsen et al. 2006)
TTC vector	GDNF (GDNF-TTC vector)	ALS	Neuro2A cells; SODG93A mice	Antiapoptotic neuronal activity; increases survival and life quality in symptoms	(Ciriza J et al. 2008)
AAV	IGF-1 (AAV vector)	ALS	SOD1 mice	Prolongs life span and delays disease progression	(Kaspar BK et al. 2003)

AAV4	IGF-1, VEGF (AAV4 vector)	ALS	SOD1 G93A mice	Improves survival but no synergistic effect with combined therapy	(Dodge et al. 2010)
Lentiviral-mediated expression of VEGF	VEGF (Lentiviral vector)	ALS	SOD1 G93A mice	Increases life expectancy	(Azzouz et al. 2004)
Plasmid that encodes ZFP-TP	VEGF (Plasmid)	ALS	SOD1 rats	Neuroprotection; improves rotaroad performance	(Kliem MA et al. 2011)
Adenovirus	CNTF (Adenoviral vector)	HD	Model of Progressive Striatal Degeneration; Lewis rats	Protects corticostriatopallidal circuits; significant behavioural benefits	(Mittoux V et al. 2002)
Lentiviral-mediated expression of GDNF	GDNF (Lentiviral vector)	HD	R6/2 Huntington mice	No attenuation of behavioral and neuropathological changes	(Popovic et al. 2005)
AAV	GDNF (AAV vector)	HD	Rat model of HD; Lewis rats	Improvement in behavioral test; reduces cell loss	(McBride et al. 2003)
AAV	GDNF (AAV vector)	HD	Mouse model of HD	Improves behavior and protects striatal neurons	(McBride JL et al. 2006)
AAV	GDNF, BDNF (AAV vector)	HD	Lesion with QA; rats	Reduces loss of both NeuNand calbindin-immunopositive striatal neurons	(Kells AP et al 2004)
AAV	Neurturin (AAV vector)	HD	N171-82Q transgenic HD mouse model	Protects striatal and cortical neurons and delays motor deficits	(Ramaswamy et al. 2009)

AAV4	BDNF (AAV4 vector)	HD	Adult rat	Sustained induction of neuronal addition to the neostriatum	(Benraiss et al. 2012)
Lentivirus	VEGF (Lentiviral vector)	HD	*In vivo* model of HD; rats	Dose-dependent Neuroprotection	(Ellison SM et al. 2013)

6. Conclusions

So far, most of the molecular, cellular, and circuit functions, genes or pathways that cause neurodegeneration in CNS diseases are not yet well investigated, and thus, nowadays the only clinical treatments for AD, PD, HD or ALS are mainly symptomatic, without managing the diseases progression.

Taking these considerations into account, the development of new therapeutic options to address the main causes of neurodegenerative diseases is urgently needed. In this sense, NTFs are considered a promising approach to attain this purpose. However, these factors present some shortcomings that limit their use in clinical application, mainly due to their poor capacity to cross the BBB, and thus to access the brain as well as their short circulation half-life and rapid degradation rate after being administered *in vivo*. With the aim to overcome these clinical restrictions, a quick progress in the area of nanomedicine has been performed, where different systems have been developed in order to protect NTFs and control their release in the brain, thus, achieving a favorable local and long term delivery. These efforts have led to a promising evolution of current therapies for the treatment of neurodegenerative disorders. According to this, in this book chapter novel nanotechnologies frequently used to achieve a controlled release of NTFs for the treatment of AD, PD, HD and ALS have been fully described. Among the different nanotechnologies mentioned, polymeric or lipidic nanocarriers could offer an exceptional ability to access the brain tissue overcoming the BBB limitation. These nanocarriers are safe and biodegradable

systems that can be administered through different administration routes. In addition, another interesting and important advantage that these nanosystems offer is the possibility of surface modification with certain ligands to attain a specific brain targeting, enabling them as suitable candidates for the sustained release of GFs in the brain tissue.

Nevertheless, despite the enormous advances that have been addressed in nanometric DDS to deliver NTFs, to date, the main clinical trials carried out to evaluate GFs for CNS disorders have been performed administering NTFs in solution. Therefore, bearing in mind the previously named problems that these proteins present after their *in vivo* administration, and taking into account the promising preclinical results obtained with the DDS entrapping NTFs described in this chapter, further research would be needed in the field nanomedicine to develop suitable DDS using GFs or neurotrophins for human application to treat neurodegenerative disorders.

7. Conflict of interest

The authors report no conflicts of interest in this work.

8. References

Acsadi G, Anguelov RA, Yang H, Toth G, Thomas R, Jani A, Wang Y, Ianakova E, Mohammad S, Lewis RA, Shy ME, 2002. Increased survival and function of SOD1 mice after glial cell-derived neurotrophic factor gene therapy. Hum Gene Ther, 13 (9), 1047-59.

Alan E. Guttmacher, M.D., and Francis S. Collins 2003. Alzheimer's Disease and Parkinson's Disease. N Engl J Med, 348, 1356-64.

Allen, S.J., Watson, J.J., Shoemark, D.K., Barua, N.U. & Patel, N.K. 2013. GDNF, NGF and BDNF as therapeutic options for neurodegeneration. Pharmacol Ther. 138 (2), 155-175.

Angelova, A., Angelov, B., Drechsler, M. & Lesieur, S. 2013. Neurotrophin delivery using nanotechnology. Drug Discov Today, 18 (23–24), 1263-1271.

Azzouz, M., Ralph, GS., Storkebaum, E, Walmsley, LE., Mitrophanous, KA., Kingsman, SM., Carmeliet, P., Mazarakis, ND,. 2004. VEGF delivery with retrogradely

transported lentivector prolongs survival in a mouse ALS model. Nature, 429, 413-417.

Barry, J.N. & Vertegel, A.A. 2013. Nanomaterials for Protein Mediated Therapy and Delivery. Nano Life, 3 (4), 1343001.

Bartus, R.T., Baumann, T.L., Siffert, J., Herzog, C.D., Alterman, R., Boulis, N., Turner, D.A., Stacy, M., Lang, A.E., Lozano, A.M. & Olanow, C.W. 2013. Safety/feasibility of targeting the substantia nigra with AAV2-neurturin in Parkinson patients. Neurology, 80 (18), 1698-1701.

Begley, D.J. 2004. Delivery of therapeutic agents to the central nervous system: the problems and the possibilities. Pharmacol Ther, 104 (1), 29-45.

Benraiss, A., Bruel-Jungerman, E., Lu, G., Economides, A.N., Davidson, B. & Goldman, S.A. 2012. Sustained induction of neuronal addition to the adult rat neostriatum by AAV4-delivered noggin and BDNF. Gene Ther, 19 (5), 483-493.

Bensimon, G., Lacomblez, L., Meininger, V., 1994. A controlled trial of riluzole in amyotrophic lateral sclerosis. ALS/Riluzole Study Group. N Engl J Med, 330 (9), 585-591.

Blasco, H., Mavel, S., Corcia, P., Gordon, PH., 2014. The glutamate hypothesis in ALS: pathophysiology and drug development. Curr Med Chem, 21 (31), 3551-3575.

Calias, P., Banks, W.A., Begley, D., Scarpa, M. & Dickson, P. 2014. Intrathecal delivery of protein therapeutics to the brain: A critical reassessment. Pharmacol Ther, 144 (2), 114-122.

Calvo, A.C., Moreno-Igoa, M., Mancuso, R., Manzano, R., Olivan, S., Munoz, M.J., Penas, C., Zaragoza, P., Navarro, X. & Osta, R. 2011. Lack of a synergistic effect of a non-viral ALS gene therapy based on BDNF and a TTC fusion molecule. Orphanet J Rare Dis, 6 (10), 1172-6-10.

Carmeliet, P. & Storkebaum, E. 2002. Vascular and neuronal effects of VEGF in the nervous system: implications for neurological disorders. Semin Cell Dev Biol, 13 (1), 39-53.

Ciesler, J. & Sari, Y. 2013. Neurotrophic Peptides: Potential Drugs for Treatment of Amyotrophic Lateral Sclerosis and Alzheimer's disease. Open J Neurosci, 3, 2.

Ciriza, J., Moreno-Igoa, M., Calvo, AC., Yague, G., Palacio, J., Miana-Mena, FJ., Muñoz, MJ., Zaragoza, P., Brûlet, P., Osta, R., 2008. A genetic fusion GDNF-C fragment of tetanus toxin prolongs survival in a symptomatic mouse ALS model. Restor Neurol Neurosci, 26 (6), 459-65.

Citron, M., 2010. Alzheimer's disease: strategies for disease modification. Nat Rev Drug Discov, 9 (5), 387-398.

Cook, AM., Mieure, KD., Owen, RD., Pesaturo, AB., Hatton, J., 2009. Intracerebroventricular administration of drugs. Pharmacotherapy, 29 (7), 832-845.

Coppola, V., Kucera, J., Palko, M.E., Martinez-De Velasco, J., Lyons, W.E., Fritzsch, B. & Tessarollo, L. 2001. Dissection of NT3 functions in vivo by gene replacement strategy. Development, 128 (21), 4315-4327.

Deierborg, T., Soulet, D., Roybon, L., Hall, V. & Brundin, P. 2008. Emerging restorative treatments for Parkinson's disease. Prog Neurobiol, 85 (4), 407-432.

Desai AK, G.G., 2005. Diagnosis and treatment of Alzheimer's disease. Neurology, 64, 34-39.

Dharmala, K., Yoo, J.W. & Lee, C.H. 2008. Development of Chitosan–SLN Microparticles for chemotherapy: In vitro approach through efflux-transporter modulation. J Control Release, 131(3), 190-197.

Dhuria, S.V., Hanson, L.R. & Frey, W.H., 2nd 2010. Intranasal delivery to the central nervous system: mechanisms and experimental considerations. J Pharm Sci, 99 (4), 1654-1673.

Dodge, J.C., Treleaven, C.M., Fidler, J.A., Hester, M., Haidet, A., Handy, C., Rao, M., Eagle, A., Matthews, J.C., Taksir, T.V., Cheng, S.H., Shihabuddin, L.S. & Kaspar, B.K. 2010. AAV4-mediated expression of IGF-1 and VEGF within cellular components of the ventricular system improves survival outcome in familial ALS mice. Mol Ther *: the journal of the American Society of Gene Therapy*, 18 (12), 2075-2084.

Eberling JL, Kells AP, Pivirotto P, Beyer J, Bringas J, Federoff HJ, Forsayeth J, Bankiewicz KS 2009. Functional effects of AAV2-GDNF on the dopaminergic nigrostriatal pathway in parkinsonian rhesus monkeys. Hum Gene Ther., 20 (5), 511-8.

Ellison, SM., Trabalza, A., Tisato, V., Pazarentzos, E., Lee, S., Papadaki, V., Goniotaki, D., Morgan, S., Mirzaei, N., Mazarakis, ND., 2013. Dose-dependent Neuroprotection of VEGF165
in Huntington's Disease Striatum. Mol Ther, 21 (10), 1862-1875.

Eslamboli, A., Georgievska, B., Ridley, R.M., Baker, H.F., Muzyczka, N., Burger, C., Mandel, R.J., Annett, L. & Kirik, D. 2005. Continuous low-level glial cell line-derived neurotrophic factor delivery using recombinant adeno-associated viral vectors provides neuroprotection and induces behavioral recovery in a primate model of Parkinson's disease. J. Neurosci, 25, 769-777.

Foster ER 2014. Themes from the special issue on neurodegenerative diseases: what have we learned, and where can we go from here?. Am J Occup Ther, 68 (1), 6-8.

Foust, KD., Flotte, TR., Reier, PJ., Mandel, RJ., 2008. Recombinant adeno-associated virus-mediated global anterograde delivery of glial cell line-derived neurotrophic factor to the spinal cord: comparison of rubrospinal and corticospinal tracts in the rat. Hum Gene Ther, 19 (1), 71-82.

Gastaldi, L., Battaglia, L., Peira, E., Chirio, D., Muntoni, E., Solazzi, I., Gallarate, M. & Dosio, F., 2014 Solid lipid nanoparticles as vehicles of drugs to the brain: Current state of the art. Eur J Pharm Biopharm, 87 (3), 433-444.

Géral, C., Angelova, A., Angelov, B., Nicolas, V. & Lesieur, S., 2012. Multicompartment Lipid Nanocarriers for Targeting of Cells Expressing Brain Receptors. Self-Assembled Supramolecular ArchitecturesJohn Wiley & Sons, Inc, 319-355.

Gobbi, M., Re, F., Canovi, M., Beeg, M., Gregori, M., Sesana, S., Sonnino, S., Brogioli, D., Musicanti, C., Gasco, P., Salmona, M. & Masserini, M.E., 2010. Lipid-based nanoparticles with high binding affinity for amyloid-beta1-42 peptide. Biomaterials, 31 (25), 6519-6529.

Gonzalez-Barrios, J.A., Lindahl, M., Bannon, M.J., Anaya-Martinez, V., Flores, G., Navarro-Quiroga, I., Trudeau, L.E., Aceves, J., Martinez-Arguelles, D.B., Garcia-Villegas, R., Jimenez, I., Segovia, J. & Martinez-Fong, D., 2006. Neurotensin polyplex as an efficient carrier for delivering the human GDNF gene into nigral dopamine neurons of hemiparkinsonian rats. Mol Ther, 14(6), 857-865.

Gordon, P.H., 2013. Amyotrophic Lateral Sclerosis: An update for 2013 Clinical Features, Pathophysiology, Management and Therapeutic Trials. Aging Dis, 4 (5), 295-310.

Guillot, S., Azzouz, M., Deglon, N., Zurn, A. & Aebischer, P., 2004. Local GDNF expression mediated by lentiviral vector protects facial nerve motoneurons but not spinal motoneurons in SOD1(G93A) transgenic mice. NeurobiolDis, 16 (1), 139-149.

Gusella, JF., MacDonald, ME., Ambrose, CM., Duyao, MP., 1993. MOlecular genetics of huntington´s disease. Arch Neurol, 50 (11), 1157-1163.

Hardy J, C.K., 2006. Amyloid at the blood vessel wall. Nat Med, 12 (7), 756-757.

Herrán, E., Requejo, C., Ruiz-Ortega, JA., Aristieta, A., Igartua, M., Bengoetxea, H., Ugedo, L., Pedraz, JL., Lafuente, JV., Hernández, RM., 2014. Increased antiparkinson efficacy by the combined administration of VEGF- and GDNF-releasing nanospheres in a partial lesion model of Parkinson's disease. Int J Nanomedicine, 9, 2677-2687.

Herrán, E., Pérez-González, R., Igartua, M., Pedraz, J.L., Carro, E. & Hernández, R.M., 2013a. VEGF-releasing biodegradable nanospheres administered by craniotomy: A novel therapeutic approach in the APP/Ps1 mouse model of Alzheimer's disease. J of Control Release, 170 (1), 111-119.

Hottinger, A.F., Azzouz, M., Deglon, N., Aebischer, P. & Zurn, A.D., 2000. Complete and long-term rescue of lesioned adult motoneurons by lentiviral-mediated expression of glial cell line-derived neurotrophic factor in the facial nucleus. JNeurosci, 20 (15), 5587-5593.

Huang, R., Ke, W., Liu, Y., Wu, D., Feng, L., Jiang, C. & Pei, Y., 2010. Gene therapy using lactoferrin-modified nanoparticles in a rotenone-induced chronic Parkinson model. J Neurol Sci, 290 (1–2), 123-130.

Huwyler, J., Wu, D. & Pardridge, W.M., 1996. Brain drug delivery of small molecules using immunoliposomes. Proc Natl Acad Sci Un S A, 93 (24), 14164-14169.

Jain, R.A., 2000. The manufacturing techniques of various drug loaded biodegradable poly(lactide-co-glycolide) (PLGA) devices. Biomaterials, 21 (23), 2475-2490.

Kabanov, A.V. & Batrakova, E.V., 2004. New technologies for drug delivery across the blood brain barrier. Curr Pharm Des, 10 (12), 1355-1363.

Kaspar, BK., Lladó, J., Sherkat, N., Rothstein, JD., Gage, FH., 2003. Retrograde Viral Delivery of IGF-1 Prolongs Survival in a Mouse ALS Model. Science, 301 (5634), 839-842.

Kaur, I.P., Bhandari, R., Bhandari, S. & Kakkar, V., 2008. Potential of solid lipid nanoparticles in brain targeting. J Control Release, 127 (2), 97-109.

Keir, SD., Xiao, X., Li, J., Kennedy, PG., 2001. Adeno-associated virus-mediated delivery of glial cell line-derived neurotrophic factor protects motor neuron-like cells from apoptosis. J Neurovirol, 7 (5), 437-36.

Kells, AP., Fong, DM., Dragunow, M., During, MJ., Young, D., Connor, B., 2004. AAV-Mediated Gene Delivery of BDNF or GDNF Is Neuroprotective in a Model of Huntington Disease. Mol Ther, 9 (5), 682-688.

Killoran, A. & Biglan, K.M., 2014. Current therapeutic options for Huntington's disease: good clinical practice versus evidence-based approaches?. Mov Disord, 29 (11), 1404-1413.

Kliem, MA., Heeke, BL., Franz, CK., Radovitskiy, I., Raore, B., Barrow, E., Snyder, BR., Federici, T., Kaye Spratt, S., Boulis, NM., 2011. Intramuscular administration of a VEGF zinc finger transcription factor activator (VEGF-ZFP-TF) improves functional outcomes in SOD1 rats. Amyotroph Lateral Scler, 12 (5), 331-9.

Koennings, S., Sapin, A., Blunk, T., Menei, P. & Goepferich, A., 2007. Towards controlled release of BDNF--manufacturing strategies for protein-loaded lipid implants and biocompatibility evaluation in the brain. J Control Release, 119 (2), 163-172.

Kordower, J.H., Palfi, S., Chen, E.Y., Ma, S.Y., Sendera, T., Cochran, E.J., Cochran, E.J., Mufson, E.J., Penn, R., Goetz, C.G. & Comella, C.D., 1999. Clinicopathological findings following intraventricular glial-derived neurotrophic factor treatment in a patient with Parkinson's disease. Ann. Neurol, 46, 419-424.

Kordower, J.H., Herzog, C.D., Dass, B., Bakay, R.A., Stansell, J.,3rd, Gasmi, M. & Bartus, R.T., 2006. Delivery of neurturin by AAV2 (CERE-120)-mediated gene transfer provides structural and functional neuroprotection and neurorestoration in MPTP-treated monkeys. Ann Neurol, 60 (6), 706-715.

Kreuter, J., 2014. Drug delivery to the central nervous system by polymeric nanoparticles: What do we know?. Adv Drug Deliv Rev, 71, 2-14.

Kuo, A. & Smith, M.T., 2014. Theoretical and practical applications of the intracerebroventricular route for CSF sampling and drug administration in CNS drug discovery research: A mini review. J Neurosci Methods, 233, 166-171.

Kurakhmaeva, KB., Voronina, TA., Kapica, IG., Kreuter, J., Nerobkova, LN., Seredenin, SB., Balabanian, VY., Alyautdin, RN., 2008. Antiparkinsonian effect of nerve growth factor adsorbed on polybutylcyanoacrylate nanoparticles coated with polysorbate-80. Bull Exp Biol Med, 145 (2), 259-262.

Kurakhmaeva, K.B., Djindjikhashvili, I.A., Petrov, V.E., Balabanyan, V.U., Voronina, T.A., Trofimov, S.S., Kreuter, J., Gelperina, S., Begley, D. & Alyautdin, R.N., 2009. Brain targeting of nerve growth factor using poly(butyl cyanoacrylate) nanoparticles. J Drug Target, 17 (8), 564-574.

Lacomblez, L., Bensimon, G., Leigh, PN., Guillet, P., Meininger, V., 1996. Dose-ranging study of riluzole in amyotrophic lateral sclerosis. Amyotrophic Lateral Sclerosis/Riluzole Study Group II. Lancet, 347 (9013), 1425-1431.

Lang, A.E., Gill, S., Patel, N.K., Lozano, A., Nutt, J.G., Penn, R., Brooks, D.J., Hotton, G., Moro, E., Heywood, P., Brodsky, M.A., Burchiel, K., Kelly, P., Dalvi, A., Scott, B., Stacy, M., Turner, D., Wooten, V.G., Elias, W.J., Laws, E.R., Dhawan, V., Stoessl, A.J., Matcham, J., Coffey, R.J. & Traub, M., 2006. Randomized controlled trial of intraputamenal glial cell line-derived neurotrophic factor infusion in Parkinson disease. Ann. Neurol, 59, 459-466.

Lapchak, P.A., Gash, D.M., Jiao, S., Miller, P.J. & Hilt, D., 1997. Glial Cell Line-Derived Neurotrophic Factor: A Novel Therapeutic Approach to Treat Motor Dysfunction in Parkinson's Disease. Exp Neurol, 144 (1), 29-34.

Larsen, K.E., Benn, S.C., Ay, I., Chian, R.J., Celia, S.A., Remington, M.P., Bejarano, M., Liu, M., Ross, J., Carmillo, P., Sah, D., Phillips, K.A., Sulzer, D., Pepinsky, R.B., Fishman, P.S., Brown, R.H., Jr & Francis, J.W., 2006. A glial cell line-derived neurotrophic factor (GDNF):tetanus toxin fragment C protein conjugate improves delivery of GDNF to spinal cord motor neurons in mice. Brain Res, 1120 (1), 1-12.

Levy, YS., Gilgun-Sherki, Y., Melamed, E., Offen, D., 2005. Therapeutic potential of neurotrophic factors in neurodegenerative diseases. BioDrugs, 19 (2), 97-127.

Linazasoro, G., 2009. A global view of Parkinson's disease pathogenesis: Implications for natural history and neuroprotection. Parkinsonism Relat Disord, 15 (6), 401-405.

Liu, X., Fawcett, J.R., Thorne, R.G., DeFor, T.A. & Frey II, W.H., 2001. Intranasal administration of insulin-like growth factor-I bypasses the blood–brain barrier and protects against focal cerebral ischemic damage. J Neurol Sci, 187 (1–2), 91-97.

Lochhead, J.J. & Thorne, R.G., 2012. Intranasal delivery of biologics to the central nervous system. Adv Drug Deliv Rev, 64 (7), 614-628.

Lu, Y.Y., Wang, L.J., Muramatsu, S., Ikeguchi, K., Fujimoto, K., Okada, T., Mizukami, H., Matsushita, T., Hanazono, Y., Kume, A., Nagatsu, T., Ozawa, K. & Nakano, I., 2003. Intramuscular injection of AAV-GDNF results in sustained expression of transgenic GDNF, and its delivery to spinal motoneurons by retrograde transport. Neurosci Res, 45 (1), 33-40.

Mahapatro, A. & Singh, D.K., 2011. Biodegradable nanoparticles are excellent vehicle for site directed in-vivo delivery of drugs and vaccines. J Nanobiotechnology, 9, 55-3155-9-55.

Marks Jr, W.J., Bartus, R.T., Siffert, J., Davis, C.S., Lozano, A., Boulis, N., Vitek, J., Stacy, M., Turner, D., Verhagen, L., Bakay, R., Watts, R., Guthrie, B., Jankovic, J., Simpson, R., Tagliati, M., Alterman, R., Stern, M., Baltuch, G., Starr, P.A., Larson, P.S., Ostrem, J.L., Nutt, J., Kieburtz, K., Kordower, J.H. & Olanow, C.W., 2010. Gene delivery of AAV2-neurturin for Parkinson's disease: a double-blind, randomised, controlled trial. Lancet Neurol, 9 (12), 1164-1172.

Marks Jr, W.J., Ostrem, J.L., Verhagen, L., Starr, P.A., Larson, P.S., Bakay, R.A., Taylor, R., Cahn-Weiner, D.A., Stoessl, A.J., Olanow, C.W. & Bartus, R.T., 2008. Safety and tolerability of intraputaminal delivery of CERE-120 (adeno-associated virus serotype 2–neurturin) to patients with idiopathic Parkinson's disease: an open-label, phase I trial. Lancet Neurol, 7 (5), 400-408.

Mathias, N.R. & Hussain, M.A., 2010. Non-invasive systemic drug delivery: developability considerations for alternate routes of administration. J Pharm Sci, 99 (1), 1-20.

McBride, J.L., During, M.J., Wuu, J., Chen, E., Leurgans, S.E. & Kordower, J.H., 2003. Structural and functional neuroprotection in a rat model of Huntington’s disease by viral gene transfer of GDNF. Exp Neurol, 181 (2), 213-223.

McBride, JL., Ramaswamy, S., Gasmi, M., Bartus, RT., Herzog, CD., Brandon, EP., Zhou, L., Pitzer, MR., Berry-Kravis, EM., Kordower, JH., 2006. Viral delivery of glial cell line-derived neurotrophic factor improves behavior and protects striatal neurons in a mouse model of Huntington’s disease. PNAS, 103, 9345-9350.

Mittal, D., Ali, A., Md, S., Baboota, S., Sahni, J.K. & Ali, J., 2014. Insights into direct nose to brain delivery: current status and future perspective. Drug Deliv, 21 (2), 75-86.

Mittoux, V., Ouary, S., Monville, C., Lisovoski, F., Poyot, T., Conde, F., Escartin, C., Robichon, R., Brouillet, E., Peschanski, M., Hantraye, P., 2002. Corticostriatopallidal Neuroprotection by Adenovirus-Mediated Ciliary Neurotrophic Factor Gene Transfer in a Rat Model of Progressive Striatal Degeneration. J Neurosci, 22 (11), 4478-86.

Mochly-Rosen, D., Disatnik, M.H. & Qi, X., 2014. The challenge in translating basic research discoveries to treatment of Huntington disease. Rare Dis, 2, e28637.

Moreno-Igoa, M., Calvo, AC., Ciriza, J., Muñoz, MJ., Zaragoza, P., Osta, R., 2012. Non-viral gene delivery of the GDNF, either alone or fused to the C-fragment of tetanus toxin protein, prolongs survival in a mouse ALS model. Restor Neurol Neurosci, 30 (1), 69-80.

Muller, R.H., Radtke, M. & Wissing, S.A., 2002. Nanostructured lipid matrices for improved microencapsulation of drugs. Internat J Pharm, 242 (1-2), 121-128.

Murlidharan, G., Samulski, R.J. & Asokan, A., 2014. Biology of adeno-associated viral vectors in the central nervous system. Front Mol Neurosci, 7, 76.

Nutt, J.G., Burchiel, K.J., Comella, C.L., Jankovic, J., Lang, A.E., Laws, E.R.,Jr, Lozano, A.M., Penn, R.D., Simpson, R.K.,Jr, Stacy, M. & Wooten, G.F., 2003. Implanted intracerebroventricular. Glial cell line-derived neurotrophic factor Randomized, double-blind trial of glial cell line-derived neurotrophic factor (GDNF) in PD. Neurology, 60, 69-73.

O'Mahony, A.M., Godinho, B.M., Cryan, J.F. & O'Driscoll, C.M., 2013. Non-viral nanosystems for gene and small interfering RNA delivery to the central nervous system: formulating the solution. J Pharm Sci, 102 (10), 3469-3484.

Pardridge, W.M., 2005. The blood-brain barrier: bottleneck in brain drug development. NeuroRx, 2 (1), 3-14.

Poon, VY., Choi, S., Park, M., 2013. Growth factors in synaptic function. Front Synaptic Neurosci, 5.

Popovic, N., Maingay, M., Kirik, D. & Brundin, P. 2005. Lentiviral gene delivery of GDNF into the striatum of R6/2 Huntington mice fails to attenuate behavioral and neuropathological changes. Exp Neurol, 193 (1), 65-74.

Ramaswamy, S., McBride, J.L., Han, I., Berry-Kravis, E.M., Zhou, L., Herzog, C.D., Gasmi, M., Bartus, R.T. & Kordower, J.H., 2009. Intrastriatal CERE-120 (AAV-

Neurturin) protects striatal and cortical neurons and delays motor deficits in a transgenic mouse model of Huntington's disease. Neurobiol Dis, 34 (1), 40-50.

Ramos-Cabrer, P. & Campos, F., 2013. Liposomes and nanotechnology in drug development: focus on neurological targets. Int J Nanomedicine, 8, 951-960.

Rosen, DR., Siddique, T., Patterson, D., Figlewicz, DA., Sapp, P., Hentati, A., Donaldson, D., Goto, J., O'Regan, JP., Deng, HX., et al 1993. Mutations in Cu/Zn superoxide dismutase gene are associated with familial amyotrophic lateral sclerosis. Nature, 362 (6415), 59-62.

Rowland LP, S.N., 2001. Amyotrophic lateral sclerosis. N Engl J Med, 344 (22), 1688-1700.

Schlachetzki, F., Zhang, Y., Boado, R.J. & Pardridge, W.M., 2004. Gene therapy of the brain: the trans-vascular approach. Neurology, 62 (8), 1275-1281.

Sendtner, M., Carroll, P., Holtmann, B., Hughes, RA., Thoenen, H., 1994. Ciliary neurotrophic factor. J Neurobiol, 25 (11), 1436-1453.

Slevin, J.T., Gash, D.M., Smith, C.D., Gerhardt, G.A., Kryscio, R., Chebrolu, H., Walton, A., Wagner, R. & Young, A.B., 2006. Unilateral intraputaminal glial cell line-derived neurotrophic factor in patients with Parkinson disease: response to 1 year each of treatment and withdrawal. Neurosurg. Focus, 20 (5).

Sofroniew, M.V., Howe, C.L. & Mobley, W.C., 2001. Nerve growth factor signaling, neuroprotection, and neural repair. Annu Rev Neurosci, 24, 1217-1281.

Stockwell, J., Abdi, N., Lu, X., Maheshwari, O. & Taghibiglou, C., 2014. Novel central nervous system drug delivery systems. Chem Biol Drug Des, 83 (5), 507-520.

Stoessl, AJ., 2014. Gene therapy for Parkinson's disease: a step closer?. Lancet, 383, 1107-1109.

Storkebaum, E., Lambrechts, D. & Carmeliet, P., 2004 VEGF: once regarded as a specific angiogenic factor, now implicated in neuroprotection. Bioessays, 26 (9), 943-954.

Tan, J., Wang, Y., Yip, X., Glynn, F., Shepherd, RK., Caruso, F., 2012. Nanoporous peptide particles for encapsulating and releasing neurotrophic factors in an animal model of neurodegeneration. Adv Mater, 24, 3362-3366.

Ventriglia, M., Zanardini, R., Bonomini, C., Zanetti, O., Volpe, D., Pasqualetti, P., Gennarelli, M. & Bocchio-Chiavetto, L., 2013. Serum brain-derived neurotrophic factor levels in different neurological diseases. Biomed. Res. Int., 2013, 1-7.

Wang, LJ., Lu, YY., Muramatsu, S., Ikeguchi, K., Fujimoto, K., Okada, T., Mizukami, H., Matsushita, T., Hanazono, Y., Kume, A., Nagatsu, T., Ozawa, K., Nakano, I., 2002. Neuroprotective Effects of Glial Cell Line-Derived Neurotrophic Factor Mediated by an Adeno-Associated Virus Vector in a Transgenic Animal Model of Amyotrophic Lateral Sclerosis. J. Neurosci., 22(16), 6920–6928.

Wohlfart, S., Gelperina, S. & Kreuter, J., 2012. Transport of drugs across the blood–brain barrier by nanoparticles. J Control Release, 161 (2), 264-273.

Wong, H.L., Wu, X.Y. & Bendayan, R., 2012. Nanotechnological advances for the delivery of CNS therapeutics. Adv Drug Deliv Rev, 64 (7), 686-700.

Xie, Y., Ye, L., Zhang, X., Cui, W., Lou, J., Nagai, T. & Hou, X., 2005. Transport of nerve growth factor encapsulated into liposomes across the blood–brain barrier: In vitro and in vivo studies. J Control Release, 105, (1–2), 106-119.

Yi, X., Manickam, D.S., Brynskikh, A. & Kabanov, A.V., 2014. Agile delivery of protein therapeutics to CNS. J Control Release, 190, 637-663.

Yusuf, M., Khan, M., Khan, RA., Ahmed, B., 2012. Preparation, characterization, in vivo and biochemical evaluation of brain targeted Piperine solid lipid nanoparticles in an experimentally induced Alzheimer's disease model. J Drug Target., 21 (3), 300-311.

Zavalishin, IA., Bochkov, NP., Suslina, ZA., Zakharova, MN., Tarantul, VZ., Naroditskiy, BS., Suponeva, NA., Illarioshkin, SN., Shmarov, MM., Logunov, DY., Tutyhina, IL., Verkhovskaya, LV., Sedova, ES., Vasiliev, AV., Brylev, LV., Ginzburg, AL., 2008. Gene therapy of amyotrophic lateral sclerosis. Bull Exp Biol Med, 145 (4), 483-6.

Zhang, C., Chen, J., Feng, C., Shao, X., Liu, Q., Zhang, Q., Pang, Z. & Jiang, X., 2014. Intranasal nanoparticles of basic fibroblast growth factor for brain delivery to treat Alzheimer's disease. Int J Pharm, 461 (1-2), 192-202.

Zhao, Y.Z., Li, X., Lu, C.T., Lin, M., Chen, L.J., Xiang, Q., Zhang, M., Jin, R.R., Jiang, X., Shen, X.T., Li, X.K. & Cai, J., 2014. Gelatin nanostructured lipid carriers-mediated intranasal delivery of basic fibroblast growth factor enhances functional recovery in hemiparkinsonian rats. Nanomedicine, 10 (4), 755-764.

Zielonka, D., Piotrowska, I., Marcinkowski, J.T. & Mielcarek, M., 2014. Skeletal muscle pathology in Huntington's disease. Front Physiol, 5, 380.

Objectives

In recent years, the prevalence of people living with neurodegenerative diseases (NDs) has dramatically increased, but to date, there is no cure for this kind of disorders. The current therapies are focused on modifying the disease progression and symptoms, with insufficient or null effect on the improvement of the disease. In this line, selective growth factors (GFs) have become an interesting therapy since they are able to provide neuroprotective, neurorestorative and stimulating effects on diseased neurons. However, these factors present some shortcomings that limit their use in clinical application, mainly due to their poor capacity to cross the blood-brain barrier (BBB), and thus to access the brain, as well as their short circulation half-life and rapid degradation rate after being administered *in vivo*. Therefore, significant attempts have already been made to design different and promising drug delivery systems (DDS) to protect neurotrophins and release them into the brain in a control manner. In addition, in the past few years intranasal drug delivery has appeared as an alternative non-invasive administration route to bypass the BBB and target drugs directly to the central nervous system (CNS).

Therefore, the main objective of this Doctoral Thesis is the development of lipid nanoparticles (NPs) as vehicles for nose-to-brain delivery of neurotrophic factors for the treatment of NDs.

Concretely, the objectives of the present study are the following:

1. Design, optimization and characterization of chitosan (CS) coated nanostructured lipid carriers (NLCs) to promote the delivery of neurotrophic factors to the brain after intranasal administration.

2. Biodistribution study of CS-NLC after intranasal administration to nude mice to explore the possibility of brain targeting by nose-to-brain delivery using fluorescence imaging (FLI) monitoring.

3. To study the *in vivo* neuroprotective effect of intranasally administered GDNF, encapsulated in CS-coated NLC (CS-NLC-GDNF), in a 6-OHDA partially lesioned rat model of Parkinson Disease.

4. To develop, characterize and validate an *in vitro* olfactory cell monolayer and to study the NPs transport across this monolayer in order to estimate their access into the brain.

Experimental design

Chapter 1

Chitosan coated nanostructured lipid carriers for brain delivery of proteins by intranasal administration

Colloids and Surfaces B: Biointerfaces 134, 304–313(2015)

Chitosan coated nanostructured lipid carriers for brain delivery of proteins by intranasal administration

Oihane Gartziandia[a,b,1], Enara Herrán[a,b,1], Jose Luis Pedraz[a,b], Eva Carro[c,d], Manoli Igartua[a,b], Rosa Maria Hernandez[a,b,*]

[a]NanoBioCel Group, Laboratory of Pharmaceutics, School of Pharmacy, University of the Basque Country (UPV/EHU), Vitoria-Gasteiz 01006, Spain.
[b]Biomedical Research Networking Center in Bioengineering, Biomaterials and Nanomedicine (CIBER-BBN), Vitoria-Gasteiz 01006, Spain.
[c]Neuroscience Laboratory, Research Institute Hospital 12 de Octubre, Madrid, Spain,
[d]Neurodegenerative Diseases Biomedical Research Centre (CIBERNED), Madrid, Spain.

ABSTRACT

The remarkable increase in the prevalence of neurodegenerative diseases has become a serious public health problem. Considering the lack of effective treatments to address these diseases and the difficulties in accessing the brain due to the blood-brain barrier (BBB), to attain a successful strategy to improve drug delivery to the brain, the administration route becomes a point of interest. The intranasal route provides a non-invasive method to bypass the BBB. Moreover, the development of new technologies for the protection and delivery of peptides is an interesting approach to consider. Thus, in this work, a suitable chitosan coated nanostructured lipid carrier (CS-NLC) formulation with the capacity to reach the brain after being intranasally administered was successfully developed and optimized. The optimal formulation displayed a particle size of 114 nm with a positive surface charge of + 28 mV. The *in vitro* assays demonstrated the biocompatibility of the nanocarrier and its cellular uptake by 16HBE14o- cells. Furthermore, no haemagglutination or haemolysis processes were observed when the particles were incubated with erythrocytes, and no toxicity signals appeared in the nasal mucosa of mice after the administration of CS-NLCs. Finally, the biodistribution study of CS-NLC-DiR demonstrated an efficient brain delivery of the particles after intranasal administration. In conclusion, CS-NLC can be considered to be a safe and effective nanocarrier for nose-to-brain drug delivery; however, to obtain a higher concentration of the drug in the brain following intranasal administration, further modifications are warranted in the CS-NLC formulation.

*Corresponding author: R.M. Hernández
[1]These two authors contributed equally to the work

Keywords: Blood-brain barrier (BBB), Intranasal administration, Nanostructured lipid carrier (NLC), Neurodegenerative disorders (ND), Biodistribution

1. Introduction

In the last decade, there has been a remarkable increase in the prevalence of neurodegenerative diseases (NDs), which have become a serious public health problem. Currently, there is no cure for most NDs, and current therapies are focused on modifying the disease progression and symptoms, presenting insufficient or null effects on the improvement of the disease [1]. A notable obstacle to identifying an adequate therapy is the presence of the blood-brain barrier (BBB), which limits the effective delivery and distribution of therapeutic agents to the central nervous system (CNS) [2]. This limitation is observed due to the function of the BBB in maintaining CNS homeostasis and preventing the free diffusion and penetration of most drugs and other foreign components from the bloodstream to the brain [3].

Considering these factors, the scientific community is making enormous efforts in the development of new successful treatment options to improve drug delivery to the brain by means of invasive or non-invasive ways. Through intracerebroventricular and intraparenchymal administration routes, drugs are administered directly into the brain, thereby avoiding the BBB. Therefore, high drug concentrations can access the target site. However, both methods are invasive techniques in which the drug diffusion from the injection site is not easy [4]. Intraperitoneal, intravenous or subcutaneous routes are much simpler techniques that are used as a less invasive alternative. Nevertheless, after parenteral administration, most of the drugs present serious difficulties in crossing the BBB, and hence, to obtain therapeutics levels in the brain, the administration of high doses is required, which may result in adverse systemic effects [5,6]. Lastly, recent research describes several studies that propose intranasal (i.n.) administration route as a non-invasive way to transport drugs directly to the CNS through the olfactory and trigeminal nerve pathways; thus, it presents the capacity to bypass the BBB [7]. Furthermore, clinical trials in humans have demonstrated that intranasal administration offers a successful

alternative to deliver drugs to the brain. In this regard, *Reger et al.* confirmed that intranasally administered insulin improves verbal memory in Alzheimer disease patients without systemic side effects [8].

Currently, there have been enormous efforts to identify new treatments to address CNS disorders. Accordingly, neurotrophic factors have become an interesting therapy due to their ability to provide neuroprotective, neurorestorative and stimulating effects on diseased neurons. However, it is interesting to mention that after their *in vivo* application, these peptides present important shortcomings, such as a short circulation half-life, a rapid degradation rate, or a poor ability to cross the BBB due to their unsuitable molecular weight, lipophilicity or surface charge [9]. Hence, new technologies for brain drug delivery have been investigated in the last few years to provide new strategies to overcome the mentioned limitations [2]. In this sense, nanometric drug delivery systems could be considered possible tools to protect drugs against degradation in the nasal cavity as well as to stimulate nose to brain drug delivery [10]. Among these substances, nanostructured lipid carriers (NLCs), which are the improved second-generation derived from solid lipid nanoparticles, represent an attractive system for this purpose. NLCs are usually composed of biodegradable and biocompatible lipid components primarily obtained from natural sources. NLCs also offer high drug entrapment efficiencies and high stability, and they have a well-established safety profile and toxicological data [11-13]. However, NLCs' major drawbacks after i.n. administration are a low residence time in the nasal cavity and incomplete drug absorption due to mucociliary clearance [14]. With the aim of solving these challenges, lipid formulations enable the possibility of surface charge modification with various cationic substances, such as chitosan (CS), with interesting characteristics. Several studies have demonstrated the excellent mucoadhesive properties of this cationic polysaccharide, enhancing the penetration across epithelial mucus and prolonging the retention time in the nasal cavity [15-17].

Accordingly, the aim of our study was to design and optimize a CS-NLC formulation to obtain mucoadhesive and positively charged nanoparticles with a particle size of approximately 100 nm for promoting the delivery of drugs to the brain after intranasal administration. *In vitro* tests were undertaken in 16HBE14o- cells to determine the cytotoxicity and cell uptake capability of our formulation. The interaction of CS-NLC with erythrocytes was analysed by haemolysis and haemaglutination assays. Additionally, the nasal toxicity of the nanoparticles was also evaluated *in vivo* in C57 mice. Finally, CS-NLCs were loaded with the near infrared dye, DiR, and administered intranasally to nude mice to explore the possibility of brain targeting by nose-to-brain delivery using fluorescence imaging (FLI) monitoring.

2. Materials and Methods

2.1. Materials

Precirol ATO®5 (Glycerol distearate), Dynasan 114® (Trimyristin) and Miglyol® (Caprylic/Capric Triglyceride) were donated by Gattefosé (France), Oxi-Med Expres S.A (Spain) and Sasol Germany GmbH, respectively. Tween 80, Lutrol® F-68 (Poloxamer 188), sodium citrate and 3.7% paraformaldehyde were purchased from Panreac (Spain). Protasan UP CL 113 Chitosan was obtained from NovaMatrix (Norway). Trehalose dihydrate, NileRed, Cell Counting Kit-8 (CCK-8), Bovine serum albumin, Vitrogen 100, Human fibronectin, Hepes, Glucose, $Na_2HPO_4.7H_2O$, Phenol Red, Polyvinilpyrrolidone, EGTA, EDTA and citric acid were bought from Sigma-Aldrich (Spain). DiR DiIC18 (7) (1,1'-Dioctadecyl-3,3,3',3'-Tetramethylindotricarbocyanine Iodide) was purchased from Molecular Probes© by Life Technologies (Spain). hIGF-I was obtained from Peprotech (UK). The 16HBE14o- cell line was bought from the Dr. Gruenert Laboratory (University of California, San Francisco). MEM, LHC basal medium, foetal bovine serum, L-Glutamine, Penicillin/Streptomycin and PBS pH 7,4 (1X) were purchased from Gibco© by Life Technologies (Spain). Sodium chloride was obtained from Labkem (Spain), K_2HPO_4, KH_2PO_4 and KCl were obtained from Scharlau (Spain) and 4',6-diamidino-2-phenylindole

(DAPI) was bought from SouthernBiotech (USA).

2.2. NLC preparation and optimization

Precirol ATO5 (melting point: 56ºC) or Dynasan 114 (melting point: 56ºC) and Miglyol (liquid at room temperature (RT)) were chosen to form lipid matrix. The lipid phase was melted 5ºC above its melting point until a clear and homogeneous phase was obtained. The aqueous solution was composed of various percentages of Tween 80 and Poloxamer 188 to obtain a final volume of 4 ml, and the solution was warmed in a water bath. The hot surfactant phase was then added to the melted oily phase and was sonicated for 60 seconds at 50 W (Branson® sonifier 250). The nanoemulsion was maintained under magnetic stirring during 15 min at RT and stored at 4 ºC for 12 h overnight to allow the re-crystallisation of the lipid for NLC-formation. On the following day, the nanoparticle dispersion was centrifuged in an Amicon filter (Amicon, "Ultracel-100k") at 2,500 rpm (MIXTASEL, P Selecta) for 15 min, the nanoparticles were washed three times with milli Q water and were finally lyophilized during 42 h (LyoBeta 15, Telstar, Spain). Prior to the lyophilization of the resultant NLC dispersion, a solution of a cryoprotectant (trehalose (15% w/w)) was added to the collected nanoparticles.

Chitosan coated NLCs were prepared as described above but followed by a chitosan coating process. The nanoparticle dispersion was added dropwise to an equal volume (4 ml) of a chitosan solution (0.5%, w/v) kept under continuous agitation at RT, and the suspension was maintained under these conditions for 20 min to allow the coating of the nanoparticles. After this step, the CS-NLC dispersion was centrifuged and lyophilized as previously mentioned. To optimize the formulation, various lipid and surfactant percentages, described in Table 1, were tested.

Table 1. Composition of the various nanoparticles developed using Precirol ATO5 (NLC-P) or Dynasan 114 (NLC-D) as solid lipids. Table shows the percentages of lipids, hIGF-I, Tween 80 (T80) and Poloxomer 188.

Formulation	% Lipid (w/v)	% hIGF-I (w/w)	% T80 (w/v)	% Poloxamer 188 (w/v)
NLC-P1	6.66	x	1.3	0.67
NLC-P2	6.66	x	3	2
NLC-P3	2.5	x	1.3	0.67
NLC-P4	2.5	x	3	2
NLC-P5	2.5	0.5	3	2
CS-NLC-P5	2.5	0.5	3	2
NLC-D1	6.66	x	3	2
NLC-D2	2.5	x	1.3	0.67
NLC-D3	2.5	x	3	2
NLC-D4	2.5	0.5	3	2
NLC-D5	1	x	1	1
NLC-D6	1	x	2	1
NLC-D7	1	x	2	2
NLC-D8	1	x	3	1
NLC-D9	1	0.5	2	1
CS-NLC-D9	1	0.5	2	1

Finally, the neurotrophic factor human insulin-like growth factor-I (hIGF-I) was loaded in the CS-NLCs at a concentration of 0.5% (w/w) to assess the suitability of the nanoparticles to encapsulate a therapeutic candidate for ND applications. Additionally, the lipophilic dye NileRed and the near infrared dye DiR were incorporated into the NLC (CS-NLC-NileRed and CS-NLC-DiR), both at a concentration of 0.5% (w/w), for cellular uptake assays and to determine the biodistribution profile. These formulations were elaborated as described above but included the corresponding neurotrophic factor or dye, depending on the formulation, in the lipid phase prior to the sonication process.

2.2.1. Nanoparticle characterization: size, zeta potential, morphology and encapsulation efficiency (EE%)

The mean diameter (Z-average diameter) and size distribution were measured by Dynamic Light Scattering, and the zeta potential was determined through Laser

Doppler Micro-Electrophoresis (Malvern® Zetasizer Nano ZS, Model Zen 3600; Malvern Instruments Ltd). Three replicate analyses were performed for each formulation, and the data are presented as the mean ± S.D. Nanoparticle surface characteristics and morphology were examined by Transmission Electron Microscopy (TEM, Philips CM120 BioTwin, 120kV).

The EE% of hIGF-I-loaded CS-NLCs was determined indirectly by measuring the free hIGF-I (non-encapsulated hIGF-I) in the supernatant obtained after the filtration/centrifugation process described in the previous section and was quantified by a specific hIGF-I ELISA development Kit (Enzo® LifeScience, USA).

2.3. In vitro dye release of Nile Red and DiR from CS-NLCs

With the objective to determine whether the dye (Nile Red or DiR) would be released from the nanoparticles after being administered to the mice, 15 mg of nanoparticles were incubated for 4 and 24 h, for Nile Red and DiR, respectively, in 1 ml of PBS (pH 7.4). Then, the nanoparticle suspension underwent centrifugal filtration (Amicon Ultra-15, Millipore©) and was centrifuged at 2,500 rpm for 15 min at 4^0C (P Selecta Mixtasel). The absorbance of the filtrates was measured with a calibration curve ranging from 5-100 µg dye/ml PBS.

2.4. Cell viability and uptake in human bronchial epithelial cell line (16HBE14o-) after CS-NLC treatment

The 16HBE14o- cell line was maintained in MEM cell culture medium containing L-glutamine, 10% foetal bovine serum, 10,000 µg/ml Streptomycin and 10,000 units/ml penicillin "G" at standardized conditions (95% relative humidity, 5% CO_2, 37ºC). Before cultivation of the cells, the flasks were coated with fibronectin coating solution (FCS) to favour cell attachment.

To evaluate the cytotoxicity of CS-NLCs, 16HBE14o- cells were seeded into 96-well plates previously coated with FCS, at a density of 5 x 10^3 cells/well and were incubated for 24 h to allow the cell attachment. Defined concentrations of CS-NLCs (0.01-0.1 mg/ml) were added to the cell cultures and were incubated for 24, 48 and 72 h at 37ºC. The cell viability

was measured using Cell Counting Kit-8, in which the absorbance was directly proportional to the number of living cells in the culture.

Fluorescent microscopy was used to perform the qualitative analysis of cellular uptake of CS-NLC labelled with NileRed (CS-NLC-NileRed) in 16HBE14o- cells. In brief, a 24-well plate with coverslips was coated with FCS, and 5 x 10^4 cells were seeded on this plate and kept in complete culture medium for 24 h. On the next day, 25 µg of CS-NLC-NileRed was administered to the cells, which were incubated for 4 h at 37ºC. Afterwards, the cells were washed twice with cold uptake buffer (0.14 M NaCl, 2 mM K_2HPO_4 and 0.4 mM KH_2PO_4), once with cold acid buffer (0.26 M citric acid•H_2O, 80 mM sodium citrate and 85 mM KCl), and finally fixed with 4% paraformaldehyde. Nuclei were then stained with 4',6-diamidino-2-phenylindole (DAPI) (500 ng/ml), and the coverslips were mounted on the slides for examination under a fluorescent microscope (Carl Zeiss Axio Observer) equipped with a structured illumination module (ApoTome) at a magnification of 40×. Images of the successive planes of the z-axis were obtained and studied.

2.5. Interaction with erythrocytes: haemolysis and haemaglutination assays

Haemolysis and haemaglutination assays were conducted following protocols previously described [18]. In both cases, fresh human blood was centrifuged at 4,000 rpm for 5 min, and plasma was discarded. The erythrocytes were washed and centrifuged three times with PBS, and the final erythrocyte fraction was diluted in PBS to a concentration of 5% (v/v) for the haemolysis assay and 2% (v/v) for the haemaglutination assay.

In the haemolysis study, CS-NLCs were added at various concentrations (5 mg/ml, 4 mg/ml, 3 mg/ml, 2 mg/ml, 1.5 mg/ml, 1 mg/ml, 0.5 mg/ml and 0.25 mg/ml) to the erythrocyte suspension and incubated for 1 h at RT. The suspension was centrifuged at 4,000 rpm for 5 min, and the supernatants were collected to determine the haemolysis by measuring haemoglobin released at 545 nm in a microplate reader (Infinite M200-Tecan). A lysis buffer was utilized as a positive control (100% haemolysis sample).

In the haemaglutination study, CS-NLCs were added at various concentrations (5 mg/ml, 4 mg/ml, 3 mg/ml, 2 mg/ml, 1.5 mg/ml, 1 mg/ml, 0.5 mg/ml and 0.1 mg/ml) to the erythrocyte suspension and incubated for 15 min at RT. One drop of each of the samples was placed in a microscope slide and was observed under light microscopy (Nikon ECLIPSE TE2000-S) to determine haemaglutination.

2.6. In vivo nasal toxicity evaluation

The nasal toxicity evaluation was conducted in C57 mice after administering CS-NLCs for 15 consecutive days. Three mice per group received 3 mg of CS-NLCs (re-suspended in 20 µl of PBS) or PBS alone for 15 consecutive days by intranasal instillation (10 µl each nostril). At the end of the treatment and 24 h after the last administration, the mice were sacrificed and the nasal mucosa was harvested, fixed (with 4% paraformaldehyde) and embedded in paraffin. Paraffin sections were cut, stained with haematoxylin/eosin and observed under a light microscope (Nikon ECLIPSE TE2000-S) to determine toxicity indicators, such as fibrosis, inflammation and atypical signs.

2.7. Brain-accumulation and whole body biodistribution of CS-NLC

Fifteen athymic nude female mice were used (22 g, Harlan Interfauna Iberica, Spain) to evaluate CS-NLCs brain targeting effect and whole-body biodistribution. DiR-labelled CS-NLCs were administered intranasally to anesthetized mice with inhalatory isoflurane using a nose cone mask. The animals were randomized into two groups: control group (i.n. PBS, 3 mice (1 mouse per end point)) and treated group (i.n. CS-NLC-DiR, 12 mice (4 mice per end point)). The formulation was administered as a single dose of 0.5 mg DiR/kg mouse body weight (135 mg CS-NLC-DiR/kg) with an administration volume of 0.8 ml/kg. A total of 8 administrations (4 per orifice) were given alternating nasal nostrils (2.5 µl/each) and waiting 3 min between each administration.

In vivo brain-accumulation and whole-body biodistribution were measured non-invasively by DiR fluorescence imaging

(FLI) monitoring from the ventral and dorsal mouse views, 0.5, 4.5, 6.5 and 23.5 h post-administration. Additionally, at 1, 7 and 24 h post-administration time points, whole brain, lung, heart, liver, spleen, kidney and skin samples were collected, and compound tissue accumulations were determined by *ex vivo* DiR FLI monitoring. Each brain was sectioned into cerebrum, cerebellum and hippocampus and *ex vivo* DiR FLI monitoring was performed. After this study, all tissues were discarded.

In vitro, in vivo and *ex vivo* FLI studies were performed with an IVIS® Spectrum imaging system. Images and measurements of fluorescent signals were acquired and analysed using Living Image® 4.3.1 software (Perkin Elmer). The fluorescent signal was quantified in radiant efficiency units (fluorescence emission radiance per incident excitation power). All the analyses and graphs were performed using GraphPad Prism 5 software.

2.8. Statistical analysis

The statistical analysis was performed using GraphPad Prism 5 software. A one-way ANOVA and a post hoc test were used in multiple comparisons. The normal distribution of samples was assessed by the Shapiro–Wilk test, and the homogeneity of variance was determined by the Levene test. Values were considered to be significant if $p < 0.05$ as the mean ± standard deviation (SD).

3. Results and Discussion

3.1. Optimization and characterization: Particle size, morphology and zeta potential

The aim of this work was to obtain a NLC formulation with an adequate particle size, morphology and zeta potential suitable to achieve an efficient nose-to-brain delivery. To attain this purpose, various concentrations of two commonly used solid lipids (Precirol ATO5 and Dynasan 114) and diverse portions of selected surfactants were tested [19]. These results are presented in Table 2 (Precirol ATO5 as solid lipid) and Table 3 (Dynasan 114 as solid lipid), which show the various particle sizes, polydispersity index (PDI) and zeta potential obtained during the optimization process. As shown in Table 2, the NLCs prepared

with Precirol ATO5 (6.6%, w/v), T80 (1.3%, w/v) and Poloxamer 188 (0.67%, w/v) (NLC-P1) exhibited a particle size of 294.50 ± 22.06 nm, with a PDI of 0.4. As expected, a notable decrease in the particle size was observed when the surfactant percentage in the aqueous phase was increased, obtaining a formulation (NLC-P2) with a particle size of approximately 103.08 ± 9.57 nm and PDI of 0.4. Moreover, when the lipid percentage decreased to 2.5% (w/v) together with the increase in the surfactant fraction (NLC-P4), particle sizes were approximately 72 nm. Additionally, NLC-P4 showed a PDI value lower than 0.4, confirming that the size distribution was more homogeneous than in the previous formulations. The study of the zeta potential revealed that all formulations presented a similar surface charge of approximately -30 mV. Considering the particle sizes and PDI values, NLC-P4 was selected as the most suitable formulation to continue with the next steps of the study.

In regard to the NLCs elaborated with Dynasan 114 solid lipid, the particle size of these formulations was higher than in those prepared with Precirol ATO5 using the same amounts of surfactants and lipid. Moreover, the PDI value of most of these formulations was above 0.4, indicating a non-stable polydisperse system. Attempts were made to obtain a formulation with a smaller particle size, such as the decrease of the lipid percentage to 1%, but the particle size was still above 150 nm, and the PDI was approximately 0.4. Therefore, because the previously described Precirol formulation (NLC-P4) presented a lower particle size and PDI value, the Dynasan prepared formulations were discarded for this application (Table 3).

Table 2. Characterization of the various nanoparticles developed using Precirol ATO5 as the solid lipid. The table shows the particle size (nm), PDI and zeta potential (mV) of the lyophilized nanoparticles. Results are expressed as the mean ± SD (n=3).

NLC-Precirol formulations			
Formulation	Size after lyoph. (nm)	PDI	Zeta potential (mV)
NLC-P1	294.50 ± 22.06	0.412 ± 0.03	(-)30.55 ± 0.49
NLC-P2	103.03 ± 9.57	0.420 ± 0.03	(-)30.28 ± 1.67
NLC-P3	81.51 ± 12.19	0.387 ± 0.11	(-)30.67 ± 0.55
NLC-P4	72.17 ± 8.55	0.364 ± 0.22	(-)28.20 ± 1.32
NLC-P5	107.12 ± 8.95	0.342 ± 0.04	(-)30.30 ± 2.12
CS-NLC-P5	114.48 ± 20.20	0.287 ± 0.05	(+)28.40 ± 2.83

Table 3. Characterization of the various nanoparticles developed using Dynasan 114 as the solid lipid. The table shows the particle size (nm), PDI and zeta potential (mV) of the lyophilized nanoparticles. Results are expressed as the mean ± SD (n=3).

NLC-Dynasan 114 formulations			
Formulation	Size after lyoph. (nm)	PDI	Zeta potential (mV)
NLC-D1	267.40 ± 2.12	0.461 ± 0.02	(-)20.81 ± 2.31
NLC-D2	127.87 ± 35.03	0.461 ± 0.08	(-)21.52 ± 3.45
NLC-D3	136.00 ± 13.57	0.376 ± 0.03	(-)20.30 ± 5.28
NLC-D4	132.65 ± 22.41	0.648 ± 0.05	(-)22.53 ± 3.32
NLC-D5	162.06 ± 20.69	0.382 ± 0.00	(-)21.23 ± 2.86
NLC-D6	129.12 ± 26.90	0.409 ± 0.12	(-)20.51 ± 3.81
NLC-D7	237.00 ± 11.92	0.250 ± 0.05	(-)20.62 ± 3.24
NLC-D8	226.05 ± 54.94	0.421 ± 0.01	(-)22.10 ± 4.52
NLC-D9	159.35 ± 9.47	0.361 ± 0.06	(-)19.12 ± 1.34
CS-NLC-D9	191.89 ± 0.74	0.386 ± 0.12	(+) 41.50 ± 18.88

Previous studies have reported that cationic nanoparticles are expected to be easily attracted to the endothelial cells due to electrostatic interactions between the negatively charged cell membranes and positively charged cationic nanoparticles, which may enhance their cellular absorption and brain delivery [20]. For this reason, with the aim of enhancing the penetration of encapsulated drugs or proteins across the nasal mucosa, the surface of NLCs was modified with chitosan. After our nanoparticle formulation was coated with chitosan, zeta potential values became positive (+ 28 mV), and the particle size increased to approximately 10 nm (CS-NLC-P5), compared with the non-coated particles,

suggesting the correct adsorption of chitosan to the surface of the nanoparticles. In addition to this change in the surface charge of the NLCs, this biopolymer exhibits good biocompatibility, biodegradability and a low toxicity. Furthermore, chitosan presents excellent mucoadhesive properties that prolong the contact of nanoparticles with the nasal epithelium, increasing the retention time in the nasal mucosa and consequently enhancing the drug uptake by the nasal epithelial cells [21, 22].

Therefore, in the next step of this work, the selected nanoparticles were loaded with a model neurotrophic factor (hIGF-I) (NLC-P5) and coated with chitosan to achieve the desired mucoadhesive properties (CS-NLC-P5). Moreover, this formulation showed a high encapsulation efficiency (90.28 ± 0.4%), and thus, it was validated as an adequate delivery system for future applications in NDs. Fig. 1A depicts a TEM micrograph of the nanoparticles, showing a uniform particle size.

3.1.1. In vitro dye release of Nile Red and DiR from CS-NLCs

To confirm that each of the dyes remained encapsulated in the CS-NLCs, the nanoparticles were incubated with PBS (pH 7.4) and were filtered. The absorbance of the filtrates was then measured, showing an absence of detectable signal, thus confirming that neither Nile Red nor DiR were released from the NP after the incubation period. These results clearly suggest that all the fluorescent tracer remained associated with the nanoparticles in the experimental period and indicate that the fluorescence signal detected in the cell cultures or tissue samples was attributed to the labelled nanoparticles and not to the free dye.

3.1.2. Cell viability and uptake in human bronchial epithelial cell line (16HBE14o-) after CS-NLC treatment

Following the intranasal administration of CS-NLCs, the nanoparticles came into contact with nasal epithelial cells, which is the first barrier that CS-NLCs must overcome to reach the brain. To emulate these conditions and evaluate the safety

and uptake capacity of the optimized CS-NLC formulation, the 16HBE14o- cell line was used. Fig. 1B displays cell viability results at 24, 48 and 72 h after CS-NLCs were incubated at increasing concentrations (0.01-0.1 mg/ml) with cells, showing viability results above 70% at all concentrations of CS-NLCs. Because it is assumed that cell viability >70% is considered “no toxicity” [23], these data suggest the biocompatibility of the formulation tested with nasal epithelial cells, maintaining cell viability.

Considering that the NLCs designed in this work are intended to be administered intranasally; thus, they would be in contact with nasal epithelial cells, the CS-NLCs cellular uptake occurred in the same cell line (16HBE14o-). In this study, NLCs labelled with Nile Red were used. The NP showed a mean size of approximately 119 nm (PDI 0.266) and zeta potential of +32.9 mV. Figure 1C illustrates a high uptake of CS-NLC-Nile Red in the 16HBE14o- cell line after 4 h of treatment. As shown, the formulation was homogeneously distributed throughout the cell cytoplasm and membrane without detectable evidence of the particles in the nucleus, as other researchers have previously reported for similar nanoparticles [24].

3.2. Interaction with erythrocytes: haemolysis and haemaglutination assays

Although these nanoparticles are designed for intranasal administration, it is interesting to address haemaglutination and haemolysis tests due to a possible systemic absorption of the particles after their i.n. administration. These assays were performed by incubating various concentrations of CS-NLCs with erythrocytes. Fig. 2A shows the haemaglutination assay results, in which an insignificant agglutination was observed when 5 mg of CS-NLCs/ml were added to the erythrocytes, and no agglutination was detected at lower CS-NLCs concentrations. Therefore, it was not expected to be clinically relevant. Fig. 2B displays the haemolytic activity of erythrocytes after CS-NLCs treatment. In this case, no haemolysis was observed at any concentration tested; thus, no sign of toxicity was detected.

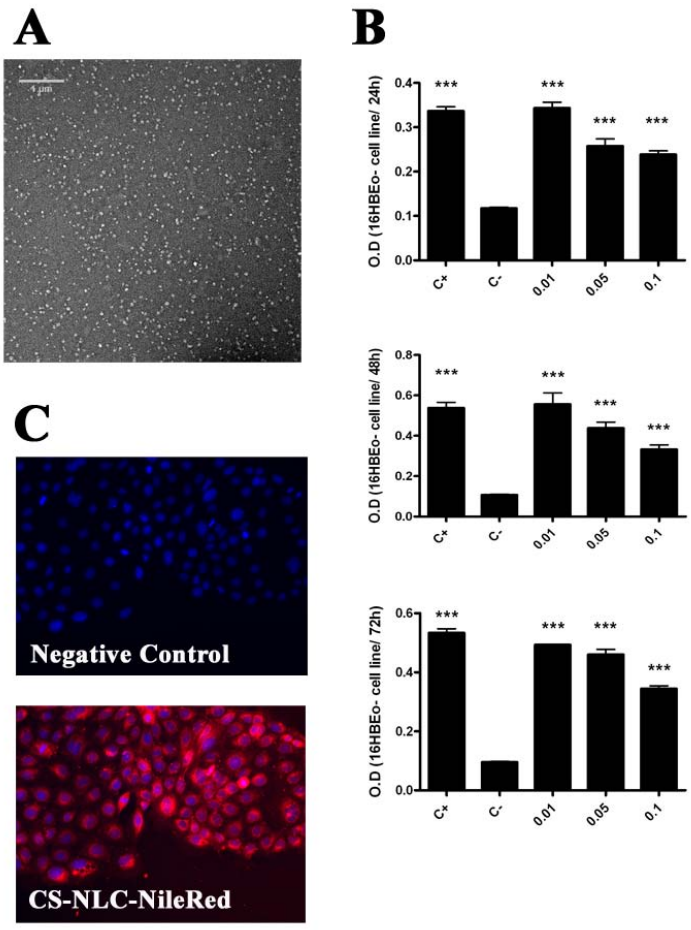

Figure 1. Morphology and *in vitro* studies of CS-NLCs A) TEM photomicrograph of CS-NLCs. **B)** Viability evaluation in 16HBE14o- cell line cultures at 24, 48 and 72 h after CS-NLCs treatment (0.01 = 0.01 CS-NLCs mg/ml; 0.05 = 0.05 CS-NLCs mg/ml; 0.1 = 0.1 CS-NLCs mg/ml; C+ (positive control) = culture medium with PBS; C- (negative control) = culture medium with 10% DMSO). The data are shown as the mean ± SD. ***p< 0.001. **C)** Cellular uptake of CS-NLC-NileRed (25 µg) after incubation with 16HBE14o- cells for 4 h. The image on the top is the negative control, in which cells were not incubated with NileRed loaded nanoparticles. The image below shows the cells incubated with the nanoparticles, NileRed labelled nanoparticles (in red) and cell nuclei stained with DAPI (in blue).

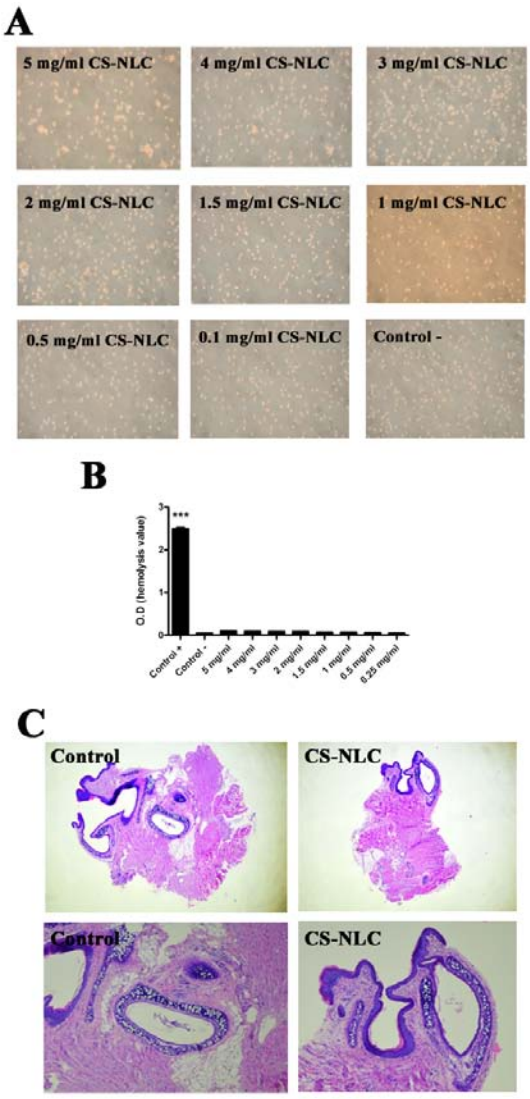

Figure 2. Haemolysis, haemaglutination and nasal toxicity studies A) Agglutination of erythrocytes when blood is untreated and treated with various concentrations of CS-NLCs **B)** Haemolytic activity of erythrocytes after their treatment with various concentrations of CS-NLCs. Lysis buffer represents the positive control haemolysis sample. Error bars represent S.D. ***$p < 0.001$ with respect to the rest of the samples. **C)** Representative photomicrographs of the entire nasal mucosa/cavity biopsies in C57 mice after i.n. administration of PBS or CS-NLCs.

3.2.1. In vivo nasal toxicity

The results reflected in Fig. 2C show PBS treated mucosa (control) and the nasal mucosa after being exposed to CS-NLCs stained with haematoxylin-eosin. Following the i.n. administration of CS-NLCs for 15 consecutive days, no histopathological lesions that could indicate toxicity were detected. Representative photomicrographs of the histopathological analysis are shown in figure 2C, revealing no changes and no noticeable lesions of the nasal epithelium in CS-NLCs treated mice, compared with the control group. All samples exhibited absence of fibrosis, inflammatory cells and atopic tissue formation.

3.3. In vivo distribution of CS-NLCs following intranasal administration

The brain drug delivery for the treatment of neurodegenerative diseases is hindered by the BBB, which limits the access of drugs to the CNS. In recent years, enormous efforts have been made towards the research of new drug delivery platforms able to improve the diffusion of drugs across the BBB using non-invasive administration routes. In 2008, *Kumar et al.* optimized a mucoadhesive nanoemulsion that demonstrated a rapid and large extent of olanzapine transport to the rat brain [25]. Furthermore, *Patel et al.* confirmed the location of risperidone in the brain after i.n. administration of solid lipid nanoparticles by gamma scintigraphy imaging [26]. In view of all that has been mentioned above, in this work, we made a step forward by studying the brain uptake of a second improved generation of lipid-based nanoparticles after i.n. administration of DiR labelled CS-NLCs. The average particle size and zeta potential values of CS-NLC-DiR were approximately 119 nm (PDI 0.268) and +37.3 mV, respectively.

As shown in Fig. 3A, DiR fluorescence was detected in mice brain after i.n. administration of CS-NLC-DiR, revealed by the *in vivo* tissue-biodistribution monitoring performed at 0.5, 4.5, 6.5 and 23.5 h post-administration. After the images were overexposed, the fluorescence signal in some animals was colocalized with the brain, confirming an *in vivo* brain-accumulation of our formulation (Figure 3B). Moreover, as

shown in figure 3A, the CS-NLC-DiR were quickly adsorbed by the olfactory tract and distributed mainly to the lungs through the respiratory track and were also detected in the trachea and olfactory bulb. It is important to note that the nanoparticles were retained in the nasal cavity 24 h post administration because they were detected by fluorescence monitoring; they were slowly cleared and biodistributed to other organs (Figure 3C). In a recent study performed by *Kumar et al.,* olanzapine Cmax and AUC in rat brain after i.n. administration of chitosan coated nanoformulations were significantly higher in comparison with the values obtained after the i.n. administration of non-coated formulations, probably due to the mucoadhesive property of chitosan that diminishes the mucociliary clearance, which enables the drug to target the olfactory region [25]. Moreover, chitosan favours the drug delivery across various cellular barriers, such as epithelial mucosa, opening the tight junctions between cells [16].

After *in vivo* fluorescence monitoring, mice were sacrificed to analyse the *ex vivo* brain and tissue fluorescence accumulations. *Ex vivo* DiR fluorescence further confirmed the brain accumulation of CS-NLC-DiR 1, 7 and 24 h after their i.n. administration (Figure 4A). As shown in figure 4A, brain accumulation was lower than lung accumulation, similar to other published works [26,27]; however, in our study, the signal was maintained during 24 h after i.n. administration, suggesting that our formulation would reach the brain over time without being cleared by nasal mucosal cilia. Moreover, although a low percentage of CS-NLCs reached the brain, this amount could be sufficient to exert biological activity when a specific drug is encapsulated. The quantification of CS-NLC-DiR tissue accumulation is shown in figure 4B, in which 0.02%, 0.03% and 0.03% per g of brain, with respect to the total tissue-accumulated fluorescence, was measured (Figure 4B) 1, 7 and 24 h post-administration. These results agree with the findings obtained by *Shadab et al.* who demonstrated the capability of chitosan nanoparticles to reach the brain after i.n. administration. Moreover, in the study performed in 2013 by *Shadab* and

colleagues, they found that the drug concentration in the brain after the i.n. administration of drug loaded chitosan nanoparticles was significantly higher than the concentration detected after i.v. drug administration [27].

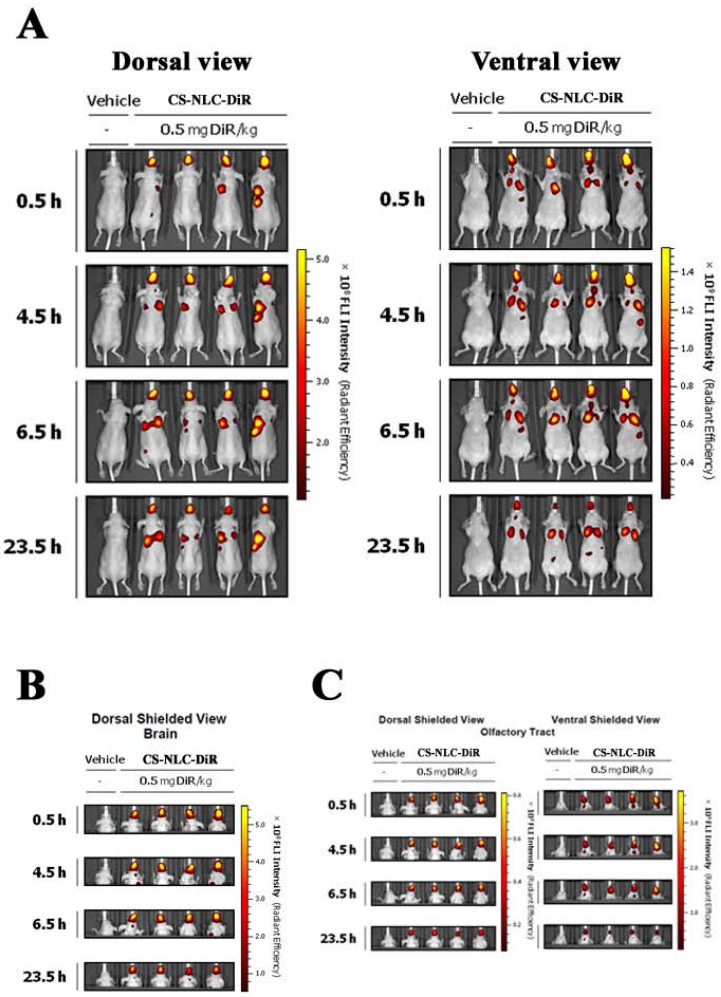

Figure 3. Non-invasive *in vivo* monitoring of CS-NLC-DiR tissue-accumulations over time A) *In vivo* CS-NLC-DiR tissue accumulation was monitored at 0.5, 4.5, 6.5 and 23.5 h post-administration of 0.5 mg DiR/kg through i.n. administration. Dorsal (left) and ventral (right) mice views are shown. Fluorescent signals were localized in the olfactory tract, lungs, trachea and spleen. **B)** Overexposed

dorsal shielded mice views are shown to visualize accumulations in the brain. **C)** Dorsal (left) and ventral (right) shielded mice views show olfactory tract accumulations. Pseudocolour scale bars were consistent for each corresponding view to show relative changes over time.

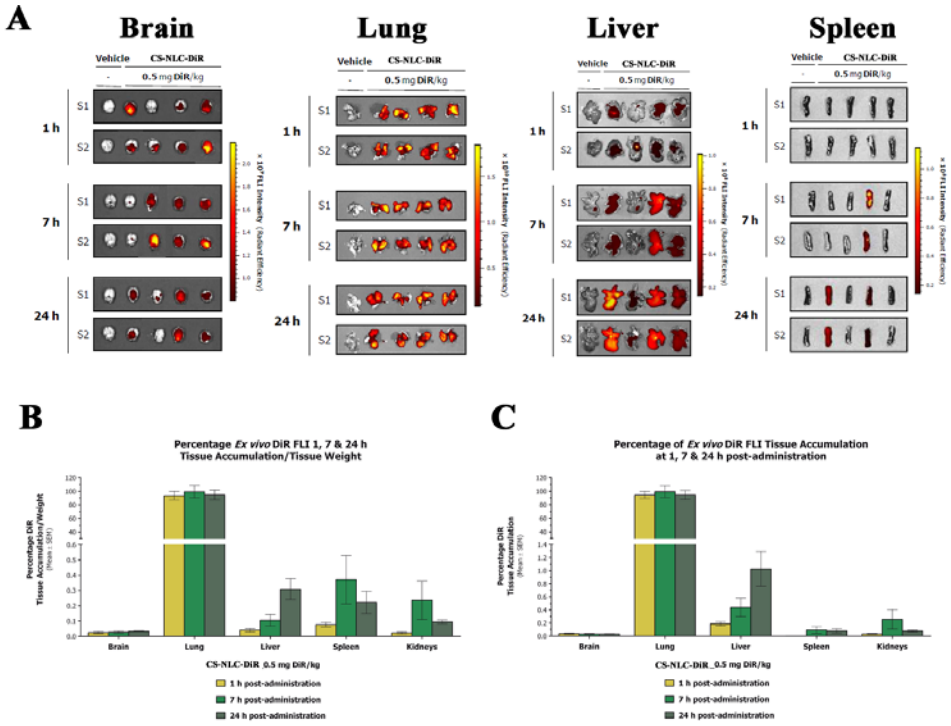

Figure 4. ***Ex vivo*** **CS-NLC-DiR brain and tissue fluorescence accumulations A)** *Ex vivo* brain, lung, liver, spleen FLI at 1, 7 and 24 h after i.n administration of CS-NLC-DiR at 0.5 mg DiR/kg. Pseudocolour scale bars were consistent for each corresponding tissue to show relative changes from 1 to 24 h. DiR tissue-accumulation per tissue weight was quantified by measuring DiR FLI intensity (Radiant Efficiency). Mean values ± SEM are displayed at each corresponding end point. S1 and S2 stands for Side 1 and 2 of the imaged tissues. **B, C)** CS-NLC-DiR tissue biodistribution. *Ex vivo* brain, lung, liver, spleen and kidney FLI per tissue weight (B) and FLI total (C) at 1, 7 and 24 h after i.n. administration of CS-NLC-DiR at 0.5 mg DiR/kg. Mean percentage values of tissue-accumulations per tissue weight with respect to the total *ex vivo* tissue-accumulated fluorescence are displayed for each time point. Mean percentage values of tissue-accumulations with respect to the total *ex vivo* tissue-accumulated fluorescence are displayed for each time point. Results are expressed as the mean ± SD (n=4).

When the brain was sectioned, significant accumulations of NLC were observed in the cerebrum, cerebellum and hippocampus brain segments, confirming that the nanoparticles not only reached the frontal brain sections but were also able to diffuse and penetrate into deeper segments (Figure 5A). Based on the data presented in Figure 5B, the percentage of CS-NLC-DiR brain segments-accumulations per whole-tissue was higher in the cerebral cortex than in the cerebellum and hippocampus at the three time-points tested. These findings are consistent with previous published works studying the direct nose-to-brain drug delivery, suggesting that the transfer of substances to the brain occurs via the olfactory and trigeminal nerve pathways by slow intra-axonal transport or by a faster transfer through the perineural space surrounding the nerve cells [28].

Further analysis in other tissues exhibited that *ex vivo* DiR fluorescence was distributed mainly in the lungs (Figure 4A). The results obtained from the analysis of accumulations of CS-NLC-DiR in the lung were 94%, 99% and 95% per g (Figure 4B) after 1, 7 and 24 h post-administration, respectively. In addition to the lungs, CS-NLC-DiR were also detected in the liver, spleen and kidneys, thereby increasing the concentrations over time, but the concentrations were below 0.4% per g in all cases. These liver- and spleen-accumulations might be attributed to the non-specific capture by the mononuclear phagocyte system. Furthermore, hepatic and renal metabolic excretion of the conjugate might also occur. Finally, no fluorescent signal was detected in the skin nor in the heart tissue, indicating that CS-NLC-DiR were not specific to cardiac tissue.

Thus, CS-NLC-DiR conjugate was biodistributed to the brain through the nose-to-brain delivery and to the lungs through the pulmonary delivery following intranasal administration, which enhanced pulmonary delivery.

4. Conclusions

This report described safe and non-toxic novel nanometric chitosan coated NLCs for i.n. administration. This CS-NLC formulation shows effective delivery to the brain after a single dose by i.n.

administration, opening new horizons to less invasive administration routes that could reach the brain avoiding the limiting step of the BBB. Moreover, considering the prolonged retention time of CS-NLCs in the nasal epithelium, this formulation could be considered an interesting alternative to decrease the dose and dosage frequency of drugs, as well as maximizing their therapeutic effect. Finally, although these results seem promising, further modifications in the CS-NLC formulation are warranted to enhance the percentage of particles reaching the brain after their i.n. administration.

Acknowledgments

This project was partially supported by the "Ministerio de Economía y Competitividad" (SAF2013-42347-R), the University of the Basque Country (UPV/EHU) (UFI 11/32), and FEDER funds. The authors thank SGIker (UPV/EHU, MICINN, GV/EJ, ESF) for their collaboration. *In vivo* biodistribution experiments were performed at the *In Vivo* Experimental Platform of the CIBER-BBN, which belongs to the Functional Validation & Preclinical Research (FVPR) Area of CIBBIM-Nanomedicine at Vall d'Hebron Research Institute (VHIR) (Barcelona, Spain). O. Gartziandia thanks the University of the Basque Country for a fellowship grant.

References

[1] Foster ER., Themes from the special issue on neurodegenerative diseases: what have we learned, and where can we go from here?, Am J Occup Ther, 68(1) (2014), 6-8

[2] Wong HL, Wu XY, Bendayan R., Nanotechnological advances for the delivery of CNS therapeutics, Adv Drug Deliv Rev, 64(7) (2012), 686-700

[3]Tajes M, Ramos-Fernandez E, Weng-Jiang X, Bosch-Morato M, Guivernau B, Eraso-Pichot A, et al., The blood-brain barrier: structure, function and therapeutic approaches to cross it, Mol Membr Biol, 31(5) (2014), 152-167

[4] Cook AM, Mieure KD, Owen RD, Pesaturo AB, Hatton J., Intracerebroventricular administration of drugs, Pharmacotherapy, 29(7) (2009), 832-845

[5] Mathias NR, Hussain MA, Non-invasive systemic drug delivery: developability considerations for alternate routes of administration, J Pharm Sci, 99(1) (2010), 1-20

[6] American Academy of Pediatrics. Committee on Drugs, Alternative routes of drug administration-advantages and disadvantages (subject review), Pediatrics, 100(1) (1997), 143-152

[7] Djupesland PG, Messina JC, Mahmoud RA, The nasal approach to delivering treatment for brain diseases: an anatomic, physiologic, and delivery technology overview, Ther Deliv, 5(6) (2014), 709-733

[8] Reger MA, Watson GS, Frey WH, Baker LD, Cholerton B, Keeling ML, et al., Effects of intranasal insulin on cognition in memory-impaired older adults: modulation by APOE genotype, Neurobiol Aging, 27(3) (2006), 451-458

[9] Begley DJ, Delivery of therapeutic agents to the central nervous system: the problems and the possibilities, Pharmacol Ther, 104(1) (2004), 29-45

[10] Graff CL, Pollack GM, Nasal drug administration: potential for targeted central nervous system delivery, J Pharm Sci, 94(6) (2005), 1187-1195

[11] Beloqui A, Solinís MA, Delgado A, Évora C, del Pozo-Rodríguez A, Rodríguez-Gascón A, Biodistribution of Nanostructured Lipid Carriers (NLCs) after intravenous administration to rats: Influence of technological factors, Eur J Pharm Biopharm, 84(2) (2013), 309-314

[12] Lim SB, Banerjee A, Önyüksel H, Improvement of drug safety by the use of lipid-based nanocarriers, J Control Release, 163(1) (2012), 34-45

[13] Gobbi M, Re F, Canovi M, Beeg M, Gregori M, Sesana S, et al., Lipid-based nanoparticles with high binding affinity for amyloid-beta1-42 peptide, Biomaterials, 31(25) (2010), 6519-6529

[14] Vyas TK, Shahiwala A, Marathe S, Misra A, Intranasal drug delivery for brain targeting, Curr Drug Deliv, 2(2) (2005), 165-175

[15] Severino P, Souto EB, Pinho SC, Santana MH, Hydrophilic coating of mitotane-loaded lipid nanoparticles: preliminary studies for mucosal adhesion, Pharm Dev Technol, 18(3) (2013), 577-581

[16] Dodane V, Amin Khan M, Merwin JR, Effect of chitosan on epithelial permeability and structure, Int J Pharm, 182(1) (1999), 21-32

[17] Dharmala K, Yoo JW, Lee CH, Development of chitosan-SLN microparticles for chemotherapy: *in vitro* approach through efflux-transporter modulation, J Control Release, 131(3) (2008), 190-197

[18] Kurosaki T, Kitahara T, Fumoto S, Nishida K, Yamamoto K, Nakagawa H, et al., Chondroitin sulfate capsule system for efficient and secure gene delivery, J Pharm Pharm Sci, 13(3) (2010), 351-361

[19] Leonardi A, Bucolo C, Romano GL, Platania CBM, Drago F, Puglisi G, et al., Influence of different surfactants on the technological properties and *in vivo* ocular tolerability of lipid nanoparticles, Int J Pharm, 470(1–2) (2014), 133-140

[20] Drin G, Cottin S, Blanc E, Rees AR, Temsamani J, Studies on the internalization mechanism of cationic cell-penetrating peptides, J Biol Chem, 278(33) (2003), 31192-31201

[21] Braz, L., Rodrigues, S., Fonte, P., Grenha, A., and Sarmento, B., Mechanisms of Chemical and Enzymatic Chitosan Biodegradability and its Application on Drug Delivery, Biodegradable Polymers: Processing, Degradation and Applications, Nova Publishers, New York, USA (2011), 325-364

[22] Cano-Cebrian MJ, Zornoza T, Granero L, Polache A. Intestinal absorption enhancement via the paracellular route by fatty acids, chitosans and others: a target for drug delivery, Curr Drug Deliv, 2(1) (2005), 9-22

[23] Doktorovova S, Souto EB, Silva AM, Nanotoxicology applied to solid lipid nanoparticles and nanostructured lipid carriers - a systematic review of *in vitro* data, Eur J Pharm Biopharm, 87(1) (2014), 1-18

[24] Gainza G, Pastor M, Aguirre JJ, Villullas S, Pedraz JL, Hernandez RM, et al., A novel strategy for the treatment of chronic wounds based on the topical administration of rhEGF-loaded lipid nanoparticles: *In vitro* bioactivity and *in vivo* effectiveness in healing-impaired db/db mice, J Control Release, 185 (2014), 51-61

[25] Kumar M, Misra A, Mishra AK, Mishra P, Pathak K, Mucoadhesive nanoemulsion-based intranasal drug delivery system of olanzapine for brain targeting, J Drug Target, 16(10) (2008), 806-814

[26] Patel S, Chavhan S, Soni H, Babbar AK, Mathur R, Mishra AK, et al., Brain targeting of risperidone-loaded solid lipid nanoparticles by intranasal route, J Drug Target, 19(6) (2011), 468-474

[27] Md S, Khan RA, Mustafa G, Chuttani K, Baboota S, Sahni JK, et al., Bromocriptine loaded chitosan nanoparticles intended for direct nose to brain delivery: Pharmacodynamic, Pharmacokinetic and Scintigraphy study in mice model, Eur J Pharm Sci, 48(3) (2013), 393-405

[28] Hanson LR, Frey WH, Intranasal delivery bypasses the blood-brain barrier to target therapeutic agents to the central nervous system and treat neurodegenerative disease, BMC Neurosci, 9 (2008), 2202-2209

Chapter 2

Intranasal administration of chitosan-coated nanostructured lipid carriers loaded with GDNF improves behavioral and histological recovery in a partial lesion model of Parkinson´s disease

Journal of Biomedical Nanotechnology (under review)

Intranasal administration of chitosan-coated nanostructured lipid carriers loaded with GDNF improves behavioral and histological recovery in a partial lesion model of Parkinson´s disease

Oihane Gartziandia[1,2], Enara Herrán[1,2], Jose Aangel Ruiz-Ortega[3,4], Cristina Miguelez[3,4], Manoli Igartua[1,2], Jose Vicente Lafuente[5,6], Jose Luis Pedraz[1,2], Luisa Ugedo[4], Rosa Maria Hernández[1,2,*]

[1]NanoBioCel Group, Laboratory of Pharmaceutics, School of Pharmacy, University of the Basque Country (UPV/EHU), Vitoria-Gasteiz 01006, Spain.
[2]Biomedical Research Networking Center in Bioengineering, Biomaterials and Nanomedicine (CIBER-BBN), Vitoria-Gasteiz 01006, Spain.
[3]Dpt. Pharmacology, School of Pharmacy, University of the Basque Country (UPV/EHU), 01006, Vitoria, Spain.
[4]Dpt. Pharmacology, Faculty of Medicine and Dentistry, University of the Basque Country (UPV/EHU), 48940, Leioa, Spain
[5]LaNCE, Dept Neurosciences, University of the Basque Country (UPV/EHU), Leioa, Spain
[6]Group Nanoneurosurgery, Institute of Health Research Biocruces, Barakaldo, Spain

ABSTRACT

Parkinson´s disease (PD) is the second most frequent neurodegenerative disorder, but current therapies are only symptomatic. A promising alternative to address the neurodegenerative process is the use of neurotrophic factors, such as the glial cell-derived neurotrophic factor (GDNF). However, its clinical use has been limited due to its short half-life and rapid degradation after *in vivo* administration, in addition to difficulties in crossing the blood-brain barrier (BBB). This barrier is a limiting factor in brain drug development, making the future progression of neurotherapeutics difficult. In the past few years, intranasal drug delivery has appeared as an alternative non-invasive administration route to bypass the BBB and target drugs directly to the CNS. Thus, the aim of this work was to study the *in vivo* neuroprotective effect of intranasally administered GDNF, encapsulated in chitosan-coated nanostructured lipid carrier (CS-NLC-GDNF), in a 6-OHDA partially lesioned rat model. The developed CS-NLC-GDNF showed a particle size of approximately 130 nm and high encapsulation efficiency. The *in vitro* study in PC-12 cells demonstrated the ability of the encapsulated GDNF to protect these cells against 6-OHDA toxin. After two weeks of daily intranasal administration of treatments, the administration of CS-NLC-GDNF achieved a behavioral improvement in rats, as well as a significant improvement in both the density of TH+ fibres in the striatum and the TH+ neuronal density in the SN. Thus, it can be concluded that the nose-to-brain delivery of CS-NLC-GDNF could be a promising therapy for the treatment of PD.

Keywords: Parkinson´s disease (PD), blood-brain barrier (BBB), intranasal, glial cell-derived neurotrophic factor (GDNF), nanostructured lipid carriers (NLC)

1. Introduction

Among central nervous system (CNS) diseases, Parkinson´s disease (PD) is the second most frequent neurodegenerative disorder after Alzheimer`s Disease (AD). It is a chronic CNS disorder clinically characterized by resting tremor, bradykinesia, rigidity, and postural instability and pathologically by the progressive loss of dopaminergic neurons in the substantia nigra pars compacta (SN). Additionally, there is a presence of Lewy bodies (ubiquinated protein deposits in the cytoplasm) and Lewy neurites (thread-like proteinaceous inclusions within neurites).[1]. Nevertheless, current therapies against PD are only symptomatic and do not halt the neurodegenerative process or provide neuroprotection of the surviving dopaminergic neurons[2]. An interesting and promising alternative to address this challenge is the use of neurotrophic factors, such as the glial cell-derived neurotrophic factor (GDNF)[3]. GDNF is a potent neurotrophic factor that acts both *in vitro* and *in vivo* in the promotion of the survival and differentiation of dopaminergic neurons and protecting the dopaminergic cells against toxins[4]. However, in practice, its clinical use has been limited due to its short half-life and rapid degradation after *in vivo* administration, in addition to difficulties in crossing the blood-brain barrier (BBB) due to its hydrophilicity, molecular weight or charge[5].

The BBB is a limiting factor in brain drug development, making the future progression of neurotherapeutics difficult. The transport of either small or large molecules across the BBB is limited because 98% of all small molecules and nearly 100% of large molecules do not cross it. Therefore, despite the large number of patients with CNS disorders, the efficient delivery of drugs to the brain is still a challenge[6]. One of the key points to approach the problem with the BBB is the selection of a suitable administration route. Among different administration routes, intraperitoneal, intravenous or subcutaneous routes are the most easy and less invasive alternatives. However, after parenteral administration, most of the drugs exhibit important difficulties in crossing the BBB, and hence, to obtain

therapeutics levels in the brain, the administration of high doses is required, which may result in adverse systemic effects[7]. There have also been several invasive methods to reach the brain avoiding the BBB, but in the past few years, intranasal drug delivery has appeared as an alternative non-invasive administration route to bypass the BBB and target drugs directly to the CNS through the olfactory and trigeminal nerve pathways[8,9]. Additionally, the nose-to-brain delivery offers the advantage of inducing minimum peripheral side-effects because nasally administered proteins are barely absorbed into the systemic circulation. Accordingly, the nasal mucosa provides several benefits as a target for drug delivery, including large surface area, rapid drug onset, potential for CNS delivery, and no first-pass metabolism. However, the major disadvantages of this administration route are the limited absorption across the nasal epithelium and the short residence time in the nasal cavity due to the mucociliary clearance, causing uncompleted drug absorption[10].

In previous reports, biodegradable carriers have been used to transport drugs through the mucosal barrier and protect them from being degraded in the nasal cavity[11-13]. Among these, lipid-based nanocarriers seem good candidates to achieve brain delivery because with their lipid nature, they can be readily transported to the brain[14-16]. Our study has focused on nanostructured lipid carriers (NLCs), which are composed of biodegradable and biocompatible lipids. NLCs are the second improved generation derived from solid lipid nanoparticles (SLN), and they show many excellent characteristics in drug delivery. The main characteristics of these delivery systems are controlled release of encapsulated drugs, increased loading capacity, and improved physical and chemical long-term stability[17]. However, there is an increasing need in the improvement of these novel drug carriers to prolong the residence time of NLCs in the nasal cavity and to improve the nose-to-brain drug delivery. In the last few years, various researchers have developed surface-modified colloidal systems for transmucosal drug delivery, showing that the coating of hydrophobic

nanoparticles with hydrophilic polymers, such as chitosan (CS), improves their transmucosal transport of the associated compounds, following nasal, oral or ocular administration[18-20]. CS is a cationic polysaccharide that exhibits good mucoadhesive properties, together with penetration enhancement properties across various mucus epithelia and enzyme-inhibiting properties[21-23]. Therefore, the coating of NLCs with chitosan could enhance the nasal transport of NLCs to the brain.

Hence, the aim of this work was to study the *in vivo* neuroprotective and neurorestorative effect of intranasally administered GDNF encapsulated in CS-NLCs in a 6-OHDA partially lesioned rat model.

2. Materials and methods

2.1. Materials

Precirol® ATO5 (Glycerol distearate) and Miglyol® (Caprylic/Capric Triglyceride) were kindly donated by Gattefosé (France) and Sasol Germany GmbH, respectively. H_2O_2 30%, Tween 80, Lutrol® F-68 (Poloxamer 188) and 3.7% paraformaldehyde were purchased from Panreac (Spain). Protasan UP CL 113 Chitosan was obtained from NovaMatrix (Norway). 6-hydroxydopamine hydrochloride, desipramine hydrochloride, chloral hydrate, amphetamine sulphate, trehalose dihydrate, cell counting kit-8 (CCK-8), 3,30'-diaminobenzidine (DAB), Triton X-100 and Trizma base were bought from Sigma-Aldrich (Spain). Human GDNF was obtained from Peprotech (UK). F-12k medium, foetal bovine serum, horse serum, L-Glutamine, Penicillin/Streptomycin and PBS pH 7,4 (1X) were purchased from Gibco© by Life Technologies (Spain). PC-12 cells were obtained from ATCC® (Spain). Normal Goat Serum (NGS) and biotinylated goat-α-rabbit were bought from ATOM. Rabbit-α-TH was purchased from Chemicon Int (USA), the ABC kit from Palex (Spain), Depex mounting medium from BDH Gum® (UK), and Isoflurane Esteve from Maipe Comercial (Spain).

2.2. Preparation of chitosan-coated nanostructured lipid carriers (CS-NLCs)

NLCs were prepared by the melt-emulsification technique[24]. First, solid and

liquid lipids (Precirol® AT05, 2.5% w/v, and Miglyol®, 0.25% w/v) with GDNF (0.15% w/w) were melted 5ºC above its melting point (56ºC). Then, an aqueous solution containing the surfactant combination of Tween 80 (3%, w/v) and Poloxamer 188 (2%, w/v) was heated at the same temperature, and it was added to the lipid phase under continuous stirring for 60 seconds at 50 W (Branson® sonifier 250). The nanoemulsion formed was maintained with magnetic stirring during 15 min at room temperature (RT) and immediately cooled at 4-8ºC overnight to obtain the NLCs due to the lipid solidification.

The next day, the formed nanoparticles were coated with chitosan. The nanoparticle dispersion was added dropwise to an equal volume of chitosan solution (0.5%, w/v) under continuous agitation at RT for 20 min. After the coating period, the NLC dispersion was centrifuged in Amicon filter (Amicon, "Ultracel-100k") at 2500 rpm (MIXTASEL, P Selecta) for 15 min, washed three times with Milli Q Water and lyophilized for 42 h (LyoBeta 15, Telstar, Tarrasa, Spain). Lyophilization of the resultant CS-NLC dispersion was conducted by using trehalose (15% w/w) as a cryoprotectant.

2.3. Characterization of nanoparticles

2.3.1. Particle size, zeta potential and morphology

The mean diameter and size distribution were measured by the Cumulant method, and zeta potential was determined using the Smoluchowski approximation (Malvern® Zetasizer Nano ZS, Model Zen 3600; Malvern Instruments Ltd). Three replicate analyses were performed for each formulation, and data are presented as the mean ± S.D. Nanoparticle morphology was examined by transmission electron microscopy (TEM, Philips CM120 BioTwin, 120 kV).

2.3.2. Encapsulation efficiency (EE %)

The EE% of GDNF in the nanoparticles was determined by an indirect method in which we measured the non-encapsulated GDNF present in the supernatant obtained after the centrifugation of the nanoparticles using the following equation:

EE%= [(Total drug content – free drug content in the supernatant)/Total drug content]*100

The free GDNF was determined by a GDNF $E_{max}^{®}$ ImmunoAssay System (Promega Corporation, Madison, USA).

2.3.3. In vitro release study

The release study was conducted in triplicate by incubating around 20 mg of CS-NLC-GDNF, (containing ~ 20 µg of GDNF), in 2 ml of 0.02 M phosphate-buffered saline (PBS) for six days. At selected intervals, the release medium was removed by filtration/centrifugation and replaced by the same quantity of PBS.

The system was maintained under orbital rotation at 25 rpm, pH 7.4, and 37 ± 0.5 °C. The amount of GDNF was detected by ELISA (GDNF $E_{max}^{®}$ ImmunoAssay System (Promega Corporation, Madison, USA)). The results are given in terms of the cumulative percentage of GDNF released over time.

2.4. In vitro neuroprotection assay on PC-12 cells

PC-12 cells were maintained in F-12k medium containing L-glutamine, 15% horse serum, 2.5% foetal bovine serum and 1% penicillin/streptomycin under standardized conditions (95% relative humidity, 5% CO2, 37ºC).

To evaluate the neuroprotective effect of GDNF against 6-OHDA on PC-12 cells, cell viability was measured with a cell counting kit-8 (CCK-8) assay after treating the cells with 25 ng/ml of GDNF (in solution or encapsulated in CS-NLCs) and empty CS-NLCs. PC-12 cells were seeded into 96-well plates at a density of 10 x 10^3 cells/well and incubated at 37ºC, 5% CO_2 for 24 h to allow cell attachment. Then, culture medium was replaced, and cells were treated for 16 h with 6-OHDA (0.1 mM) (a concentration established by our research group in previous studies as the ideal dose to damage half of the cells[4]), together with GDNF in solution and CS-NLC-GDNF. Additionally, an amount of empty CS-NLCs (CS-NLC-

Blank) corresponding to the dose of CS-NLC-GDNF was added as control.

2.5. Animals and lesion with 6-OHDA

Male albino Sprague-Dawley rats (230 g) were used to obtain the hemiparkinsonian model. Rats were housed in standard conditions with a constant temperature of 22°C, a 12-h dark/light cycle and *ad libitum* access to water and food. All experimental procedures were performed in compliance with the Ethical Committee of Animal Welfare (CEBA) at the University of the Basque Country (140128/1552/I1/RUIZORTE).

The 6-OHDA lesion procedures were performed according to previous studies[4]. Thirty minutes before 6-OHDA injection, the rats were pre-treated with desipramine (25 mg/kg, i.p.), and then, they were anesthetized with isoflurane inhalation (1.5-2 %) and mounted on a Kopf stereotaxic instrument. The lesions were generated by the injection of a 3 µg/µl 6-OHDA solution into the striatum of the right hemisphere of the rats. Three injections of 2.5 µl of 6-OHDA solution (a total volume of 7.5 µl) were administered at a rate of 0.5 µl/ min at three coordinates, relative to the bregma and dura, with the toothbar set at -2.4: AP +1.3 mm, ML +2.8 mm, DV -4.5 mm; AP -0.2 mm, ML +3.0 mm, DV -5.0 mm and AP -0.6 mm, ML +4.0 mm, DV -5.5 mm.

2.6. Intranasal administration of treatments

After the lesion, rats were randomly divided into four groups (5 rats/group): (1) Sham, (2) CS-NLC-Blank, (3) CS-NLC-GDNF (2.5 µg GDNF/day) and (4) GDNF solution (2.5 µg GDNF/day). Immediately after the surgery, rats started a two-week daily treatment by the intranasal route. Anesthetized rats (isoflurane) were maintained in a supine position, and the corresponding preparations suspended in 20 µl of PBS were administered to alternating nostrils (2 administrations of 5 µl per each nostril, leaving 3 minutes between administrations) using an automatic micropipette (2-20 µl). The procedure was performed gently and slowly, allowing the rats to inhale all of the preparations.

2.7. Behavioral studies

2.7.1. Amphetamine-induced rotational behavioral test

One week after inducing the 6-OHDA lesion, the rats were tested once a week for 7 weeks by the amphetamine-induced rotational behavioral test. Animals were weighed throughout the study before amphetamine administration. Amphetamine (5 mg/kg) was injected intraperitoneally to the rats, and they were transferred to a rotameter. After 15 minutes of latency, the total number of full turns in the ipsilateral direction to the lesion was counted for 90 minutes with an automated rotameter (Harvard Apparatus multicounter LE3806). The results are expressed as the number of ipsilateral turns per minute.

2.7.2. Cylinder test

Forelimb use asymmetry was assessed using the cylinder test at weeks 3, 5 and 7 of the *in vivo* study, as described previously[25]. Rats were individually placed in a 20-cm-diameter glass cylinder and allowed to explore freely. Mirrors were placed behind the cylinder to allow a 360º view of the exploratory activity. Each animal was left in place until at least 20 supporting front paw touches were made on the walls of the cylinder. The session was videotaped and later analysed. Touches performed with the contralateral or ipsilateral front limb were counted, and data are expressed as the percentage of ipsilateral placements, calculated as [(ipsilateral paw placement/(ipsilateral + contralateral paw placements)]*100. Figure 1 shows a schematic illustration of the experimental design for the *in vivo* study.

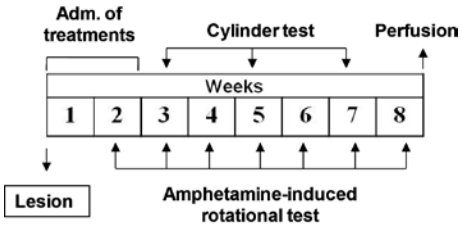

Figure 1. Schematic illustration of the *in vivo* study.

2.8. Tyrosine hydroxylase (TH) immunohistochemistry

The rats were transcardially perfused with 0.9% (w/v) NaCl and 4% (v/v) paraformaldehyde in 0.1 M PBS, pH 7.4. The brains were removed and post-fixed

for 24 h in paraformaldehyde and then transferred to a 25% (w/v) sucrose solution in 0.1 M PBS for dehydration. After at least 3 days, brains were coronally sectioned on a freezing microtome (50 µm thick) and collected in 12 and 6 series of the striatum (ST) and substantia nigra (SN), respectively, in a cryoprotection solution for a TH immunochemistry assay.

The degree of dopamine denervation in the striatum and substantia nigra (SN) was analysed using a Tyrosine Hydroxylase (TH) immunostaining[4,25]. For TH immunostaining, sections were rinsed three times in potassium phosphate buffered saline (KPBS), and then the endogenous peroxidases were quenched using 3% H_2O_2 (v/v) and 10% (v/v) methanol in potassium phosphate-buffered saline (KPBS) (0.02 M, pH 7.1) for 30 min at room temperature (RT). After three rinsing steps in KPBS, the brain sections were preincubated with 5% (w/v) normal goat serum (NGS) and 1% (w/v) Triton X-100 in KPBS (KPBS/T) for 1 h to block nonspecific binding sites and then incubated overnight with rabbit polyclonal anti-tyrosine hydroxylase (1:1000) in 5% (w/v) NGS KPBS/T at RT. After rinsing twice with KPBS and once with 2.5% w/v NGS KPBS/T, the sections were incubated for 2 h with a secondary biotinylated goat anti-rabbit IgG, which was diluted 1:200 in KPBS/T containing 2.5% w/v NGS. All sections were processed with an avidin-biotin-peroxidase complex (Elite ABC kit) for 1 h, and the reaction was visualised using 3,3'-diaminobenzidine (DAB) as the chromogen, after rinsing three times with KPBS. Finally, the brain sections were mounted on gelatin-coated slides, dehydrated in an ascending series of alcohols, cleared in xylene and coverslipped with DPX mounting media.

2.9. Integrated optical densitometry (IOD)

The optical density of the TH immunoreactive dopaminergic fibres in the striatum was measured using a computerized image analysis system (Mercator-7 Image Analysis system, Explora Nova, La`Rochelle, France), reading optical densities as grey levels. Images from sections were taken with a 1200 ppp resolution digital scan (Epson).

The IOD reading was corrected for background staining by subtracting the values of an area outside of the tissue from the obtained IOD of the striatum. Ten slices from each animal were used to represent all levels of the striatum. Optical density values for the striatum on the ipsilateral side were expressed as the percentage of the contralateral non-lesioned side, which was set at 100%.

2.10. Neuronal density

A stereological tool (optical fractionator) provided by the previously referred Mercator-7 system was used to measure TH+ neuronal density. Probes of 50 x 50 µm separated by 100 µm were launched into the previously delimited area corresponding to the SN region (4X objective). The counting was performed using a 40X objective (numerical aperture = 0.75). Positive cells that were present inside the probe or crossing on the right side of the X–Y axis were counted, and the volume (mm^3) of this region was calculated to determine the neuronal density. A minimum of eight histological sections per animal and five animals from each experimental group were used. Neuronal density values for the SN on the ipsilateral side are expressed as the percentage of the contralateral non-lesioned side, which was set at 100%.

2.11. Statistical analysis

Experimental data were analysed using the computer program GraphPad Prism (v. 5.01, GraphPad Software, Inc.). One-way ANOVA, two-way ANOVA or repeated measures two-way ANOVA followed by Bonferroni post hoc test were used for analysing *in vitro* assays, histological evaluation and behavioral data, respectively. The normal distribution of samples was assessed by the Shapiro-Wilk test, and the homogeneity of variance was determined by the Levene test. Linear regression analyses were used to assess correlations between histological and behavioral data. Values were considered statistically significant if $*p < 0.05$. Data are presented as group means ± standard error of the mean (S.E.M.).

3. Results

3.1. Characterization of NLCs

The mean particle size was 136.70 ± 14.14 nm for CS-NLC-GDNF and 133.23 ± 4.29 nm for CS-NLC-Blank. The PDI values demonstrated a narrow size distribution. Both formulations showed a similar zeta potential of approximately +30 mV, confirming the presence of chitosan (Figure 2A). In the external morphological study made using TEM, the NLCs appeared uniform in size (Figure 2B). The EE % was 98.10 ± 0.36%.

The *in vitro* GDNF release profile of CS-NLC-GDNF was displayed in Figure 2C. Nearly 20 % GDNF was detected in the supernatant after 1h incubation (burst release), corresponding to the percentage of surface-associated protein (SAP: 23.87 ± 0.275%). Thereafter, a fast release phase from 8 h to 24 h (~ 55% of the total GDNF) was observed, and finally a sustained release phase from 24 to 144 h, reaching 70% of GDNF released by 144 h.

3.2. In vitro neuroprotection assay against 6-OHDA

In this assay, we tested whether GDNF, encapsulated in NLCs or not, was able to protect PC-12 cells from 6-OHDA toxicity. As shown in Figure 2C, GDNF-loaded CS-NLCs and GDNF solution ($p<0.0001$, $F_{(3,8)}=30.43$, one-way ANOVA) were able to protect PC-12 cells against neurotoxicity induced by 6-OHDA *in vitro*, whereas as expected, blank CS-NLCs did not show any neuroprotection. Thus, the ability of GDNF to protect cells against 6-OHDA was maintained after the nanoencapsulation in CS-NLCs, and hence, these results demonstrate that the encapsulation process does not affect the bioactivity of GDNF.

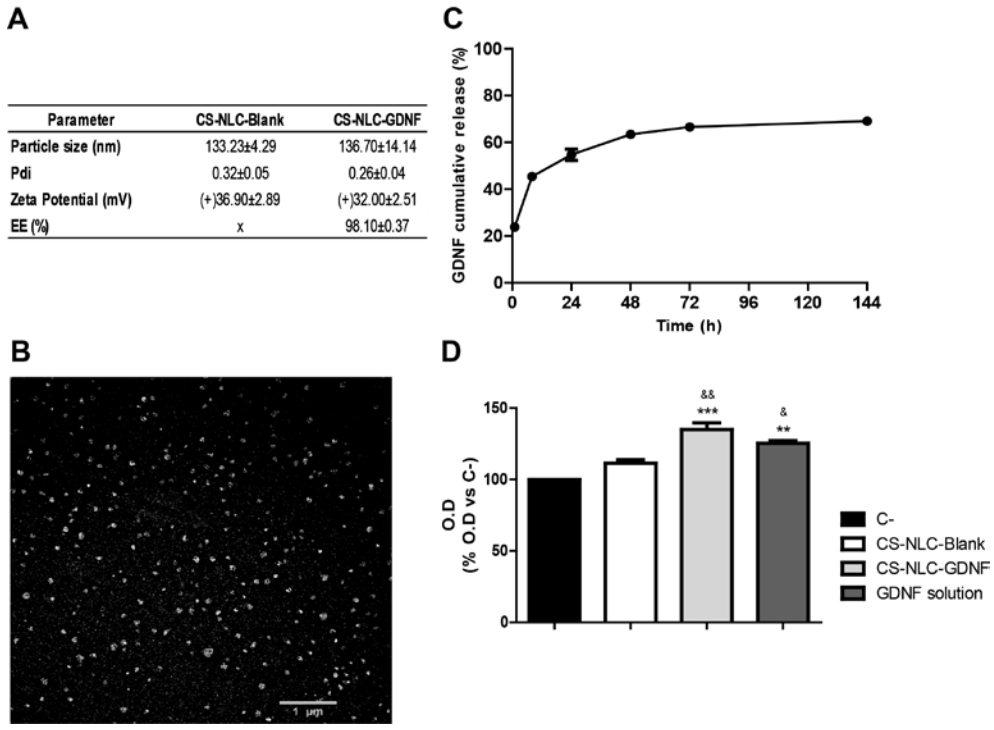

Figure 2. Physicochemical characterization and morphology study of CS-NLCs, and *in vitro* neuroprotection assay. A: Physicochemical properties of GDNF-loaded CS-NLC and blank CS-NLC. The data are shown as the mean ± S.D (n=3). **B:** Microphotograph of CS-NLC-GDNF obtained by TEM. **C:** Cumulative *in vitro* release profile of GDNF from CS-NLC-GDNF. **D:** PC-12 cell viability evaluation after 6-OHDA-induced toxicity *in vitro*. Effect of 25 ng/ml of GDNF administered in solution (GDNF solution) or encapsulated in CS-NLC (CS-NLC-GDNF), and CS-NLC-Blank treatment on cell viability. The results are expressed as cell viability percentage with respect to the C- group, which is considered to have 100% cell viability. The data are shown as the mean ± SEM (n=3), **p< 0.01, ***p< 0.001 with respect to the control group, $^{\&}$p< 0.05, $^{\&\&}$p< 0.01 with respect to the CS-NLC-Blank group, Bonferroni post hoc test.

3.3. Behavioral studies: Amphetamine-induced rotational behavioral test and cylinder test

The *in vivo* effectiveness of the GDNF-loaded NLCs was determined by the amphetamine-induced rotational behavioral test. Significant differences

were found for the factor interaction depicting that encapsulated GDNF had a more beneficial effect in movement recovery than GDNF in solution ($p<0.05$, $F_{(1,14)}=7.1$, for interaction factor, repeated measures two-way ANOVA). After performing this study during 7 consecutive weeks, the CS-NLC-GDNF group showed a significantly lower number of rotations per minute with respect to the basal number of rotations from the 3rd testing session until the end of the study in which a reduction of 80% was achieved (for statistical details, see Figure 3A). The other three groups included in the study showed stable rotational behaviour during the 7 weeks of the study.

The behavioral improvement seen in the rotational behaviour was also supported by a reduction in forelimb asymmetry in the cylinder test ($F_{(1,14)}=4.54$, $p<0.05$, for interaction factor, repeated measures two-way ANOVA). As depicted in Figure 3B, in the CS-NLC-GDNF group, the use of the ipsilateral paw was significantly decreased at all analysed time points. Accordingly, the use of the ipsilateral paw in this group was significantly lower than in the other three groups, from the first session, and these differences became larger two weeks later in the second session (for statistical details, see Figure 3B).

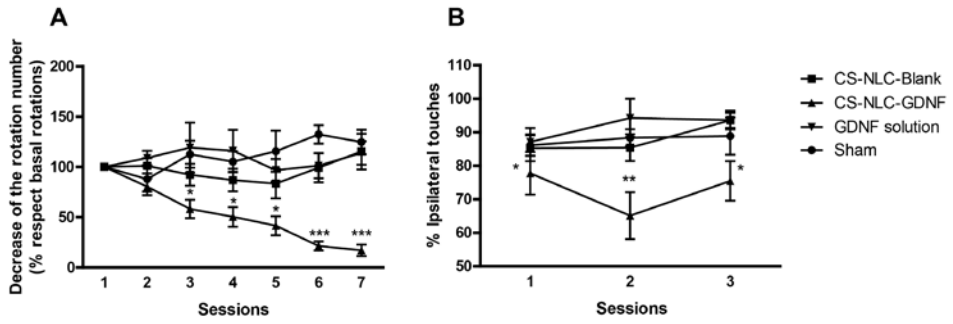

Figure 3. Graphical representation of the behavioral assessment of 6-OHDA lesioned animals. A: Amphetamine-induced rotational behaviour test. The graphic shows the percentage change in the ipsilateral number of rotations per minute, with respect to the basal rotation values obtained in the first session (100%). **B:** The graphic shows the percentage of touches performed with the ipsilateral

forelimb in the cylinder test. The data are shown as the mean ± SEM (n=5), *p< 0.05, **p<0.01 and ***p< 0.001, CS-NLC-GDNF group with respect to the other three groups, Bonferroni post hoc test.

3.4. Histological evaluation

In addition to the behavioral tests, immunohistochemical techniques were also used to analyse the efficacy of the treatment in hemiparkinsonian rats. For this purpose, integrated optical density (IOD) of TH+ fibres of the striatum and density of dopaminergic neurons in the SN were measured.

Figures 4A-D show the photomicrographs of the TH immunostained striatums (rostral, medial and caudal). The study of the ipsilateral coronal sections of the striatum showed a different degree of neurodegeneration after the intranasal administration of different treatments.

As shown in Figure 4E, 7 weeks after finishing the 2-week daily i.n. treatment, the percentage of TH+ fibres in the striatum of the ipsilateral or lesioned side, compared to the contralateral or non-lesioned hemisphere, was higher in the CS-NLC-GDNF treatment group ($F(1, 14)=8.96$ $p<0.01$, for interaction factor, two-way ANOVA). In this group, the increase in striatal TH+ fibres in the lesioned side was 72%, whereas the other three groups recovered by approximately 40%, demonstrating that the encapsulated GDNF treatment improved the restoration of TH+ structures better than the treatments with GDNF solution, PBS or empty CS-NLCs (CS-NLC-Blank) (for statistical details, see Figure 4E). Although these differences were maintained through the striatum, they were more pronounced in the caudal ($F(1, 14)=8.953$ $p<0.05$, for interaction factor, two-way ANOVA, Figure 4G) than in the rostral striatum ($F(1, 14)=2.5$ $p>0.05$, for interaction factor, two-way ANOVA, Figure 4F). These results may be because in the parkinsonism model, the neuronal loss affects mainly the caudal areas of the striatum, and thus, there are no significant differences in the striatal rostral areas[26].

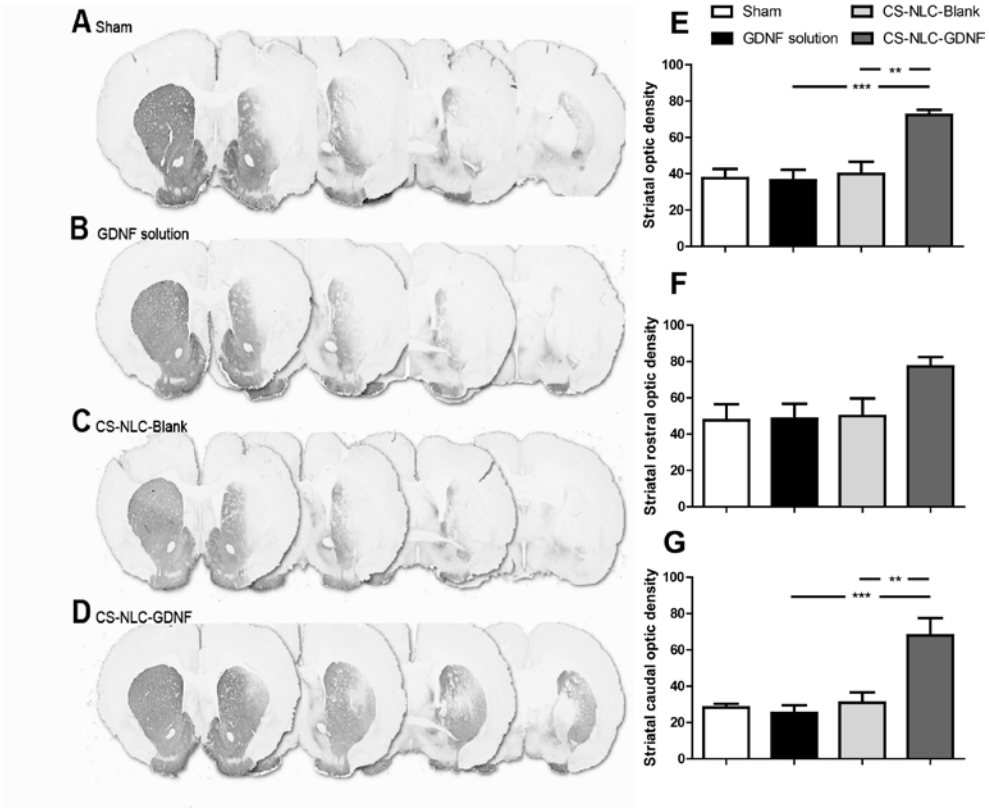

Figure 4. Histological evaluation of the striatum. A: Representative photomicrographs of the TH immunostained striatums (rostral, medial and caudal) compared with the non-lesioned side (on the left) of 6-OHDA lesioned rats, after the intranasal administration of PBS (Sham), **B:** Representative photomicrographs of the TH immunostained striatums (rostral, medial and caudal) compared with the non-lesioned side (on the left) of 6-OHDA lesioned rats, after the intranasal administration of GDNF solution, **C:** Representative photomicrographs of the TH immunostained striatums (rostral, medial and caudal) compared with the non-lesioned side (on the left) of 6-OHDA lesioned rats, after the intranasal administration of CS-NLC-Blank and **D:** Representative photomicrographs of the TH immunostained striatums (rostral, medial and caudal) compared with the non-lesioned side (on the left) of 6-OHDA lesioned rats, after the intranasal administration of CS-NLC-GDNF. The degeneration degree of various ipsilateral coronal sections of the striatum. **E:** The integrated optical density (IOD) of TH+ fibres of the entire striatum in the lesioned hemisphere compared to the non-lesioned hemisphere. **F:** The integrated optical density (IOD) of TH+ fibres of the rostral striatum in the lesioned hemisphere compared to the non-lesioned hemisphere. **G:** The integrated optical density (IOD) of TH+ fibres of the caudal striatum in the lesioned hemisphere compared to the non-lesioned hemisphere. The results are expressed as a percentage of the intact hemisphere compared to the lesioned side. The data are shown as the mean ± SEM (n=5), **p<0.01 and ***p<0.001 *vs* the CS-NLC-GDNF group, Bonferroni post hoc test.

The results of the quantitative analysis of TH+ neurons in the SN confirmed these results ($F_{(1, 14)}$=71.37 p<0.001, for interaction factor, two-way ANOVA, Figure 5A). The TH+ neuronal density in the entire SN of the CS-NLC-GDNF group was significantly higher than that in the other three groups, as shown in the stereological study (for statistical details, see Figure 5A). Accordingly, the percentage of neuronal density in the entire SN of the lesioned side compared to the non-lesioned side was approximately 25.74%, 18.44%, 25.82% and 69.79% in the Sham, GDNF solution, CS-NLC-Blank and CS-NLC-GDNF groups, respectively. This neuronal density was similar through the nucleus because similar results were obtained in rostral and caudal SN ($F_{(1, 14)}$= 51.50 p<0.001, for interaction factor, two-way ANOVA, Figure 5B; $F_{(1, 14)}$= 43.31 p<0.001, for interaction factor, two-way ANOVA, 5C).

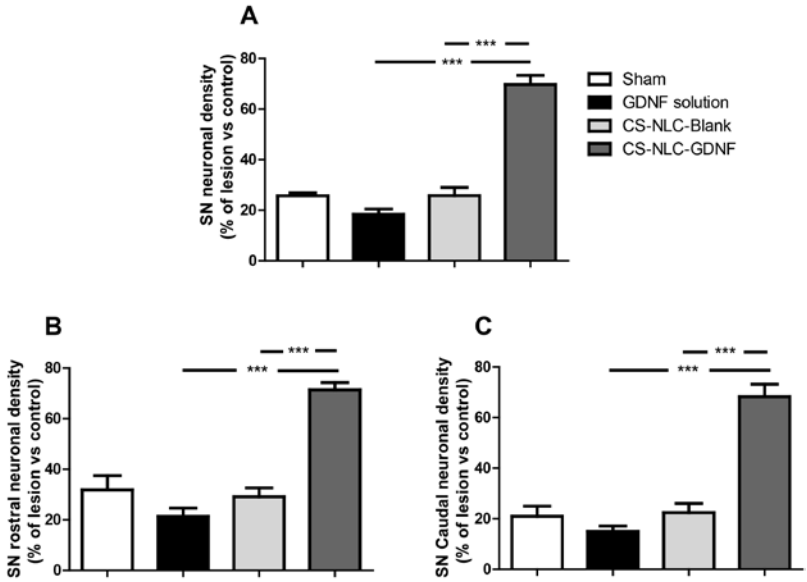

Figure 5. Histological evaluation of the SN. A: Density of TH+ neurons in the entire SN. The results are expressed as a percentage of lesioned hemisphere compared to the intact side. **B:** Density of TH+ neurons in the rostral SN. The results are expressed as a percentage of lesioned hemisphere

compared to the intact side. **C:** Density of TH+ neurons in the caudal SN. The results are expressed as a percentage of lesioned hemisphere compared to the intact side. The data are shown as the mean ± SEM, ***p < 0.001 *vs* the CS-NLC-GDNF group, Bonferroni post hoc test.

After the behavioral and histological evaluation, whether a correlation exists between the behaviour of rats and brain histological results was investigated. In this regard, correlation analysis was performed between TH+ striatal density or the number of dopaminergic neurons in the SN and the percentage of rotations induced by amphetamine. The results indicated that rotational performance was significantly correlated with both striatal density ($r = 0.85$, $p < 0.001$, Figure 6A) and neuronal density in the SN ($r = 0.89$, $p < 0.001$, Figure 6B). In this regard, rats that showed low ipsilateral rotation percentage at the end of the study exhibited high levels of optical density in the striatum and TH+ cells in the SN of the ipsilateral side of the brain. Rats with high ipsilateral rotation percentages at the end of the study showed low levels of optical density in the striatum and neuronal density in the SN. It is possible to hypothesise, therefore, that the cell recovery in the SN and the higher density of TH positive innervation contributed to the behavioral improvement observed in the CS-NLC-GDNF group.

As seen in the rotational behaviour, a significant correlation was also observed between behavioral improvement during the last testing session of the cylinder test and both optical density in the striatum ($r = 0.58$, $p < 0.05$, Figure 6C) and TH+ cells in the SN ($r = 0.74$, $p < 0.001$, Figure 6D) of the rats. Thus, rats that showed a decrease in the percentage of ipsilateral touches exhibited higher levels of striatal TH+ fibres and neuronal density in the SN ipsilateral to the lesion. These results support the relationship between forelimb asymmetry and dopaminergic neuronal loss in the SN[27].

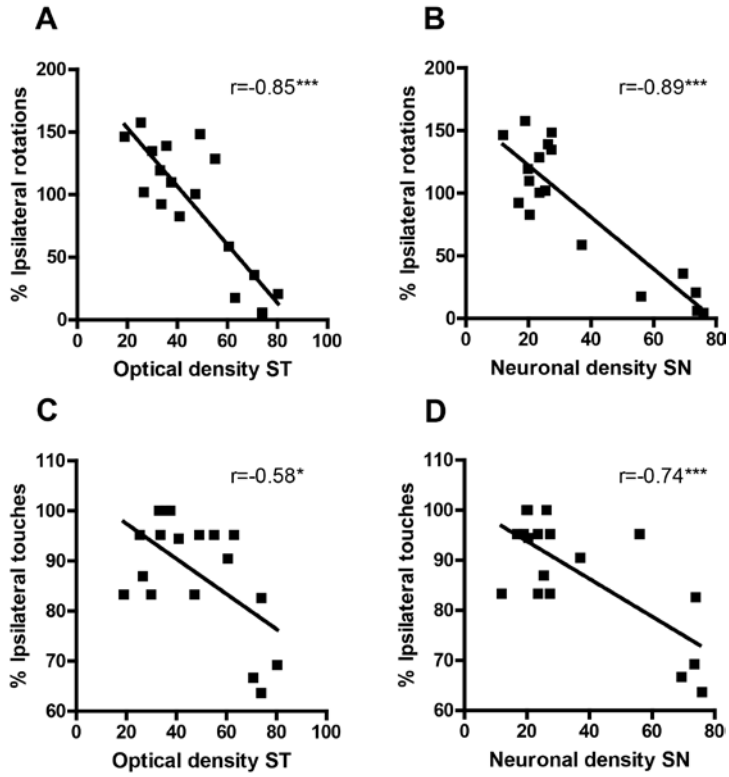

Figure 6. Graphical representation of the correlation between behavioral assays and histological changes in the striatum and the SN of rats. A, B: The graphics show the correlation between ipsilateral rotation percentage at the end of the study and the optical density of the striatum (A) or neuronal density of the SN (B). **C, D:** The graphics show the correlation between the percentage of ipsilateral touches at the end of the study and the optical density of the striatum (C) and neuronal density of the SN (D). *p< 0.05 and ***p< 0.001.

4. Discussion

In the last few years, several works using growth factors have been reported to be useful in the treatment of PD. Concerning neurotrophic factors, GDNF is promising, particularly for the treatment of this neurological disorder due to its efficacy in the up-regulation of mechanisms that are involved in neurogenic processes and therefore in the evolution of the disease. Many of these studies have demonstrated the *in vitro* neuroprotective ability of this factor against various toxins such as lipopolysaccharide (LPS), 1-methyl-4-

phenylpyridinium (MPP) or 6-OHDA[4,28,29]; they have also demonstrated that the administration of GDNF alone or in combination decreases neuronal degeneration and hence improves behavioral alterations in various Parkinson animal models[30-35]. However, GDNF is a hydrophilic molecule with crucial shortcomings that limit its use, such as a short circulation half-life and a rapid degradation rate after its *in vivo* administration. Moreover, considering the presence of the BBB, in most of these *in vivo* studies, invasive administration routes such as intraparenchymal or intracerebroventricular routes have been used to directly access the brain.

In the search for a non-invasive administration route in this research, the intranasal route has been used as a safe alternative to reach the brain by bypassing the BBB. There are relatively few studies in the area of intranasal delivery of GDNF for the treatment of hemiparkinsonian rats. In an interesting study, *Zaho et al.* designed phospholipid-based gelatin nanoparticles encapsulating basic fibroblast growth factor (bFGF) to target the brain via nasal administration, showing therapeutic effects in hemiparkinsonian rats[12]. Nevertheless, in an article published recently by *Migliore et al.*, GDNF was intranasally administered to a unilateral 6-OHDA model of PD. They observed that the treatment with GDNF-loaded liposomes induced a neurorestorative effect in the SN, as the number of TH+ neurons was significantly higher than in controls receiving the PBS treatment[36].

Therefore, with the aim of achieving a successful delivery to the brain tissue, various drug delivery systems (DDS) loaded with GDNF have been developed[37-40]. In this work, we developed for the first time a chitosan-coated NLC-GDNF formulation for nose-to-brain delivery and analysed its neuroprotective ability against 6-OHDA damage areas, as well as its potential to improve behavioral deficits in a hemiparkinsonism rat model.

The characterization study of our formulation revealed that the NLCs were uniform in size with a particle size of approximately 130 nm, suitable for the i.n. administration, in accordance with

other authors, who administered NLCs with a similar particle size by the nasal route[41]. Additionally, the NLCs were coated with the natural polysaccharide chitosan to obtain mucoadhesive nanoparticles to enhance their retention time and penetration across the nasal mucosa and thus to increase access to the brain. Their positive zeta potential value of approximately +30 mV suggested that chitosan was adsorbed to the surface of the nanoparticles, and as mentioned in previous studies, cationic nanoparticles are expected to be easily attached to the endothelial cells[42]. Moreover, a high encapsulation efficiency value was obtained, confirming the high loading capacity of this type of nanoparticles.

After the physicochemical characterization of the formulation, the *in vitro* neuroprotective capacity of GDNF-loaded CS-NLCs was determined to prove its bioactivity after the encapsulation process. For this purpose, the PC-12 cell line was used as a specific cell lineage of dopaminergic neurons, and the cells were exposed to 6-OHDA neurotoxin, the same toxin used to establish the partially lesioned model of PD. In this assay, the neuroprotective ability of GDNF was demonstrated either in solution or encapsulated in CS-NLCs. Thus, it was confirmed that the encapsulation process does not affect the bioactivity of the neurotrophic factor.

After proving the neuroprotective effect of CS-NLC-GDNF in PC-12 cells, the *in vivo* effectiveness of the formulation was also investigated. Thus, 6-OHDA-lesioned rats were used as a partially lesioned model of PD with the aim of studying the neuroprotective and neurorestorative effect of GDNF-loaded nanoparticles in the performance of behavioral tests and in the loss of dopaminergic neurons, after their intranasal administration during 15 consecutive days. By performing the *in vivo* experiments with a partially lesioned rat model of PD, we attempted to study the potential effect of CS-NLC-GDNF in the initial stage of the disease. For this purpose, the 6-OHDA toxin was injected into the rats brain, and we immediately started the two-week daily intranasal treatment to prove whether the GDNF was able to protect rats against the 6-OHDA lesion, in contrast to previous

studies conducted by our research group in which treatments were intrastriatally administered three weeks after the injury, after the lesion was fully established[4]. In the first week of the amphetamine-induced rotational test, all groups exhibited an elevated number of rotations per minute, confirming that they were well injured. However, it is interesting to note that the CS-NLC-GDNF group showed the lowest rotations per minute (CS-NLC-GDNF: 14.55 rot/min, GDNF solution: 24.98 rot/min, CS-NLC-Blank: 21.14 rot/min, Sham: 19.11 rot/min), probably due to the neuroprotective effect exerted by the nanoencapsulated GDNF. Moreover, during the 7 weeks of the study, the results obtained in the amphetamine-induced rotational test and in the cylinder test demonstrated the behavioral improvement of rats after the intranasal CS-NLC-GDNF treatment, which was not observed in the group treated with the GDNF solution. These results demonstrated that the encapsulation of GDNF in our lipid-based nanoparticles promotes the nose-to-brain delivery of GDNF. As it has been mentioned above, in this study, the effectiveness of GDNF encapsulated in CS-NLC and administered by a minimally invasive route, such as the intranasal route, has been proved for the first time to improve the motor functions of hemiparkinsonian rats using two different behavioral tests. Moreover, the results obtained in the amphetamine-induced rotational test were better than those obtained by our research group using the intrastriatal administration route[4]. These results could be because in the present study, the treatments were simultaneously administered with the neurotoxin to study the neuroprotective effect of our GDNF-loaded nanoparticles, as has been mentioned above. After these encouraging results, it would be interesting for future works to investigate the neurorestorative ability of CS-NLC-GDNF after the lesion is fully established.

These findings were also confirmed with the histological evaluation of the brains. The injection of 6-OHDA is directly related to the loss of dopaminergic neurons, and thus, the density of TH+ fibres in the striatum and the density of dopaminergic neurons in the SN of the lesioned side of the brain were evaluated.

As in the behavioral tests, only the CS-NLC-GDNF treatment group showed an improvement in both the density of TH+ fibres in the striatum and the TH+ neuronal density in the SN, in contrast to *Migliore et al.´*s findings in which the treatment with GDNF in PBS was also effective[36]. This difference could be explained by the dose and dosing frequency because they administered a higher single dose of GDNF, whereas we administered repeated low doses of GDNF. It can thus be suggested that the encapsulation provides a more effective delivery of the neurotrophic factor to the brain tissue avoiding its loss, compared with the non-encapsulated GDNF.

Moreover, in the current study, a correlation between the behavioral improvements and the degree of injury in the striatum and SN of the ipsilateral hemisphere of the brain was also demonstrated. Hence, these results provide further support for the hypothesis that the progress of motor function in rats is evidenced by the recovery of the striatal TH+ fibres and dopaminergic neurons in the SN of the lesioned-side of the brain[27].

5. Conclusion

The results obtained from the *in vivo* studies suggest that the encapsulation of GDNF in CS-coated NLCs improves the nose-to-brain delivery of the neurotrophic factor after intranasal administration. Furthermore, we demonstrated the neuroprotective and neurorestorative effect of CS-NLC-GDNF in a partially lesioned rat model of PD. Thus, it can be concluded that GDNF-loaded CS-NLCs administered by a non-invasive route such as the intranasal route could be a promising therapy for the treatment of PD.

Despite the hopeful results obtained during this experimental work, it must bear in mind that we performed a neuroprotection study. However, diagnosis is only enabled late in the disease, when the motor symptoms reflecting the degeneration of dopaminergic neurons in the substantia nigra appear. Thus, it would be interesting for future works to investigate the neurorestorative ability of CS-NLC-GDNF in more advances stages of the disease.

6. Acknowledgements

This project was partially supported by the "Ministerio de Economía y Competitividad" (SAF2013-42347-R), the University of the Basque Country (UPV/EHU) (UFI 11/32), Basque Government (Saiotek S-PE13UN048), (GIC IT 794/13) and FEDER funds. The authors thank SGIker (UPV/EHU, MICINN, GV/EJ, ESF) for their collaboration. O. Gartziandia thanks the University of the Basque Country for a fellowship grant.

7. References

1. Alan E. Guttmacher, M.D., and Francis S. Collins, Alzheimer's Disease and Parkinson's Disease, N Engl J Med. 348, 1356-64 **(2003)**.

2. Deierborg T, Soulet D, Roybon L, Hall V, Brundin P, Emerging restorative treatments for Parkinson's disease, Prog Neurobiol. 85(4), 407-432 **(2008)**.

3. George J. Siegela, Neelima B. Chauhanb, Neurotrophic factors in Alzheimer's and Parkinson's disease brain, Brain Res Rev. 33, 199-227 **(2000)**.

4. Herrán E, Requejo C, Ruiz-Ortega JA, Aristieta A, Igartua M, Bengoetxea H, Ugedo L, Pedraz JL, Lafuente JV, Hernández RM, Increased antiparkinson efficacy by the combined administration of VEGF- and GDNF-releasing nanospheres in a partial lesion model of Parkinson's disease, Int J Nanomedicine. 9, 2677-87 **(2014)**.

5. Levy YS, Gilgun-Sherki Y, Melamed E, Offen D, Therapeutic potential of neurotrophic factors in neurodegenerative diseases, BioDrugs. 19(2), 97-127 **(2005)**.

6. Pardridge WM, The blood-brain barrier: bottleneck in brain drug development, NeuroRx. 2(1), 3-14 **(2005)**.

7. Mathias NR, Hussain MA, Non-invasive systemic drug delivery: developability considerations for alternate routes of administration, J Pharm Sci. 99(1), 1-20 **(2010)**.

8. Graff CL, Pollack GM, Nasal drug administration: potential for targeted central nervous system delivery, J Pharm Sci. 94(6), 1187-1195 **(2005)**.

9. Dhuria SV, Hanson LR, Frey WH, Intranasal delivery to the central nervous system: mechanisms and experimental considerations, J Pharm Sci. 99(4), 1654-1673 **(2010)**.

10. Costantino HR, Illum L, Brandt G, Johnson PH, Quay SC, Intranasal delivery: Physicochemical and therapeutic aspects. Int J Pharm. 337(1–2), 1-24 **(2007)**.

11. Zhang C, Chen J, Feng C, Shao X, Liu Q, Zhang Q, et al, Intranasal nanoparticles of basic fibroblast growth factor for brain delivery to treat Alzheimer's disease, Int J Pharm. 461(1-2), 192-202 **(2014)**.

12. Zhao YZ, Li X, Lu CT, Lin M, Chen LJ, Xiang Q, et al, Gelatin nanostructured lipid carriers-mediated intranasal delivery of basic fibroblast growth factor enhances

functional recovery in hemiparkinsonian rats, Nanomedicine. 10(4), 755-764 **(2014)**.

13. Sharma D, Maheshwari D, Philip G, Rana R, Bhatia S, Singh M, et al, Formulation and optimization of polymeric nanoparticles for intranasal delivery of lorazepam using Box-Behnken design: in vitro and in vivo evaluation, Biomed Res Int. 156010 **(2014)**.

14. Kaur IP, Bhandari R, Bhandari S, Kakkar V, Potential of solid lipid nanoparticles in brain targeting, J Control Release. 127(2), 97-109 **(2008)**.

15. Gobbi M, Re F, Canovi M, Beeg M, Gregori M, Sesana S, et al, Lipid-based nanoparticles with high binding affinity for amyloid-beta1-42 peptide, Biomaterials. 31(25), 6519-6529 **(2010)**.

16. Blasi P, Giovagnoli S, Schoubben A, Ricci M, Rossi C, Solid lipid nanoparticles for targeted brain drug delivery, Adv Drug Deliv Rev. 59(6), 454-477 **(2007)**.

17. Muller RH, Radtke M, Wissing SA, Nanostructured lipid matrices for improved microencapsulation of drugs, Int J Pharm. 242(1-2), 121-128 **(2002)**.

18. Garcia-Fuentes M, Torres D, Alonso MJ, New surface-modified lipid nanoparticles as delivery vehicles for salmon calcitonin, Int J Pharm. 296(1-2), 122-132 **(2005)**.

19. Prego C, Garcia M, Torres D, Alonso MJ, Transmucosal macromolecular drug delivery, J Control Release. 101(1-3), 151-162 **(2005)**.

20. Vila A, Sanchez A, Tobio M, Calvo P, Alonso MJ, Design of biodegradable particles for protein delivery, J Control Release. 78(1-3), 15-24 **(2002)**.

21. Sandri G, Bonferoni MC, Gökçe EH, Ferrari F, Rossi S, Patrini M, Caramella C, Chitosan-associated SLN: in vitro and ex vivo characterization of cyclosporine A loaded ophthalmic systems, J Microencapsul. 27(8), 735-746 **(2010)**.

22. Severino P, Souto EB, Pinho SC, Santana MH, Hydrophilic coating of mitotane-loaded lipid nanoparticles: preliminary studies for mucosal adhesion, Pharm Dev Technol. 18(3), 577-581 **(2013)**.

23. Dharmala K, Yoo JW, Lee CH, Development of Chitosan–SLN Microparticles for chemotherapy: In vitro approach through efflux-transporter modulation, J Control Release. 131(3), 190-197 **(2008)**.

24. Gartziandia O., Herrán E., Pedraz J.L., Carro E., Igartua M., Hernández R.M, Chitosan coated nanostructured lipid carriers for brain delivery of proteins by intranasal administration, Colloids Surf B Biointerfaces. 134, 304-313 **(2015)**.

25. Miguelez C, Aristieta A, Cenci MA, Ugedo L, The locus coeruleus is directly implicated in L-DOPA-induced dyskinesia in parkinsonian rats: an electrophysiological and behavioural study, PLoS One. 6(9), e24679 **(2011)**.

26. C. Requejo, J. A. Ruiz-Ortega, H. Bengoetxea, A. Garcia-Blanco, E. Herrán, A. Aristieta, M. Igartua, L. Ugedo, J. L. Pedraz, R. M. Hernández, J. V. Lafuente, Topographical Distribution of Morphological Changes in a Partial

Model of Parkinson's Disease—Effects of Nanoencapsulated Neurotrophic Factors Administration, Mol Neurobiol. In press **(2015)**.

27. Schallert T, Fleming SM, Leasure JL, Tillerson JL, Bland ST, CNS plasticity and assessment of forelimb sensorimotor outcome in unilateral rat models of stroke, cortical ablation, parkinsonism and spinal cord injury, Neuropharmacology. 39(5), 777-787 **(2000)**.

28. Xing B, Xin T, Zhao L, Hunter RL, Chen Y, Bing G. Glial cell line-derived neurotrophic factor protects midbrain dopaminergic neurons against lipopolysaccharide neurotoxicity. J Neuroimmunol. 225(1–2), 43-51 **(2010)**.

29. Zeng X, Chen J, Deng X, et al, An in vitro model of human dopaminergic neurons derived from embryonic stem cells: MPP+ toxicity, Neuropsychopharmacology. 31(12), 2708-2715 **(2006)**.

30. Yue X, Hariri DJ, Caballero B, Zhang S, Bartlett MJ, Kaut O, et al, Comparative study of the neurotrophic effects elicited by VEGF-B and GDNF in preclinical in vivo models of Parkinson's disease, Neuroscience. 258, 385-400 **(2014)**.

31. Chen Y, Ai Y, Slevin JR, Maley BE, Gash DM, Progenitor proliferation in the adult hippocampus and substantia nigra induced by glial cell line-derived neurotrophic factor, Exp Neurol. 196(1), 87-95 **(2005)**.

32. Kordower JH, Emborg ME, Bloch J, Ma SY, Chu Y, Leventhal L, et al, Neurodegeneration prevented by lentiviral vector delivery of GDNF in primate models of Parkinson's disease, Science. 290(5492), 767-773 **(2000)**.

33. Garbayo E, Ansorena E, Blanco-Prieto MJ, Drug development in Parkinson's disease: From emerging molecules to innovative drug delivery systems, Maturitas. 76(3), 272-278 **(2013)**.

34. Grandoso L, Ponce S, Manuel I, Arrúe A, Ruiz-Ortega JA, Ulibarri I, et al, Long-term survival of encapsulated GDNF secreting cells implanted within the striatum of parkinsonized rats, Int J Pharm. 343(1–2):69-78 **(2007)**.

35. Herrán E, Ruiz-Ortega JÁ, Aristieta A, Igartua M, Requejo C, Lafuente JV, et al, In vivo administration of VEGF- and GDNF-releasing biodegradable polymeric microspheres in a severe lesion model of Parkinson's disease. Eur J Pharm Biopharm. 85(3, Part B), 1183-1190 **(2013)**.

36. Migliore MM, Ortiz R, Dye S, Campbell RB, Amiji MM, Waszczak BL, Neurotrophic and neuroprotective efficacy of intranasal GDNF in a rat model of Parkinson's disease, Neuroscience. 274, 11-23 **(2014)**.

37. Eberling JL, Kells AP, Pivirotto P, Beyer J, Bringas J, Federoff HJ, Forsayeth J, Bankiewicz KS, Functional effects of AAV2-GDNF on the dopaminergic nigrostriatal pathway in parkinsonian rhesus monkeys, Hum Gene Ther. 20(5), 511-8 **(2009)**.

38. Huang R, Ke W, Liu Y, Wu D, Feng L, Jiang C, et al, Gene therapy using lactoferrin-modified nanoparticles in a rotenone-induced chronic Parkinson

model. J Neurol Sci. 290(1–2), 123-130 **(2010)**.

39. Jollivet C, Aubert-Pouessel A, Clavreul A, Venier-Julienne M, Remy S, Montero-Menei CN, et al, Striatal implantation of GDNF releasing biodegradable microspheres promotes recovery of motor function in a partial model of Parkinson's disease, Biomaterials. 25, 933-942 **(2004)**.

40. Garbayo E, Ansorena E, Lanciego JL, Blanco-Prieto MJ, Aymerich MS, Long-term neuroprotection and neurorestoration by glial cell-derived neurotrophic factor microspheres for the treatment of Parkinson's disease, Mov Disord. 26(10), 1943-1947 **(2011)**.

41. Madane RG, Mahajan HS, Curcumin-loaded nanostructured lipid carriers (NLCs) for nasal administration: design, characterization, and in vivo study, Drug Deliv. 4, 1-9 **(2014)**.

42. Drin G, Cottin S, Blanc E, Rees AR, Temsamani J, Studies on the internalization mechanism of cationic cell-penetrating peptides, J Biol Chem. 278(33), 31192-31201 **(2003)**.

Chapter 3

Nanoparticle transport across *in vitro* olfactory cell monolayers

International Journal of Pharmaceutics 499, 81-89 (2016)

Nanoparticle transport across *in vitro* olfactory cell monolayers

Oihane Gartziandia[1,2,3], Susana Patricia Egusquiaguirre[1,2], John Bianco[3,4], José Luis Pedraz[1,2], Manoli Igartua[1,2], Rosa Maria Hernandez[1,2], Véronique Préat[3,*], Ana Beloqui[3,*]

[1]NanoBioCel Group, Laboratory of Pharmaceutics, School of Pharmacy, University of the Basque Country (UPV/EHU), Vitoria-Gasteiz 01006, Spain.
[2]Biomedical Research Networking Center in Bioengineering, Biomaterials and Nanomedicine (CIBER-BBN), Vitoria-Gasteiz 01006, Spain.
[3]Université catholique de Louvain, Louvain Drug Research Institute, Advanced Drug Delivery and Biomaterials, Brussels, Belgium
[4]Integrated Center for Cell Therapy and Regenerative Medicine, International Clinical Research Center (FNUSA-ICRC), St. Anne's University Hospital Brno, Pekařská 53, 656 91, Brno, Czech Republic

ABSTRACT

Drug access to the CNS is hindered by the presence of the blood-brain barrier (BBB), and the intranasal route has risen as a non-invasive route to transport drugs directly from nose-to-brain avoiding the BBB. In addition, nanoparticles (NPs) have been described as efficient shuttles for direct nose-to-brain delivery of drugs. Nevertheless, there are few studies describing NP nose-to-brain transport. Thus, the aim of this work was (i) to develop, characterize and validate *in vitro* olfactory cell monolayers and (ii) to study the transport of polymeric- and lipid-based NPs across these monolayers in order to estimate NP access into the brain using cell penetrating peptide (CPPs) moieties: Tat and Penetratin (Pen). All tested poly(D,L-lactide-co-glycolide) (PLGA) and nanostructured lipid carrier (NLC) formulations were stable in transport buffer and biocompatible with the olfactory mucosa cells. Nevertheless, 0.7 % of PLGA NPs was able to cross the olfactory cell monolayers, whereas 8 % and 22 % of NLC and chitosan-coated NLC (CS-NLC) were transported across them, respectively. Moreover, the incorporation of CPPs to NLC surface significantly increased their transport, reaching 46 % of transported NPs. We conclude that CPP-CS-NLC represent a promising brain shuttle via nose-to-brain for drug delivery.

*Corresponding authors: Ana Beloqui and Véronique Préat

Keywords: Nose-to-brain delivery, NLC, nanoparticles, lipid nanoparticles, CPP, olfactory mucosa

1. Introduction

The search for an effective treatment to address central nervous system (CNS) diseases is a big challenge for the scientific community, taking into account the difficulties that present most drugs to access into the brain (Begley, 2004). Drug access to the CNS is hindered by the presence of the blood-brain barrier (BBB), which limits the free entrance and diffusion of most drugs and other external contents from the bloodstream to the brain (Tajes et al., 2014). In the last years, the intranasal route has risen as a non-invasive route to transport drugs directly from nose-to-brain avoiding the BBB (Illum, 2000). This route of administration links the brain with the nasal cavity at the respiratory epithelium or olfactory neuroepithelium through the trigeminal nerve and the olfactory system, respectively. Due to the fact that these are the only areas of the CNS that are externally exposed, this route represents the most promising non-invasive access into the brain (Mistry, Stolnik and Illum, 2009).

Regarding the olfactory epithelium, it consists of three different cell types: the supporting, the basal and the olfactory neural cells (Illum, 2000). Basal cells supply mechanical support to other cells and are progenitor of supporting cells. The olfactory cells, which are located between the supporting cells, start in the olfactory bulb in the CNS and end at the olfactory epithelium. Therefore, when a drug formulation gets in contact with the nasal mucosa, it is directly transported into the brain via the olfactory pathway (Wu, Hu and Jiang, 2008).

Nevertheless, despite the various benefits of the nasal-to-brain route, such as rapid drug onset, bypassing the BBB, and the avoidance of the first-pass metabolism, it presents certain limitations like the short drug residence time and the insufficient drug absorption across the nasal epithelium due to the mucociliary clearance (Costantino et al., 2007). In order to overcome these drawbacks, several drug delivery systems (DDS) have been developed in order to efficiently transport drugs through the olfactory pathway while protecting them from degradation within the nasal cavity

(Gartziandia et al., 2015, Agrawal et al., 2015, De Luca et al., 2015 and Kaur et al., 2015). Concretely, nanoparticles (NPs) have been described as efficient shuttles for direct nose-to-brain delivery of drugs (Mistry, Stolnik and Illum, 2009).

Among the nanocarriers described so far towards nose-to-brain delivery, polymeric NPs, such as PLGA NPs, offer a controlled drug release, enhanced drug stability and improved entrapment efficiency (Sharma et al., 2014). More recently, these have been evaluated for brain delivery via nasal route (Musumeci et al., 2014). Nevertheless, in the last few years several lipid-based NPs have been designed to transport and deliver drugs to the brain (De Luca et al., 2015, Alam et al., 2014, Devkar, Tekade and Khandelwal, 2014 and Yasir and Sara, 2014). Among these, nanostructured lipid carriers (NLC) have recently shown to efficiently reach the brain upon nasal administration (Gartziandia et al., 2015 and Beloqui et al., 2015). These nanocarriers are made by natural biodegradable and biocompatible lipids, and provide high encapsulation efficiencies and high stability. Moreover, NLC offer well-recognized safety profile and toxicological data (Lim, Banerjee and Önyüksel, 2012). However, several strategies could be followed in order to enhance the access of NLC into the brain. NLC could be surface-modified with the aim of solving their low residence time in the nasal cavity (Vyas et al., 2005). Accordingly, the cationic polysaccharide chitosan (CS) has been reported to offer great mucoadhesive characteristics to NLC increasing their retention time in the nasal cavity and enhancing their penetration through the olfactory cells (Severino et al., 2013 and Dodane, Amin Khan and Merwin, 1999).

Another strategy towards increased NP transport through olfactory cells could be the use of cell-penetrating peptides (CPPs). These short peptides are known for their ability to get into the cells by penetrating cell membranes (Trabulo et al., 2010). Therefore, the adsorption of a CPPs in the nanoparticles' surface could facilitate their entrance across the olfactory cells in order to reach the brain. Among different CPPs, Tat and Penetratin (Pen) are well-known, and have been used to enhance the nose-to-brain delivery of

drugs and/or NPs (Kanazawa et al., 2011 and Kamei and Takeda-Morishita, 2015).

Nevertheless, although there are several studies on brain targeting of NPs after intranasal administration *in vivo* (Patel et al., 2011, Md et al., 2013, Zhang et al., 2014), there are few studies describing nanoparticle nose-to-brain transport (Mistry, Stolnik and Illum, 2009). Thus, the aim of this work was (i) to develop, characterize and validate *in vitro* olfactory cell monolayers and (ii) to study the transport of both polymeric- and lipid-based NPs across these monolayers in order to estimate NP access into the brain using commonly used CPP moieties: Tat and Pen.

2. Materials and Methods

2.1. Materials

Precirol ATO®5 (Glycerol distearate) and Miglyol® 812N/F (Caprylic/Capric Triglyceride) were kindly donated by Gattefosé (France) and Sasol GmbH (Germany), respectively. Tween 80 (polysorbate 80) was purchased from Panreac (Spain) and Lutrol® F-68 (Poloxamer 188) was donated by BASF (Germany). Protasan UP CL 113 CS was obtained from NovaMatrix (Norway). Trehalose dehydrate, poly(vinyl alcohol) (PVA, with an average MW of 30-70 kDa, 87-90% hydrolysis degree), polyethyleneimine (PEI with a MW of 25 kDa, branched), as well as bovine serum albumin (BSA), were bought from Sigma-Aldrich (Spain). DiR DiIC18 (7) (1,1'-Dioctadecyl-3,3,3',3'-Tetramethylindotricarbocyanine Iodide) (DiR) was purchased from Molecular Probes© by Life Technologies (Spain). The polymer poly(D,L-lactide-co-glycolide) PLGA (Resomer RG® 503) 50:50 (lactic/glycolic %), with a MW of 33.9 kDa and an intrinsic viscosity of 0.32–0.4 dl/g was purchased from Boehringer Ingelheim (Germany), and Tat and Pen CPPs from ChinaPeptides, Co., Ltd. (China). MTT (3-[4,5-dimethylthiazol-2-yl]-2,5 diphenyltetrazolium bromide; thiazolyl blue), magnesium chloride ($MgCl_2$), calcium chloride ($CaCl_2$), D-glucose and L-Ascorbic acid were obtained from Sigma-Aldrich (Belgium). Dimethyl sulfoxide (DMSO), sodium carbonate (Na_2CO_3), disodium hydrogen phosphate

dehydrate (Na_2HPO_4 x $2H_2O$) and 4% paraformaldehyde (PFA) were bought from Merck (Germany). Sodium chloride (NaCl) and potassium chloride (KCl) were purchased from VWR Chemicals (Belgium). FluoSpheres® carboxylate 0.2 µm yellow-green (505/515) were purchased from Molecular Probes® by Invitrogen, and Alexa 488-phalloidin and goat anti-mouse IgG (H+L) Alexa 568 from Molecular Probes© by Life Technologies (Belgium). Finally, monoclonal antibody to Mucin-5AC and Matrigel™ were obtained from Acris antibodies, Inc. (USA) and BD Bioscience (Belgium), respectively.

2.2. Cell culture reagents

Dulbecco´s Modified Eagle Medium/Nutrient Mixture F-12 (DMEM-F12), Penicillin-streptomycin (P/S), heat inactivated fetal bovine serum (FBS), Hank's Balanced Salt Solution (HBSS), Trypsin 0.2% EDTA and Dulbecco's phosphate-buffered saline (DPBS) were purchased from Gibco® by Life technologies (Belgium).

2.3. Nanoparticle preparation, characterization and stability studies

2.3.1. Preparation of NLC

NLC were prepared using the melt-emulsification technique (Gartziandia et al., 2015). Firstly, solid and liquid lipids (Precirol AT0®5, 2.5% w/v, and Miglyol®, 0.25% w/v) were melted 5ºC above their melting point (56ºC). Then, 4 ml of an aqueous solution containing the surfactant combination of tween 80 (3%, w/v) and poloxamer 188 (2%, w/v) was heated at the same temperature and added to the lipid phase under continuous stirring for 60 seconds at 50 W (Branson® sonifier 250). The resulting nanoemulsion was maintained under magnetic stirring during 15 min at room temperature (RT) and was immediately cooled down at 4-8ºC overnight to obtain NLCs by lipid solidification.

For the preparation of CS-NLC, NPs were coated with CS. The NP dispersion was added dropwise to an equal volume (4 ml) of a CS solution (0.5%, w/v) under continuous agitation at RT for 20 min. After the coating process, the NLC dispersion was centrifuged in Amicon filters (Amicon, “Ultracel-100k”, Millipore, USA) at 2,500 rpm

(MIXTASEL, P Selecta, Spain) for 15 min, washed three times with Milli Q water and lyophilized for 42 h (LyoBeta 15, Telstar, Spain).

The lyophilization of the resultant NLC and CS-NLC dispersion was carried out adding trehalose (15% w/w) as a cryoprotectant.

The preparation of CPP-CS-NLC was carried out as aforesaid, but prior to the coating process, CPPs were covalently linked to CS by a surface activation method (1-ethyl-3-(-3-dimethylaminopropyl) carbodiimide hydrochloride (EDC)/sulfo-N-hydroxysuccinimide (NHS) chemistry) (Layek, 2013 and Egusquiaguirre et al., 2015b). Briefly, 250 µl of EDC in solution (1 mg/ml) and 250 µl of sulfo-NHS (1 mg/ml) in 0.02 M PBS were added dropwise to a 4 ml CS solution (0.5%, w/v, in PBS 0.02 M), under magnetic stirring (2 h at RT). For the coupling of the CPPs, 250 µl of the CPP solution (1 mg/ml) in PBS (0.02 M; pH 7.4) was added dropwise to the activated CS, under gentle agitation. The CPP-CS solution was maintained under agitation for another 4 h at RT and then incubated at 4°C overnight. On the following day, the NLCs were coated with CPP-CS as described in section 2.3.1; NLC dispersion previously prepared was added dropwise to the CPP-CS solution under continuous agitation for 20 min at RT, followed by the centrifugation and the lyophilization of the resultant CPP-CS-NLC dispersion.

For the preparation of DiR labeled NLC, CS-NLC and CPP-CS-NLC, DiR (0.5% w/w) was incorporated into the lipid phase before the melting step.

2.3.2. Preparation of PLGA nanoparticles

DiR labeled PLGA NPs were prepared by a water-in-oil-in-water ($w_1/o/w_2$) double emulsion solvent evaporation method slightly modified (Egusquiaguirre et al., 2015b). In brief, the primary emulsion (w_1/o) was formed by emulsifying 100 µl of an aqueous solution in 2 ml of a dichloromethane (DCM) solution containing 100 mg of PLGA and 0.5 mg of DiR (0.5 %, w/w) using a probe sonicator (Branson Ultrasonic Sonifier® 250) for 30 s in an ice bath. Subsequently, the primary emulsion was poured into 10

ml of 5% (w/v) PVA aqueous solution and sonicated during 60 s to form a double emulsion ($w_1/o/w_2$). The secondary emulsion was then diluted into 20 ml of 2% (v/v) isopropanol and stirred for 2 h to allow the organic solvent to evaporate. The NPs were then collected by ultracentrifugation at 25,000 g for 20 min at 4°C, and washed three times to remove the excess surfactant. The pellet of NPs was re-suspended in a cryoprotectant solution of trehalose 15% (w/w), prior to lyophilization (LyoBeta 15, Telstar, Spain). The cationic PEI-PLGA NPs preparation was conducted as aforsesaid for PLGA NPs but adding 1.3% (w/w) of PEI in the organic phase.

The covalent link of CPPs onto the PLGA NPs' surface was carried out using an activation method by means of EDC/sulfo-NHS chemistry (Egusquiaguirre et al., 2015b and Yadav, Kumari and Yadav, 2011). Briefly, 100 mg of the NPs were suspended in 5 ml of phosphate buffered saline (PBS; 0.02 M, pH 7.4). After, 250 µl of EDC solution (1 mg/ml) and 250 µl of sulfo-NHS (1 mg/ml) in 0.02 M PBS were added dropwise to the NPs suspension under magnetic stirring agitation (4 h at RT). Then, the unreacted EDC and sulfo-NHS were removed by ultracentrifugation at 25,000 g for 15 min at 4°C, and the activated NPs were recovered. For the coupling of the CPPs, the activated NPs were re-suspended in 2 ml of PBS followed by the addition of 50 µl of the CPP solution (1 mg/ml) in PBS dropwise under gentle agitation. The NPs suspension was left under magnetic stirring (2 h at RT) and then incubated at 4°C overnight. Finally, the unconjugated CPP was removed the next day by ultracentrifugation. The resulting pellet was re-suspended in 15% (w/w) of trehalose solution and lyophilized.

2.3.3. Nanoparticle characterization

The mean diameter (Z-average diameter) and size distribution were measured by Dynamic Light Scattering (DLS), and the zeta potential was determined by Laser Doppler Micro-Electrophoresis (Malvern® Zetasizer Nano ZS, Model Zen 3600; Malvern Instruments Ltd, UK). Three replicate analyses were performed for each formulation, and the data were presented as the mean ± S.D.

2.3.4. Stability of the nanoparticles in transport buffer (HBSS) and artificial cerebrospinal fluid (CSF)

The *in vitro* stability of all the NP formulations was tested first in HBSS, to assess the stability of formulations in the transport buffer and secondly, in a biomimetic media, CSF (6.15g NaCl, 0.216g KCl, 0.447g $MgCl_2$, 0.255g $CaCl_2$, 6.009g Na_2CO_3, 0.057g Na_2HPO_4, 0.613g D-glucose, 0.2g L-ascorbic acid, 0.3g BSA per litre of Milli Q water adjusted to pH 7.35) (Hajos and Mody, 2009), in order to evaluate the stability of the NPs in a more relevant media, thus assessing a foreseen *in vivo* application.

For this purpose, 5 mg of NPs were dispersed in 20 ml of HBSS or CSF and were maintained for 2h at 37ºC under magnetic stirring. The stability assay was carried out in triplicate for each formulation. Samples were withdrawn at time 0 and after 2h of incubation, and the NP size was measured following the procedure described in Section 2.3.3.

The absence of DiR release from NLC and PLGA nanoparticles in transport buffer was assessed by our group in previous studies and thus, not included within the present work (Gartziandia et al., 2015 and Egusquiaguirre et al., 2015a).

2.4. Nasal in vitro cell monolayers

2.4.1. Cell extraction and cell culture

The olfactory mucosa primary cells were extracted from the nasal cavity of 4 female Wistar rats in accordance with the *Université catholique de Louvain* animal committee (2013/UCL/MD/004), following the protocol described by Bianco et al. (Bianco et al., 2004). Briefly, animals were anaesthetized by isoflurane inhalation and killed by decapitation. After removing the lower jaw and surrounding musculature, the lateral and medial cheekbones, and the incisors, the nasal turbinates were exposed. Thereafter, the salivary glands, nasal turbinates, and cartilage were taken out from both sides of the nasal septum to reveal the olfactory mucosa, which was dissected and immediately placed in 1 ml of HBSS and maintained during 10 min at RT. The lamina propria was transferred into 1 ml of Trypsin-0.2% EDTA and incubated at 37°C, 5% CO_2. Five to ten

min later, trypsin activity was stopped by adding 9 ml of HBSS. The cell suspension was then centrifuged at 400 *g* for 5 min and the cell pellet was re-suspended in DMEM/F12 supplemented with 10% FBS and 1% P/S before being placed on culture flasks.

The cells were maintained in DMEM-F12 cell culture medium containing L-glutamine, 10% FBS and 1% P/S at standard conditions (95% relative humidity, 5% CO_2, 37ºC).

2.4.2. Cell monolayer integrity

Olfactory cell monolayers were developed following the previous experience of our research group with other *in vitro* cell models (des Rieux et al., 2007, Rieux et al., 2005, Mathot et al., 2007 and Beloqui et al., 2013). Briefly, Transwell® inserts (1 µm pore diameter, 0.9 cm^2 area) (Corning Costar1, NY) in 12-well plates were coated with Matrigel®, prepared in supplement-free DMEM-F12 to a final 100 µg/ml concentration. Then, 300 µl of this solution was poured onto the inserts (30 µg/cm^2), which were then left at room temperature for 1h. Supernatants were then removed and inserts were twice washed with 500 µl of DMEM-F12. Three different cell ratios, 1.5 x 10^5, 3 x 10^5 and 5 x 10^5 of olfactory mucosa cells, suspended in 500 µl of supplemented DMEM-F12, were seeded on the upper insert side.

The trans-epithelial electrical resistance (TEER) was measured every two days during 21 days to check the TEER values at time points and using the aforesaid cell ratios in order to select the optimum cell ratio and day to perform the transport studies. The measurements were carried out at 37°C in HBSS using an electrode connected to an EVOM® volt-ohmmeter (World Precision Instruments, USA).

2.4.3. Immunocytochemistry (ICC) of Mucin-5AC

The ICC of cells was carried out in Transwell® inserts previously seeded with olfactory cells. The inserts were first fixed in 4% PFA (v/v) and then gently washed in DPBS to thoroughly clean the cells from PFA left-overs. After the washing step, the fixed cells were incubated for 1 h with DPBS + 2.5% BSA to block unspecific binding of the antibodies. The cells were then incubated overnight at 4ºC

with a mouse anti-Mucin5AC antibody, after washing three times with DPBS. This Mucin5AC protein specific antibody was used to characterize the phenotype of olfactory cells (Yunus et al., 2014). Following the incubation with the primary antibody, the inserts were washed 3 times with DPBS and incubated for 1.5 h with a polyclonal (secondary) conjugated antibody (goat anti-mouse IgG (H+L) Alexa 568) for fluorescent staining of proteins, following a 10 min incubation with Alexa 488-phalloidin for staining the actin of the cells. Subsequently, inserts were washed in HBSS, cut and mounted on glass slides. Images were captured using a Zeiss™ confocal microscope (LSM 150). All antibodies were diluted in DPBS + 0.1 % (w/v) BSA + 0.2% (v/v) Triton X-100.

2.4.4. Cytotoxicity studies

To evaluate the cytotoxicity of the different formulations in olfactory mucosa cells, cell viability was assessed after the incubation of 20,000 olfactory cells/well on a 96-well tissue culture plate (Costar® Corning® CellBIND Surface) with the aforementioned NP formulations in dispersion in culture medium (0.01-1.5 mg/ml). Cells were co-incubated for 2 h at 37ºC. After 2 h, the supernatants of each well were removed and the cells were incubated again for 3 h with 100 µL 0.5 mg/mL 3-(4,5-dimethylthiazol-2-yl)-(2,5-diphenyltetrazolium bromide) (Sigma-Aldrich, BE) (MTT assay) (Beloqui et al., 2014). The absorbance was measured at 560 nm using a MultiSkan EX plate reader (Thermo Fisher Scientific, MA, USA). All the studies were made in triplicate.

2.5. NP transport across olfactory cell monolayers

Transport of NPs across olfactory cells was studied quantitatively by fluorescence measurement and qualitatively by confocal laser scanning microscopy (CLSM), for which DiR (λ_{em}=750 nm, λ_{ex}=779 nm) labeled NPs were employed.

The transport of the different NP formulations was evaluated in olfactory mucosa cells 21 days after seeding on Transwell® inserts at a density of 5 x 10^5 cells/insert. Inserts with TEER values above 160 $\Omega \cdot cm^2$ were selected to conduct the transport studies. These

parameters were established based in the results obtained from section 2.4.2.

The experiments were conducted at 37°C by adding a volume of 500 µL at 1 mg/mL NP concentration in HBSS on the apical side of the inserts and 1 mL of HBSS on the basolateral side. After 2 h of incubation, samples were collected from the basolateral side and NP concentration was determined by fluorescence measurement (SpectraMaxM3 (Molecular Devices), software SoftMaxPro 6.2.2.). NP transport was expressed as mean of transported NPs in percentage ± SD.

For the assessment of olfactory mucosa *in vitro* monolayer integrity, the transport of commercial fluorescent carboxylated NPs (0.2 µm) was evaluated under the aforementioned conditions. A NP suspension (500 µL) with final concentration of 4.5×10^9 NPs/mL was added on the apical side and inserts were incubated at 37°C for 2 h (Beloqui et al., 2013). After this incubation time, basolateral solutions were withdrawn and the number of transported NPs was measured using a flow cytometer (BD FACSVerse). NP transport was expressed as mean ± SD. This control was conducted in parallel to each NP transport study to assess the monolayer integrity.

The integrity of the monolayer was also corroborated by measuring the TEER before and after the transport studies on day 21. TEER values were not significantly different to initial values unless otherwise stated.

After transport experiments, cell monolayers were washed twice in cold HBSS and fixed in PFA 4% for subsequent staining.

For the CLSM study, the Transwell® inserts fixed in 4% PFA were gently washed in HBSS. Actin was stained with 200 µL of Alexa 488– phalloidin (1:100) in buffered HBSS+0.2% (v/v) Triton X-100 for 10 min in the dark to reveal cell borders. Subsequently, inserts were washed in HBSS, cut and mounted on glass slides with a Mowiol + DAPI mounting media. Images were captured using a Zeiss™ confocal microscope (LSM 150). Data were analyzed by the Axio Vision software (version 4.8) to obtain *y–z*, *x–z* and *x–y* views of the cell monolayers.

2.6. Statistics

Statistical analysis was performed using the GraphPad Prism 5 program (CA, USA). Normal distribution was assessed with the Shapiro–Wilk normality test. Unpaired student's t-test with Welch correction was applied to compare the transport studies of different formulations, according to the result of the Bartlett's test of homogeneity of variances. All other analyses were performed using a Student's t-test. Differences were considered statistically significant at $*p<0.05$. Results are expressed as mean ± SD.

3. Results and discussion

3.1. Characterization of the nanoparticles

In this study eight different formulations were prepared: four lipid-based NPs and four polymeric NPs. Regarding to lipid-based NPs, four different NLC were developed differing in the surface characteristics (CS-coated or CPP-CS-coated). The PLGA NPs were also modified to obtain four different formulations (PLGA NPs, PEI-coated or CPP-coated PLGA NPs). Table 1 summarizes the mean diameter size and zeta potential of all assayed formulations. All NLC formulations exhibited a mean particle size between 100 and 139 nm, depending on their surface characteristics, since the coating of NPs with CS ($*p < 0.05$), and with CS and CPPs ($**p < 0.01$), led to a significant increased particle size. These particle sizes could be considered appropriate for nose-to-brain delivery, since it has been reported that NPs with average diameters up to 200 nm could be easily transported transcellularly *via* intranasal route (Madane, Mahajan 2015). The coating process had also an effect in the zeta potential, obtaining positively charged nanoparticles (approximately + 35 mV) ($***p < 0.001$). In addition, with the incorporation of CPPs in the NPs, the zeta potential value of CPP-CS coated NLC was significantly increased to + 45 mV ($*p< 0.05$ and $**p < 0.01$, for Tat-CS-NLC and Pen-CS-NLC, respectively) probably due to the positive charge of these moieties (Zorko and Langel, 2005). The average particle size and zeta potential values did not significantly differ ($*p > 0.05$) when NLC were labeled with DiR, demonstrating that its incorporation in NLC does not

alter the physicochemical parameters of the NPs.

Table 1. Physicochemical characterization of blank and DiR labeled NLC and PLGA formulations: size, polydispersity index (PDI) and zeta potential. n=3, data are expressed as mean ± S.D. $p^* < 0.05$, $p^{**} < 0.01$ and $p^{***} < 0.001$ with respect to uncoated NLCs; $p^{\&} < 0.05$ and $p^{\&\&} < 0.01$ with respect to CS-NLCs; $p^{\#\#\#} < 0.001$ with respect to PLGA NPs.

Formulation	Size (nm)	PDI	Zeta potential (mV)
NLC	98.4 ± 10.6	0.29 ± 0.03	(-) 20.2 ± 0.9
NLC-DiR	97.2 ± 14.7	0.35 ± 0.06	(-) 23.4 ± 5.2
CS-NLC	132.7* ± 10.9	0.26 ± 0.01	(+) 37.3*** ± 0.3
CS-NLC-DiR	128.1 ± 3.7	0.31 ± 0.02	(+) 34.7 ± 14.1
Tat-CS-NLC	139.6** ± 9.1	0.28 ± 0.02	(+) 46.8***$^{\&}$ ± 3.7
Tat-CS-NLC-DiR	136.6 ± 11.3	0.30 ± 0.04	(+) 43.4 ± 16.8
Pen-CS-NLC	137.3** ± 6.7	0.35 ± 0.03	(+) 49.5***$^{\&\&}$ ± 3.9
Pen-CS-NLC-DiR	136.9 ± 16.3	0.29 ± 0.06	(+) 43.5 ± 3.4
PLGA	206.6 ± 8.1	0.29 ± 0.01	(-) 20.4 ± 0.3
PLGA-DiR	214.1 ± 0.3	0.11 ± 0.04	(-) 23.1 ± 5.4
PEI-PLGA	243.3 ± 6.1	0.35 ± 0.01	(+) 27.0$^{\#\#\#}$ ± 0.5
PEI-PLGA-DiR	253.3 ± 5.8	0.27 ± 0.04	(+) 23.1 ± 0.2
Tat-PLGA	220.1 ± 9.1	0.22 ± 0.04	(+) 3.2$^{\#\#\#}$ ± 0.2
Tat-PLGA-DiR	236.1 ± 8.2	0.11 ± 0.04	(+) 6.3 ± 0.6
Pen-PLGA	220.5 ± 6.9	0.10 ± 0.01	(+) 4.3$^{\#\#\#}$ ± 0.1
Pen-PLGA-DiR	237.7 ± 8.3	0.29 ± 0.01	(+) 8.1 ± 0.7

Regarding PLGA NPs, the mean particle sizes were found to be around 200 nm, obtaining higher but not significant values after coating them with CPPs ($^*p > 0.05$). The zeta potential of these NPs was around – 20 mV, and as with NLC, the linkage of the CPPs to the NPs led to a significant change in the surface charge, from negative to positive values (around + 5 mV) ($^{\#\#\#}p < 0.001$), confirming the

presence of the CPPs. The incorporation of DiR to the NPs did not significantly change these values (*p > 0.05).

3.2. Stability of the formulations in HBSS and CSF

Table 2 summarizes the particle size and PDI of NLC and PLGA formulations before and after 2 h of incubation in HBSS and CSF. All formulations resulted highly stable in HBSS and in CSF, since the particle size obtained before and after 2 h of incubation in both media were not significantly different (*p > 0.05). Thus, these results demonstrated that all the formulations tested in this study were stable to carry out *in vitro* studies in HBSS, and also for a foreseen *in vivo* application toward targeting the brain, since they resulted stable in the CSF.

Table 2. NP size and PDI measurements after the incubation of NLC and PLGA formulations during 2 h in HBSS and CSF. n = 3, data are expressed as mean ± SD.

		Before incubation		**2h after incubation**	
Formulation	**Medium**	**Size (nm)**	**PDI**	**Size (nm)**	**PDI**
NLC	HBSS	104.4 ± 3.6	0.32 ± 0.03	98.3 ± 20.9	0.33 ± 0.02
	CSF	103.1 ± 23.2	0.31 ± 0.03	111.4 ± 10.3	0.32 ± 0.04
CS-NLC	HBSS	131.6 ± 1.1	0.32 ± 0.03	131.2 ± 0.7	0.28 ± 0.03
	CSF	142.8 ± 7.8	0.29 ± 0.03	142.4 ± 8.6	0.28 ± 0.02
Tat-CS-NLC	HBSS	151.5 ± 9.6	0.28 ± 0.02	152.9 ± 3.7	0.29 ± 0.02
	CSF	155.0 ± 0.2	0.26 ± 0.01	153.3 ± 5.8	0.26 ± 0.01
Pen-CS-NLC	HBSS	155.0 ± 8.8	0.30 ± 0.05	152.3 ± 7.2	0.27 ± 0.01
	CSF	153.2 ± 4.5	0.36 ± 0.05	152.3 ± 2.7	0.35 ± 0.02
PLGA	HBSS	218.3 ± 0.8	0.28 ± 0.01	238.2 ± 19.5	0.32 ± 0.08
	CSF	230.3 ± 9.9	0.24 ± 0.01	244.9 ± 6.8	0.28 ± 0.06
PEI-PLGA	HBSS	245.5 ± 4.8	0.37 ± 0.02	246.8 ± 5.6	0.26 ± 0.08
	CSF	231.1 ± 2.2	0.37 ± 0.02	232.3 ± 3.8	0.36 ± 0.01
Tat-PLGA	HBSS	224.2 ± 4.6	0.08 ± 0.01	229.1 ± 1.2	0.07 ± 0.01
	CSF	217.0 ± 2.7	0.07 ± 0.02	218.1 ± 1.2	0.06 ± 0.01
Pen-PLGA	HBSS	225.1 ± 5.7	0.07 ± 0.03	222.4 ± 5.2	0.03 ± 0.02
	CSF	241.3 ± 7.1	0.14 ± 0.04	237.9 ± 4.2	0.11 ± 0.02

3.3. Validation and characterization of nasal cell monolayers

3.3.1. Assessment of cell monolayer integrity

These monolayers have been developed based on other *in vitro* models (des Rieux et al., 2007), but taking into account the behavioral differences that exist between the different cell lines. The first step was to establish the optimum cellular ratio of olfactory cells in order to form a monolayer in the inserts, and thus, to perform the transport studies. As shown in Figure 1A, after measuring the TEER at three different seeding ratios during 21 days, the ratio 500,000 cells/insert showed the highest TEER value at day 21. Moreover, with this ratio the cells were growing progressively until reaching a constant TEER value from day 16, while the other two ratios showed more irregular TEER values. Thus, it could be hypothesized that cells were not growing in a regular way, and that there were not enough cells to form a monolayer.

The integrity of the monolayer was further confirmed by measuring the number of commercial carboxylated particles transported by flow cytometry (des Rieux et al., 2007, Gullberg et al., 2000 and Rieux et al., 2005). The number of nanoparticles transported was less than 0.001 %.

Therefore, the 500,000 cells/insert ratio and inserts with TEER values above 160 $\Omega \cdot cm^2$ at day 21 were selected to carry out the transport studies.

3.3.2. ICC of Mucin-5AC

Cells were characterized by ICC analysis in order to confirm that extracted and cultured cells were olfactory cells which maintain their specific characteristics, such as the mucus secretion (Illum, 2000). ICC is a useful technique for this purpose, since it is used to stain cells by specific protein markers, allowing their characterization depending on the type of proteins contained. Figure 1B shows positive expression of Mucin-5AC in the cell cytoplasm, a specific protein found in airway epithelium mucus-secreting cells (Yunus et al., 2014), proving that the extracted cells were indeed olfactory cells.

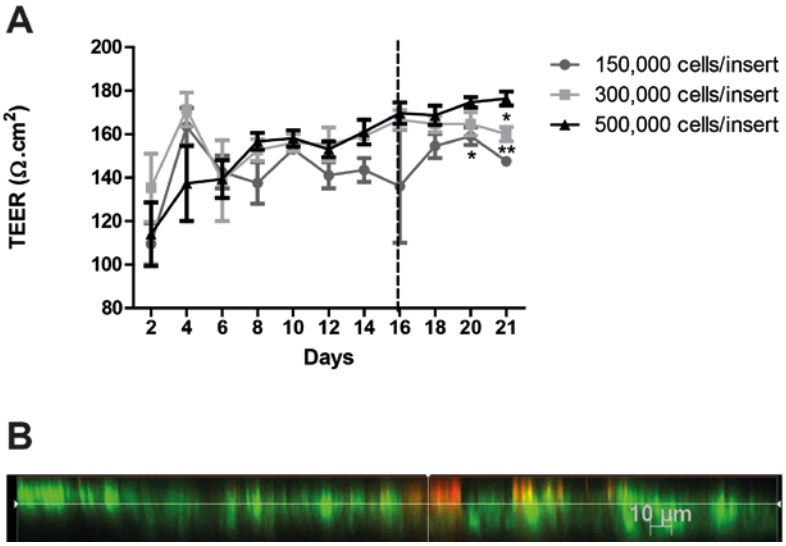

Figure 1. Optimization of the cellular seeding ratio into Transwell® inserts. A) TEER measurement at three different cell ratios (150,000, 300,000 and 500,000 olfactory cells/insert) during 21 days. n=3, results are expressed as mean ± S.D. *p< 0.05 and **p< 0.01, with respect to 500,000 cells/insert ratio. B) *y–z* section of CLSM image of positive Mucin-5AC expression in the cytoplasm (orange). Cells membranes are stained in green with Alexa 488-phalloidin. (For interpretation of the references to color in this figure legend, the reader is referred to the web version of the article).

3.4. Cell viability of olfactory mucosa cells after NP treatment

Before performing the NP transport studies, it was important to assess the safety of the tested formulations for the cells, and to establish the NP concentration that induced no harm. For this purpose, the cell viability was evaluated after 2 h of incubation with all NPs assayed at increasing concentrations (0.01-1.5 mg/ml). As displayed in Figure 2, cell viability was higher than 70% with all formulations whatever the concentration, and therefore, these results demonstrated that all NPs were not toxic and thus, biocompatible with olfactory mucosa cells (Doktorovova, Souto and Silva, 2014).

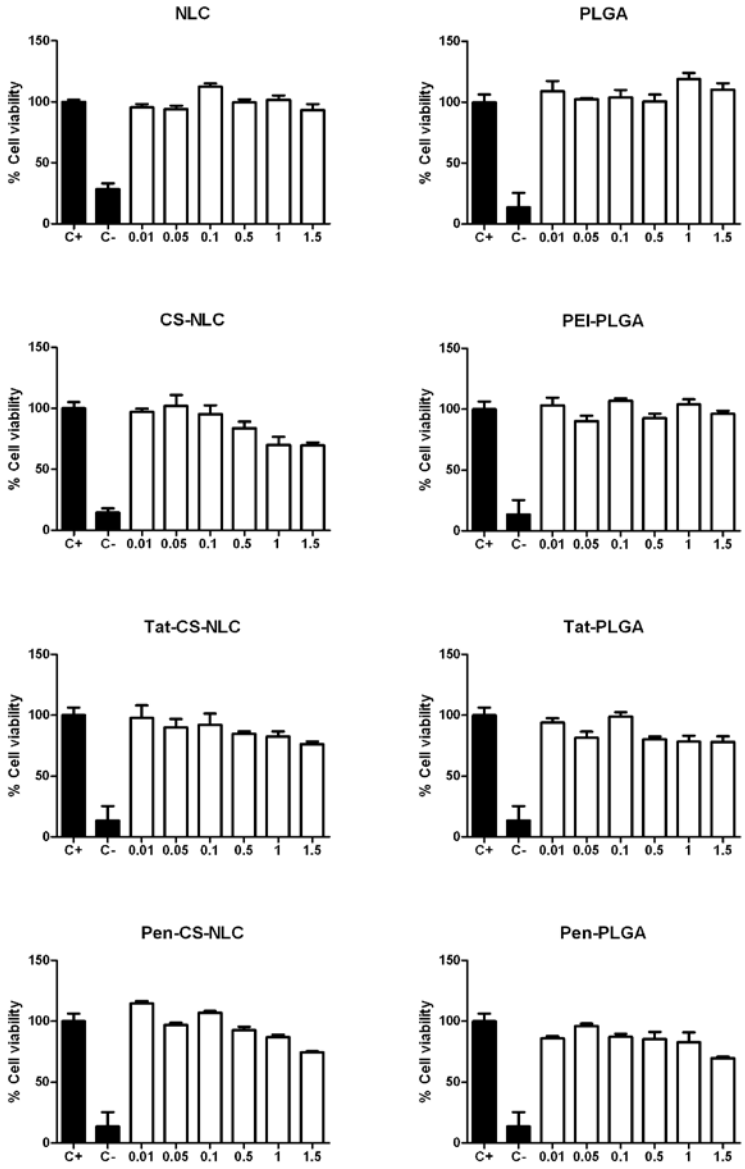

Figure 2. Olfactory mucosa primary cell viability after 2 h of co-incubation with lipid- and polymeric-based NPs (0.01=0.01 NP mg/ml; 0.05=0.05 NP mg/ml; 0.1=0.1 NP mg/ml; 0.5=0.5 NP

mg/ml; 1=1 NP mg/ml; 1.5=1.5 NP mg/ml; C+ (positive control) = culture medium; C- (negative control) = culture medium with 10% DMSO). Results are expressed as cell viability percentage with respect to C+ cell viability, which represents values of 100 %. n=3, results are expressed as mean ± S.D.

3.5. NP transport

Once the nasal *in vitro* cell monolayers were established, and after proving that all NLC and PLGA formulations were stable in the transport buffer and biocompatible with the olfactory mucosa cells, the final step of the study was to evaluate the ability of the different NPs to cross this monolayer. Taking into account that after the nasal administration the olfactory mucosa is the first barrier that NPs have to cross to access directly into the brain (Wu, Hu and Jiang, 2008), selecting the ideal NP formulation in order to achieve the highest possible accumulation in the brain *via* the intranasal administration route remains of great interest. According to Mistry et al., there are three main routes of nanoparticle entrance after a nasal administration: (i) the transport through the nasal epithelium into the systemic circulation (systemic pathway), (ii) the paracellular or transecellular pathway *via* the olfactory neuron (olfactory neural pathway) or the olfactory epithelium (olfactory epithelial pathway) or (iii) the transport *via* the trigeminal nerves (trigeminal pathway) (Mistry et al., 2015). This study was focused on analyzing the ability of NLC to cross a nasal *in vitro* model (olfactory mucosa cell monolayer), and thus, their access to the brain *via* the transepithelial pathways.

Previous studies carried out in our laboratory demonstrated that CS-NLC where accumulated in the brain after being intranasally administered to nude mice (Gartziandia et al., 2015). In order to get a better understanding of modified-NLC transport across the nasal epithelium and to improve this transport, CS-NLC and CPP-modified CS-NLC transports was evaluated *in vitro* across this nasal model. NLC transport was compared to PLGA NP transport in order to evaluate whether lipidic rather than polymeric NPs are better NP candidates towards brain delivery *via* nasal route.

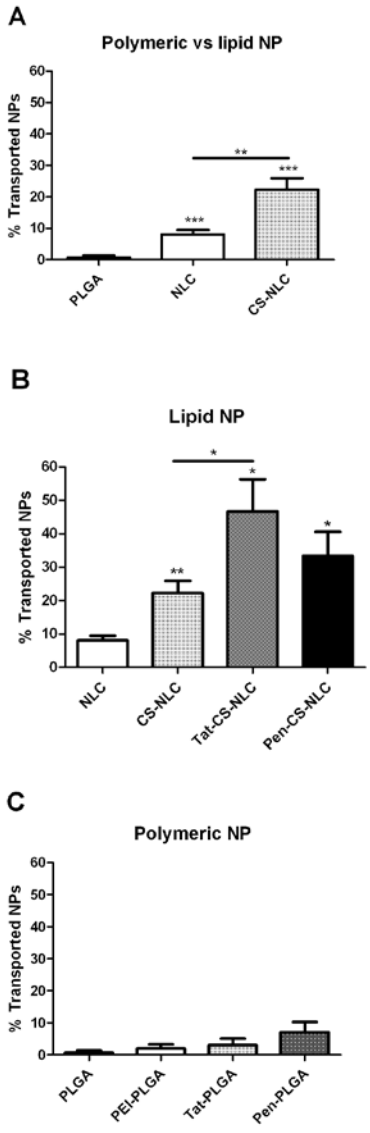

Figure 3. NP transport study across a nasal in vitro model. Percentage of transported NPs across olfactory mucosa cell monolayers after 2 h of co-incubation with different coated and uncoated NLC and PLGA NPs. n= 7-9, results are expressed as mean ± S.D, *p < 0.05, **p < 0.01, ***p < 0.001.

As shown in Figure 3A, on the one hand, when comparing these lipidic nanocarriers with PLGA NPs, the transport of both, coated and uncoated NLC, resulted significantly higher than the percentage of transported PLGA NPs (***p < 0.001). Accordingly, only a 0.7 % of PLGA NPs was able to cross the olfactory cell monolayer, whereas an 8 % and a 22 % of NLC and CS-NLC were transported across the nasal monolayers, respectively. These results bring to mind the data obtained by other researchers after studying the transport of PLGA-based NPs in M cells, where these NPs were successfully transported, whereas in caco-2 cells not, suggesting that the transport of different nanocarriers depends on the cell type (Garinot et al., 2007). Thus, our finding suggests that lipid-based NPs could result more appropriate than polymeric NPs for the intranasal administration. It is true that some authors have reported the use of PLGA NPs for nose-to-brain delivery (Sharma et al., 2015 and Seju, Kumar and Sawant, 2011). In these studies the authors detected the

encapsulated compound in the brain, but not the NP itself, and it is possible, therefore, that the NPs were retained in the nasal mucosa and the encapsulated compound released to the brain (Sharma et al., 2015 and Seju, Kumar and Sawant, 2011). On the other hand, comparing CS-coated with uncoated NLCs, the percentage of transported NPs was significantly higher when NLC were coated with the cationic polysaccharide CS (CS-NLC) (**$p < 0.01$). Thus, it has been demonstrated the ability of positively charged cationic NPs for being easily attracted by endothelial cells, probably due to electrostatic interactions between positively charged NPs and negatively charged cell membranes, enhancing the cellular absorption of these NPs across the olfactory cells (Severino et al., 2013 and Dodane, Amin Khan and Merwin, 1999). Moreover, CS NPs possess intrinsic properties that include mucoadhesion and the ability of transiently open the tight junctions (Behrens et al., 2002, Trapani et al., 2010 and Rassu et al., 2015). Regarding to the unalterated TEER values after the co-incubation of cells with CS-coated NLC, we discarded the tight junction opening as an alternative mechanism of transport of these NPs across olfactory cells. CS-coated NLC might adhere to the surface of the olfactory cells, thus increasing their interaction and transport across olfactory cells. However, further mechanistic studies need to be conducted in order to unravel this mechanism of transport. These results justify the use of lipid NPs over polymeric and the use of CS as coating agent towards increased nasal penetration.

After confirming that the coating of NLC with CS had a significant influence in the enhancement of the transported NPs across the olfactory cells, the other aim of this work was to evaluate whether the incorporation of a CPP to the CS-NLC formulation could improve CS-NLC transport. The CPPs are known for their ability to effectively penetrate across the cell membrane without the need of a receptor (Drin et al., 2003). Concretely, in this study Tat and Pen peptides were incorporated into CS-NLCs, which have been shown to increase the nasal absorption of NPs (Kanazawa et al., 2011, Kamei, Takeda-Morishita 2015).

Interestingly, we observed a significant increase in the percentage of transported Tat-CS-NLC compared to CS-NLC and NLC (*$p < 0.05$, Figure 3B), reaching 46 % of transported Tat-CS coated NLC. Regarding to Pen-CS-NLC, the percentage of transported NPs was found to be 33 %, but not significantly higher than CS-NLC ($p > 0.05$). The absence of significance could be due to the high variability (SD = 18.99%). Although the cationic (PEI-PLGA) and CPP coated (Tat-PLGA and Pen-PLGA) NPs showed higher transport than uncoated PLGA NPs, no significant differences were observed on PLGA transport across the nasal cell monolayers whatever the formulation ($p>0.05$), and the values ranged from 0.7 to 7 % of transported NPs. All formulations, either coated or uncoated, lipid or polymeric were located within the nasal cell monolayers (data not shown). Figure 4 shows the *y-z* sections of NLC, CS-NLC and Pen-CS-NLC. It can be observed that the presence of NLC (in red) within the monolayers corresponds to the amounts encountered for the basolateral chambers of the Transwell® (NLC<CS-NLC<Pen-CS<Tat-CS-NLC). Figure 4B shows the localization of Tat-CS-NLC, the formulation exhibiting the highest transport rate, within the olfactory cells.

These findings demonstrated the ability of lipid-based *versus* polymeric NPs to cross the nasal epithelium. The incorporation of a CPP to the CS-NLC formulation enhanced the *in vitro* transport of CS-NLC across a nasal cell monolayer. Hence, CPP-CS-NLC represent promising nose-to-brain delivery systems to be tested in future *in vivo* studies, needed to provide quantitative proof of the nanoparticle access to the brain.

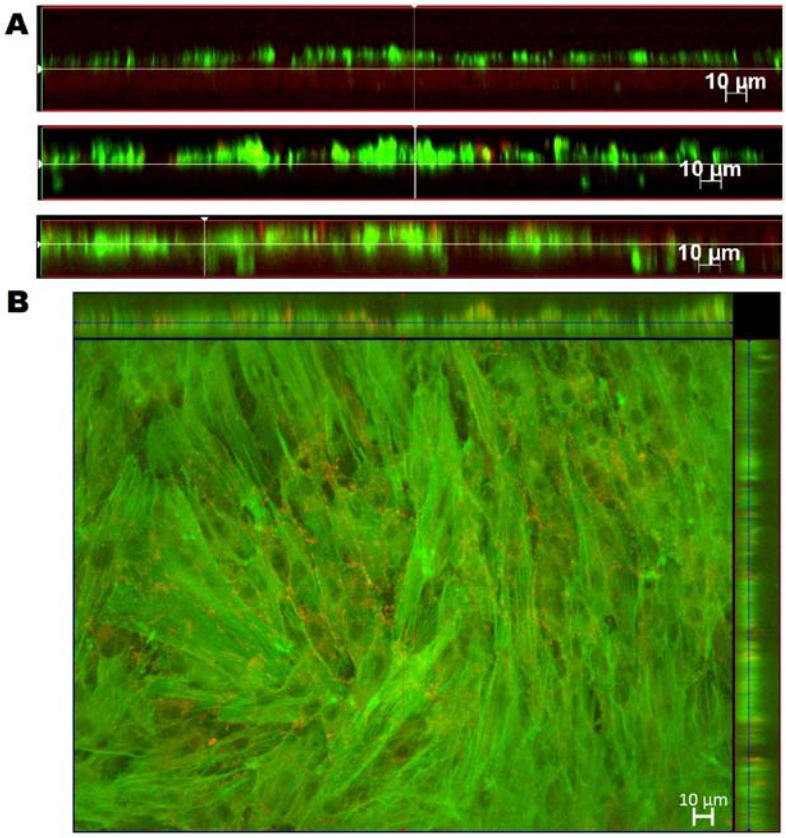

Figure 4. CLSM images corresponding to NLC formulations. A) y-z sections of NLC, CS-NLC and Pen-CS-NLC, top-bottom, respectively. B) *y-z*, *x–y* and *x-z* sections of Tat-CS-NLC CLSM image with which the higher uptake rate was recorded after 2 h of co-incubation with olfactory cells. Cell membranes are stained in green with Alexa488-phalloidine. NPs are stained in red.

4. Conclusion

In this study an *in vitro* olfactory cell monolayer has been validated to evaluate NP nasal-to-brain delivery. This system is a valuable tool to evaluate the potential of different NPs to access the brain through the nasal route. All tested NLC formulations were able to cross the olfactory cell monolayer, and their transport was significantly enhanced with the incorporation of CPPs and CS to their surface. All in all, CPP-CS-NLC seem to

be promising brain shuttles *via* nose-to-brain route. However, to further confirm CPP-CS-NLC nasal-penetration, these *in vitro* results should be verified in the *in vivo* animal studies.

5. Acknowledgements

This project was partially supported by the "Ministerio de Economía y Competitividad" (SAF2013-42347-R), the University of the Basque Country (UPV/EHU) (UFI 11/32), and FEDER funds. O. Gartziandia thanks the University of the Basque Country for a fellowship grant. J. Bianco is a recipient of subsidies from the *Fonds National de la Recherche Scientifique* (FNRS/FRSM) and was supported by European Regional Development Fund – Project FNUSA-ICRC (No. CZ.1.05/1.1.00/02.0123) and by the project ICRC-ERA-HumanBridge (No. 316345) funded by the 7th Framework Programme of the European Union. A. Beloqui is a postdoctoral researcher from the Belgian *Fonds National de la Recherche Scientifique* (F.R.S. — FNRS).

6. References

Agrawal, U., Chashoo, G., Sharma, P.R., Kumar, A., Saxena, A.K., Vyas, S.P. 2015. Tailored polymer–lipid hybrid nanoparticles for the delivery of drug conjugate: Dual strategy for brain targeting. Colloids Surf. B Biointerfaces. 126, 414-425.

Alam, M.I., Baboota, S., Ahuja, A., Ali, M., Ali, J., Sahni, J.K., Bhatnagar, A. 2014. Pharmacoscintigraphic evaluation of potential of lipid nanocarriers for nose-to-brain delivery of antidepressant drug. Int. J. Pharm. 470, 99-106.

Begley, D.J. 2004. Delivery of therapeutic agents to the central nervous system: the problems and the possibilities. Pharmacol. Ther.104, 29-45.

Behrens, I., Pena, A.I., Alonso, M.J., Kissel, T. 2002. Comparative uptake studies of bioadhesive and non-bioadhesive nanoparticles in human intestinal cell lines and rats: the effect of mucus on particle adsorption and transport. Pharm. Res. 19, 1185-1193.

Beloqui, A., Solinis, M.A., Gascon, A.R., del Pozo-Rodriguez, A., des Rieux, A., Préat, V. 2013. Mechanism of transport of saquinavir-loaded nanostructured lipid carriers across the intestinal barrier. J. Control. Release. 166, 115-123.

Beloqui, A., Solinís, M.Á., Rieux, A.d., Préat, V., Rodríguez-Gascón, A. 2014. Dextran–protamine coated nanostructured lipid carriers as mucus-penetrating nanoparticles for lipophilic drugs. Int. J. Pharm. 468, 105-111.

Beloqui, A., Solinís, M.Á., Rodríguez-Gascón, A., Almeida, A.J., Préat, V. 2016. Nanostructured Lipid Carriers: promising drug delivery systems for

future clinics. Nanomedicine. 12, 143-161.

Bianco JI, Perry C, Harkin DG, Mackay-Sim A, Féron F. 2004. Neurotrophin 3 Promotes Purification and Proliferation of Olfactory
Ensheathing Cells From Human Nose. Glia. 45, 111-123.

Costantino, H.R., Illum, L., Brandt, G., Johnson, P.H. & Quay, S.C. 2007. Intranasal delivery: Physicochemical and therapeutic aspects. Int J Pharm. 337 (1–2), 1-24.

De Luca, M.A., Lai, F., Corrias, F., Caboni, P., Bimpisidis, Z., Maccioni, E., Fadda, A.M., Di Chiara, G. 2015. Lactoferrin- and antitransferrin-modified liposomes for brain targeting of the NK3 receptor agonist senktide: Preparation and in vivo evaluation. Int. J. Pharm. 479, 129-137.

des Rieux, A., Fievez, V., Théate, I., Mast, J., Préat, V., Schneider, Y. 2007. An improved in vitro model of human intestinal follicle-associated epithelium to study nanoparticle transport by M cells. Eur. J. Pharm. Sci. 30, 380-391.

Devkar, T.B., Tekade, A.R. & Khandelwal, K.R. 2014. Surface engineered nanostructured lipid carriers for efficient nose to brain delivery of ondansetron HCl using Delonix regia gum as a natural mucoadhesive polymer. Colloids Surf. B Biointerfaces. 122, 143-150.

Dodane, V., Amin Khan, M., Merwin, J.R. 1999. Effect of chitosan on epithelial permeability and structure. Int. J. Pharm. 182, 21-32.

Doktorovova, S., Souto, E.B., Silva, A.M. 2014. Nanotoxicology applied to solid lipid nanoparticles and nanostructured lipid carriers - a systematic review of in vitro data. Eur. J. Pharm. Biopharm. 87, 1-18.

Drin, G., Cottin, S., Blanc, E., Rees, A.R., Temsamani, J. 2003. Studies on the internalization mechanism of cationic cell-penetrating peptides. J. Biol. Chem. 278, 31192-31201.

Egusquiaguirre, S.P., Beziere, N., Pedraz, J.L., Hernandez, R.M., Ntziachristos, V., Igartua, M. 2015a. Optoacoustic imaging enabled biodistribution study of cationic polymeric biodegradable nanoparticles. Contrast Media Mol Imaging. In press.

Egusquiaguirre, S.P., Manguán-García, C., Pintado-Berninches, L., Iarriccio, L., Carbajo, D., Albericio, F., Royo, M., Pedraz, J.L., Hernández, R.M., Perona, R., Igartua, M. 2015b. Development of surface modified biodegradable polymeric nanoparticles to deliver GSE24.2 peptide to cells: A promising approach for the treatment of defective telomerase disorders. Eur. J. Pharm. Biopharm. 91, 91-102.

Garinot, M., Fiévez, V., Pourcelle, V., Stoffelbach, F., des Rieux, A., Plapied, L., Theate, I., Freichels, H., Jérôme, C., Marchand-Brynaert, J., Schneider, Y., Préat, V. 2007. PEGylated PLGA-based nanoparticles targeting M cells for oral vaccination. J. Control. Release. 120, 195-204.

Gartziandia, O., Herran, E., Pedraz, J.L., Carro, E., Igartua, M., Hernandez, R.M. 2015. Chitosan coated nanostructured lipid carriers for brain delivery of proteins

by intranasal administration. Colloids Surf. B Biointerfaces. 134, 304-313.

Gullberg, E., Leonard, M., Karlsson, J., Hopkins, A.M., Brayden, D., Baird, A.W., Artursson, P. 2000. Expression of Specific Markers and Particle Transport in a New Human Intestinal M-Cell Model. Biochem. Biophys. Re.s Commun. 279, 808-813.

Hajos, N., and Mody, I. 2009. Establishing a physiological environment for visualized in vitro brain slice recordings by increasing oxigen supply and modifying aCSF content. J Neurosci Methods. 183, 107-113.

Illum, L. 2000. Transport of drugs from the nasal cavity to the central nervous system. Eur. J. Pharm. Sci. 1, 1-18.

Kamei, N. and Takeda-Morishita, M. 2015. Brain delivery of insulin boosted by intranasal coadministration with cell-penetrating peptides. J. Control. Release. 197, 105-110.

Kanazawa, T., Taki, H., Tanaka, K., Takashima, Y., Okada, H. 2011. Cell-penetrating peptide-modified block copolymer micelles promote direct brain delivery via intranasal administration. Pharm. Res. 28, 2130-2139.

Kaur, P., Garg, T., Vaidya, B., Prakash, A., Rath, G., Goyal, A.K. 2015. Brain delivery of intranasal in situ gel of nanoparticulated polymeric carriers containing antidepressant drug: behavioral and biochemical assessment. J. Drug Target. 23, 275-286.

Layek B, S.J. 2013. Cell penetrating peptide conjugated polymeric micelles as a high performance versatile nonviral gene carrier. Biomacromolecules. 14, 4071-4081.

Lim, S.B., Banerjee, A., Önyüksel, H. 2012. Improvement of drug safety by the use of lipid-based nanocarriers. J. Control. Release. 163, 34-45.

Madane, R.G. and Mahajan, H.S. 2015. Curcumin-loaded nanostructured lipid carriers (NLCs) for nasal administration: design, characterization, and in vivo study. Drug Deliv. 1-9.

Mathot, F., des Rieux, A., Ariën, A., Schneider, Y., Brewster, M., Préat, V. 2007. Transport mechanisms of mmePEG750P(CL-co-TMC) polymeric micelles across the intestinal barrier. J. Control. Release. 124, 134-143.

Md, S., Khan, R.A., Mustafa, G., Chuttani, K., Baboota, S., Sahni, J.K., Ali, J. 2013. Bromocriptine loaded chitosan nanoparticles intended for direct nose to brain delivery: Pharmacodynamic, Pharmacokinetic and Scintigraphy study in mice model. Eur. J. Pharm. Sci. 48, 393-405.

Mistry, A., Stolnik, S., Illum, L. 2009. Nanoparticles for direct nose-to-brain delivery of drugs. Int. J. Pharm. 379, 146-157.

Mistry, A., Stolnik, S., Illum, L. 2015. Nose-to-brain delivery: investigation of the transport of nanoparticles with different surface characteristics and sizes in excised porcine olfactory epithelium. Mol. Pharm. 12, 2755-66.

Musumeci, T., Pellitteri, R., Spatuzza, M., Puglisi, G. 2014. Nose-to-brain delivery: evaluation of polymeric nanoparticles on

olfactory ensheathing cells uptake. J. Pharm. Sci. 103, 628-635.

Patel, S., Chavhan, S., Soni, H., Babbar, A.K., Mathur, R., Mishra, A.K., Sawant, K. 2011. Brain targeting of risperidone-loaded solid lipid nanoparticles by intranasal route. J. Drug Target. 19, 468-474.

Rassu, G., Soddu, E., Cossu, M., Gavini, E., Giunchedi, P., Dalpiaz, A. 2015. Particulate formulations based on chitosan for nose-to-brain delivery of drugs. A review. J. Drug Deliv. Sci. Technol. In press.

Rieux, A.d., Ragnarsson, E.G.E., Gullberg, E., Préat, V., Schneider, Y., Artursson, P. 2005. Transport of nanoparticles across an in vitro model of the human intestinal follicle associated epithelium. Eur. J. Pharm. Sci. 25, 455-465.

Seju, U., Kumar, A., Sawant, K.K. 2011. Development and evaluation of olanzapine-loaded PLGA nanoparticles for nose-to-brain delivery: In vitro and in vivo studies", Acta Biomater. 7, 4169-4176.

Severino, P., Souto, E.B., Pinho, S.C., Santana, M.H. 2013. Hydrophilic coating of mitotane-loaded lipid nanoparticles: preliminary studies for mucosal adhesion. Pharm. Dev. Technol. 18, 577-581.

Sharma, D., Maheshwari, D., Philip, G., Rana, R., Bhatia, S., Singh, M., Gabrani, R., Sharma, S.K., Ali, J., Sharma, R.K., Dang, S. 2014. Formulation and optimization of polymeric nanoparticles for intranasal delivery of lorazepam using Box-Behnken design: in vitro and in vivo evaluation. Biomed. Res Int. 156010.

Sharma, D., Sharma, R.K., Sharma, N., Gabrani, R., Sharma, S.K., Ali, J., Dang, S. 2015. Nose-To-Brain Delivery of PLGA-Diazepam Nanoparticles. AAPS PharmSciTech.

Tajes, M., Ramos-Fernandez, E., Weng-Jiang, X., Bosch-Morato, M., Guivernau, B., Eraso-Pichot, A., Salvador, B., Fernandez-Busquets, X., Roquer, J., Munoz, F.J. 2014. The blood-brain barrier: structure, function and therapeutic approaches to cross it. Mol. Membr. Biol. 31, 152-167.

Trabulo, S., Cardoso, A.L., Mano, M., MCP, D.L. 2010. Cell-penetratingpeptides—mechanisms of cellular uptake and generation of delivery systems. Pharmaceuticals. 3, 961-993.

Trapani, A., Lopedota, A., Franco, M., Cioffi, N., Ieva, E., Garcia-Fuentes, M. & Alonso, M.J. 2010. A comparative study of chitosan and chitosan/cyclodextrin nanoparticles as potential carriers for the oral delivery of small peptides. Eur. J. Pharm. Biopharm. 75, 26-32.

Vyas TK, Shahiwala A, Marathe S, Misra A. 2005. Intranasal drug delivery for brain targeting. Curr. Drug Deliv. 2, 165-175.

Wu, H., Hu, K., Jiang, X. 2008. From nose to brain: understanding transport capacity and transport rate of drugs. Expert Opin. Drug Deliv. 5, 1159-1168.

Yadav, S.C., Kumari, A., Yadav, R. 2011. Development of peptide and protein nanotherapeutics by nanoencapsulation and nanobioconjugation. Peptides. 32, 173-187.

Yasir, M. and Sara, U.V.S. 2014. Solid lipid nanoparticles for nose to brain

delivery of haloperidol: in vitro drug release and pharmacokinetics evaluation. Acta Pharmaceutica Sinica B. 4, 454-463.

Yunus, M.H., Siang, K.C., Hashim, N.I., Zhi, N.P., Zamani, N.F., Sabri, P.P., Busra, M.F., Chowdhury, S.R., Idrus, R.B. 2014. The effects of human serum to the morphology, proliferation and gene expression level of the respiratory epithelium in vitro. Tissue Cell. 46, 233-240.

Zhang, C., Chen, J., Feng, C., Shao, X., Liu, Q., Zhang, Q., Pang, Z., Jiang, X. 2014. Intranasal nanoparticles of basic fibroblast growth factor for brain delivery to treat Alzheimer's disease. Int. J. Pharm. 461, 192-202.

Zorko, M. and Langel, Ü. 2005. Cell-penetrating peptides: mechanism and kinetics of cargo delivery. Adv. Drug Deliv. Rev. 57, 529-545.

Discussion

In recent years, the prevalence of people living with neurodegenerative diseases (NDs) has dramatically increased. These disorders are characterized by a progressive loss of neuronal structure and function in the brain and spinal cord, leading to alterations in different motor, cognitive, sensory and emotional functions of the patients. NDs include different unusual disorders such as Huntington`s disease (HD) and amyotrophic lateral sclerosis (ALS), while Alzheimer's disease (AD) and Parkinson's disease (PD) are among the most common age-related NDs (Foster ER 2014).

Although the treatments of AD and PD are the main priority for the neurologist community, to date, there is no cure for these two diseases, neither for HD nor ALS, and the current therapies are focused on modifying the disease progression and symptoms, with insufficient or null effect on the improvement of the disease (Deierborg, et al. 2008). Moreover, due to the high economic burden of the treatments, the patient care is abundant and growing. In this sense, recent research advances have been focused on new therapies able to overcome the neurodegenerative process and to provide neuroprotection to the surviving cells.

In this line, selective growth factors (GFs) have become an interesting therapy since they are able to provide neuroprotective, neurorestorative and stimulating effects on diseased neurons. GFs are a group of different molecular families and individual proteins with the ability to enhance cellular growth, proliferation and differentiation. Furthermore, they are also well known for playing important roles in tissue morphogenesis, angiogenesis, cell differentiation and neurite outgrowth (Ciesler and Sari 2013; Levy, et al. 2005; Poon, Choi and Park 2013). However, these factors present some shortcomings that limit their clinical application, mainly due to their poor capacity to cross the blood-brain barrier (BBB), and thus to access into the brain, as well as to their short circulation half-life and rapid degradation rate after *in vivo* administration. Therefore, significant attempts have already been made to design different and promising drug delivery systems (DDS) to protect neurotrophins and release them into the brain in a control manner, thereby, dealing with the limitations that these factors present to access into the brain.

In this regard, poly (lactic-co-glycolic acid) microspheres (PLGA-MS) and nanospheres (PLGA-NS) loaded with neurotrophic factors have been extensively studied by our research group (Herrán, et al. 2013a; Herrán, et al. 2013b; Herrán, et al. 2014) and other researchers (Garbayo, et al. 2011; Jollivet, et al. 2004), obtaining promising results to deal with the PD and AD. Accordingly, in one of these works carried out by our research group both glial-derived neurotrophic factor (GDNF) alone and the combination of GDNF and vascular endothelial growth factor (VEGF) microencapsulated into PLGA-MSs demonstrated regenerative effects in a severely lesioned rat model of PD, after their intrastriatal administration (Herrán, et al. 2013b). In a second study, VEGF and GDNF were encapsulated in PLGA-NSs to evaluate the synergistic effect of these two GFs in a partial lesion model of PD. Following the striatal implantation of both formulations, a synergistic effect was observed in the group which received the combined therapy, where the number of amphetamine-induced rotations decreased more significantly compared to the groups that received one of the GFs. Moreover, tyrosine hydroxylase (TH) immunohistochemical analysis in the striatum and external substantia nigra (SN) confirmed a notable enhancement of neurons in the group treated with VEGF and GDNF-loaded NS (Herrán, et al. 2014). Finally, in a third study carried out by our research group, VEGF-loaded PLGA-NS administered by craniotomy demonstrated to be a potential therapeutic strategy to achieve behavioral improvements in an APP/Ps1 mouse model of AD. Moreover, Aβ deposits were significantly decreased in the whole brain, including cerebral cortex, striatum and hippocampus, and VEGF-NS were also able to promote angiogenesis (Herrán, et al. 2013a). In addition, these VEGF loaded PLGA-NS were able to induce the activation of the proliferation and maturation of neuronal precursors, which in turn may enhance the improvements in memory deficits in APP/Ps1 mice (Herran, et al. 2015).

Nevertheless, in the aforementioned works the treatments were administered using invasive approaches in order to avoid the BBB, and that limits their use for a possible clinic application. Therefore, in the search for less invasive techniques, in the past few years intranasal drug delivery has appeared as an alternative non-invasive administration route to bypass the BBB and target drugs directly to the central nervous system (CNS) through the

olfactory and trigeminal nerve pathways (Dhuria, et al. 2010; Graff and Pollack 2005). Due to the fact that these are the only areas of the CNS that are externally exposed, this route represents the most promising non-invasive access into the brain (Mistry, et al. 2009). Accordingly, the nasal mucosa provides several benefits as a target for drug delivery, including large surface area, rapid drug onset, potential for CNS delivery, and no first-pass metabolism. However, the major disadvantages of this administration route are the limited absorption across the nasal epithelium and the short residence time in the nasal cavity due to the mucociliary clearance, causing uncompleted drug absorption (Costantino, et al. 2007). In order to overcome these drawbacks, nanoparticles (NPs) have been described as efficient shuttles to efficiently transport drugs through the olfactory pathway while protecting them from degradation within the nasal cavity (Mistry, et al. 2009). Among these, lipid-based nanocarriers seem good candidates to achieve brain delivery as they could be readily transported to the brain due to their lipid nature (Blasi, et al. 2007; Gobbi, et al. 2010; Kaur, et al. 2008).

Bearing these considerations in mind, in this doctoral thesis we have focused on the preparation of nanostructured lipid carriers (NLCs) for intranasal (i.n.) administration. These lipid-based nanocarriers, which are the second improved generation derived from solid lipid nanoparticles (SLN), are composed of biodegradable and biocompatible lipids and provide high encapsulation efficiencies and high stability (Beloqui, et al. 2016). Moreover, NLCs offer well-recognized safety profile and toxicological data (Lim, et al. 2012). In addition, several strategies could be followed in order to enhance their access into the brain. NLCs could be surface-modified with the aim of solving their low residence time in the nasal cavity (Vyas, et al. 2005). Accordingly, the cationic polysaccharide chitosan (CS) exhibits good mucoadhesive properties, together with penetration enhancement characteristics across various mucus epithelia and enzyme-inhibiting properties (Dharmala, et al. 2008; Sandri, et al 2010; Severino, et al. 2013). Therefore, the coating of NLCs with CS could result a good approach to try to enhance the nasal transport of NLCs to the brain.

All in all, the first step of this work was the design and optimization of a CS-NLC formulation to obtain mucoadhesive and positively charged NPs with an adequate particle size for promoting the delivery of neurotrophic factors to the brain after intranasal administration. To attain this purpose, various concentrations of commonly used solid (Precirol® ATO5 or Dynasan® 114) and liquid (Miglyol® 812N/F) lipids, and various percentages of selected surfactants were tested (Leonardi, et al. 2014), and NPs were prepared using the melt-emulsification method (Gartziandia, et al. 2015). After process optimization, the composition of the selected NLC formulation was: Precirol 2.5% (w/v), Miglyol 0.25% (w/v), Tween 80 (T80) 3% (w/v) and Poloxamer 2% (w/v). The NLCs presented a particle size of 72.17 ± 8.55 nm, with a PDI of 0.364 ± 0.22 and a zeta potential of -28.2 ± 1.32 mV. After being coated with CS and loaded with a model neurotrophic factor (IGF-I) (0.5%, w/w) the particle size increased to 114.48 ± 20.20 nm, with a PDI of 0.287 ± 0.05, and a positive zeta potential value (+ 28.4 ± 2.83 mV), suggesting that CS was adhered to the NPs surface. The CS-NLC-IGF-I exhibited a spherical morphology and uniform size (Figure 1A), with a high encapsulation efficiency, around 90%, and thus, it was considered as an adequate delivery system for future applications in NDs.

In regard to the NLCs elaborated with Dynasan 114 solid lipid, the particle size of these formulations was higher than in those prepared with Precirol ATO5 using the same amounts of surfactants and lipid. Moreover, the PDI value of most of these formulations was above 0.4, indicating a non-stable polydisperse system. Therefore, because the previously described Precirol formulation presented a lower particle size and PDI value, the Dynasan formulations were discarded for this application.

Following the intranasal administration of CS-NLCs, the NPs came into contact with the nasal epithelial cells, which are the first barrier that CS-NLCs must overcome to reach the brain. Thus, in order to determine the cytotoxicity and cell uptake capability of our formulation, *in vitro* tests were undertaken in 16HBE14o- cells, a cell line widely used for *in vitro* studies of NPs developed for nose-to-brain delivery (Sapsforda, et al. 1990; Xia, et al. 2011). Since it is assumed that cell viability >70% is considered “no toxicity”

(Doktorovova, et al. 2014), the data obtained from this study suggest the biocompatibility of the formulation tested with 16HBE14o- cells, maintaining cell viability during 72h (Figure 1B). As shown in Figure 1C, the cellular uptake of CS-NLCs by these cells was also confirmed.

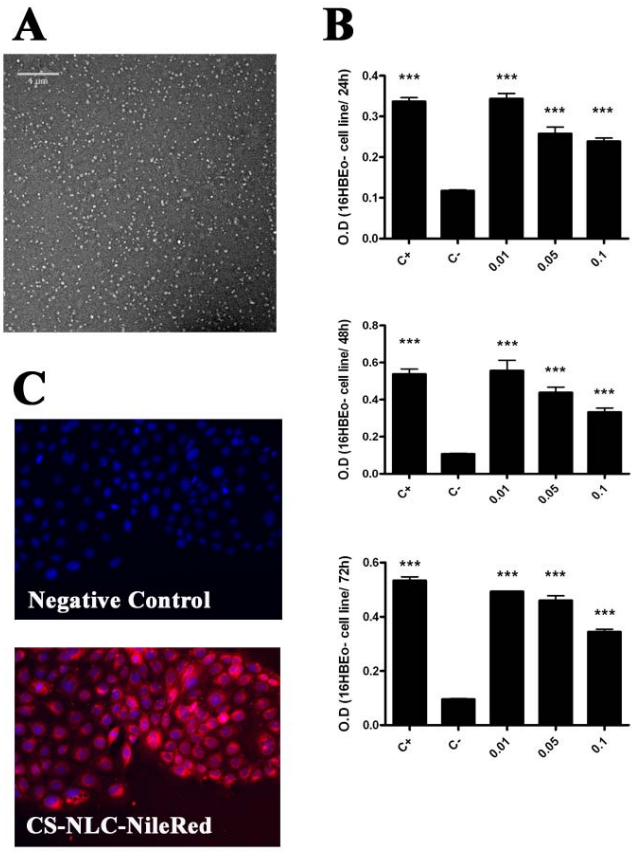

Figure 1. Morphology and *in vitro* studies of CS-NLCs A) TEM photomicrograph of CS-NLCs. **B)** Viability evaluation in 16HBE14o- cell line cultures at 24, 48 and 72 h after CS-NLCs treatment (0.01, 0.05, 0.1 CS-NLCs mg/ml; C+ (positive control) = culture medium with PBS; C- (negative control) = culture medium with 10% DMSO). The data are shown as the mean ± SD. ***p< 0.001. **C)** Cellular uptake of CS-NLC-NileRed (25 µg) after incubation with 16HBE14o- cells for 4 h. The image on the top is the negative control, in which cells were not incubated with NileRed loaded nanoparticles. The image below shows the cells incubated with the nanoparticles, NileRed labelled nanoparticles (in red) and cell nuclei stained with DAPI (in blue).

Furthermore, in order to assess the in vivo nasal toxicity of our formulation, the CS-NLCs were i.n. administered to C57 mice for 15 consecutive days. After the histopathological analysis of the harvested mice nasal mucosa, no histopathological lesions that could indicate toxicity were detected (Figure 2).

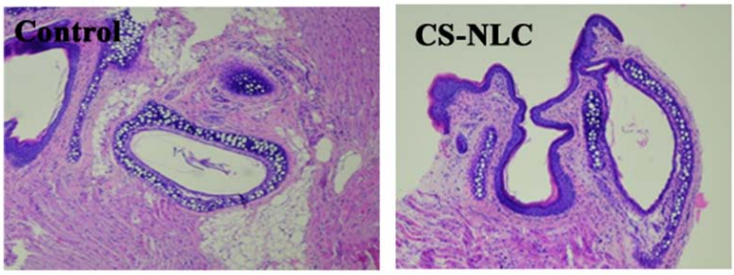

Figure 2. Nasal toxicity study. Representative photomicrographs of the entire nasal mucosa/cavity biopsies in C57 mice after i.n. administration of PBS (control) or CS-NLCs. Nasal sections were stained with haematoxylin/eosin and observed under a light microscope (40X).

As mentioned before, the drug delivery to the brain for the treatment of NDs is hindered by the BBB, which limits the access of drugs to the CNS. In recent years, enormous efforts have been made towards the research of new drug delivery platforms able to improve the diffusion of the drugs across the BBB using non-invasive administration routes (Kumar, et al. 2008; Patel, et al. 2011). Therefore, after proving the safety of the CS-NLCs, we made a step forward by studying their brain uptake after i.n. administration. For that purpose DiR labelled CS-NLCs were prepared in order to study the nanoparticles biodistribution by DiR fluorescence imaging (FLI) monitoring. It is important to note that the incorporation of DiR in CS-NLCs did not alter their physicochemical parameters and that the fluorescent tracer remained associated with the NPs in the experimental period, indicating that the fluorescence signal detected in the tissue samples was attributed to the labelled NPs and not to the free dye.

In vivo brain-accumulation and whole-body biodistribution were measured at 0.5, 4.5, 6.5 and 23.5 h post i.n. administration of CS-NLC-DiR to athymic nude mice. Figure 3 shows *in vivo* biodistribution results performed with the IVIS® Spectrum imaging system.

Whole body *in vivo* fluorescent imaging revealed a brain accumulation of CS-NLC-DiR after i.n. administration. Moreover, the CS-NLC-DiR were quickly adsorbed by the olfactory tract and distributed mainly to the lungs through the respiratory track and were also detected in the trachea and olfactory bulb. It is worth mentioning that the NPs were retained in the nasal cavity up to 24 h post administration and were slowly cleared and biodistributed to other organs.

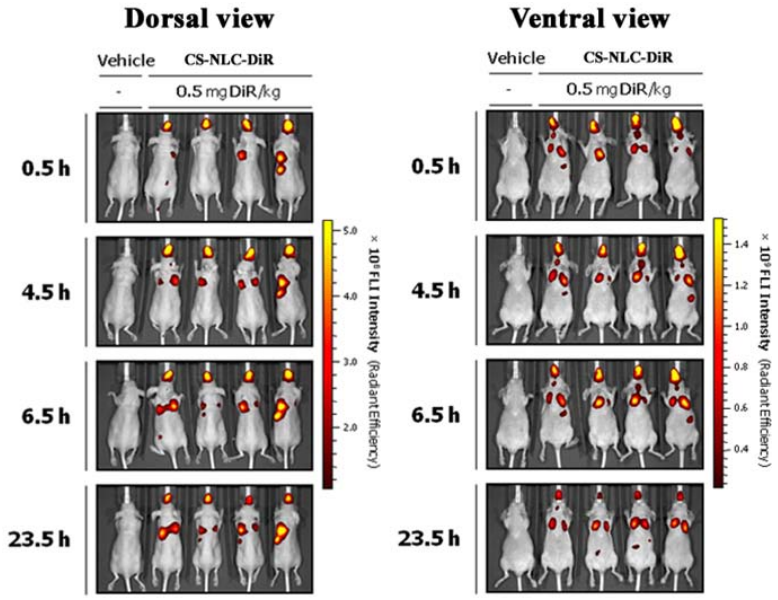

Figure 3. *In vivo* CS-NLC-DiR tissue accumulation at 0.5, 4.5, 6.5 and 23.5 h post-administration.

Additionally, at 1, 7 and 24 h post-administration time points, whole brain, lung, heart, liver, spleen, kidney and skin samples were collected, and NP tissue accumulations were determined by *ex vivo* DiR FLI monitoring. Each brain was sectioned into cerebrum, cerebellum and hippocampus and *ex vivo* DiR FLI monitoring was performed. The *ex vivo* imaging of extracted organs (Figures 4A and 4B) and selected areas of the brain (Figure 4C) confirmed that the NP reached the brain, but presented an significant retention in the lungs, similar to other published works (Md, et al. 2013; Patel, et al. 2011). However, in

our study, the signal was maintained during 24 h after i.n. administration, suggesting that our formulation would reach the brain over time without being cleared by nasal mucosal cilia.

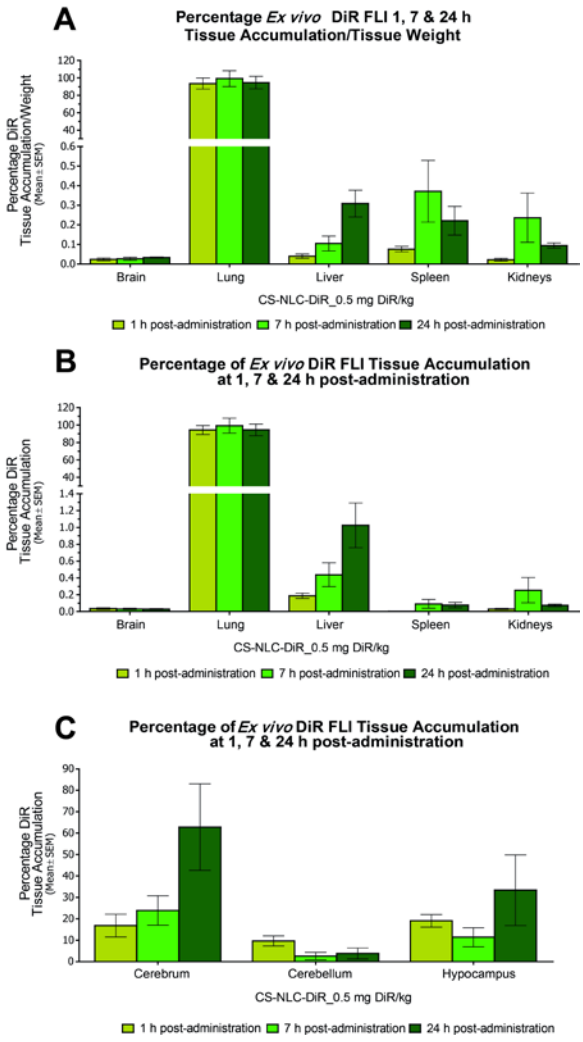

Figure 4. *Ex vivo* brain, lung, liver, spleen and kidney FLI per tissue weight (A), and FLI total (B) at 1, 7 and 24 h after i.n. administration of CS-NLC-DiR. *Ex vivo* cerebrum, cerebellum and hippocampus FLI total at 1, 7 and 24 h after i.n. administration of CS-NLC-DiR (C).

Thus, according to our results safe and non-toxic novel nanometric CS coated NLCs for i.n. administration have been developed. This CS-NLC formulation showed effective delivery to the brain after a single dose i.n. administration, opening new horizons to less invasive administration routes that could reach the brain avoiding the limiting step of the BBB. Moreover, considering the prolonged retention time of CS-NLCs in the nasal epithelium, this formulation could be considered an interesting alternative to decrease the dose and dosage frequency of drugs, as well as maximizing their therapeutic effect.

In a second step, in order to assess the *in vivo* efficacy of previously optimized CS-NLCs, the *in vivo* neuroprotective and neurorestorative effect of intranasally administered GDNF encapsulated in CS-NLCs was studied in a 6-OHDA partially lesioned rat model of PD. The neurotrophic factor GDNF is a potent candidate for the treatment of PD due to the high specificity that it presents towards dopaminergic neurons, and that is why it was selected for being encapsulated in our formulation (Lapchak, et al. 1997, Allen, et al. 2013).

After the physicochemical characterization of the formulation and before performing the *in vivo* study, the *in vitro* neuroprotective capacity of GDNF-loaded CS-NLCs was determined to prove its bioactivity after the encapsulation process. For this purpose, the PC-12 cell line was used as a specific cell lineage of dopaminergic neurons, and the cells were exposed to 6-OHDA neurotoxin, the same toxin used to establish the partially lesioned model of PD. In this assay, the neuroprotective ability of GDNF was demonstrated either in solution or in CS-NLC-GDNF. Thus, it was confirmed that the encapsulation process does not affect the bioactivity of the neurotrophic factor.

After proving the neuroprotective effect of CS-NLC-GDNF in PC-12 cells, the *in vivo* effectiveness of the formulation was also investigated with the aim of studying the neuroprotective effect of GDNF-loaded NPs in the performance of behavioural tests and against the loss of dopaminergic neurons, after their intranasal administration during 15 consecutive days. By performing the *in vivo* experiments with a partially lesioned rat model of PD, we attempted to study the potential effect of CS-NLC-GDNF in the initial stage of the disease. For this purpose, the 6-OHDA toxin was injected into the rats brain, and we

immediately started the two-week daily intranasal treatment to prove whether the GDNF was able to protect rats against the 6-OHDA lesion, in contrast to previous studies conducted by our research group in which treatments were intrastriatally administered three weeks after the injury, after the lesion was fully established (Herrán, et al. 2014).

During the 7 weeks of the study, the results obtained in the amphetamine-induced rotational test and in the cylinder test demonstrated the behavioural improvement of rats after the intranasal CS-NLC-GDNF treatment, which was not observed in the group treated with the GDNF solution (Figure 5A and 5B). Regarding to amphetamine-induced rotational test, significant differences were found for the interaction factor depicting that encapsulated GDNF had a more beneficial effect in movement recovery than GDNF in solution ($p<0.05$, $F_{(1,14)}=7.1$, for interaction factor, repeated measures two-way ANOVA). The behavioural improvement seen in the rotational behaviour was also supported by a reduction in forelimb asymmetry in the cylinder test ($F_{(1,14)}=4.54$, $p<0.05$, for interaction factor, repeated measures two-way ANOVA). These results demonstrated that the encapsulation of GDNF in our lipid-based NPs promotes the nose-to-brain delivery of GDNF.

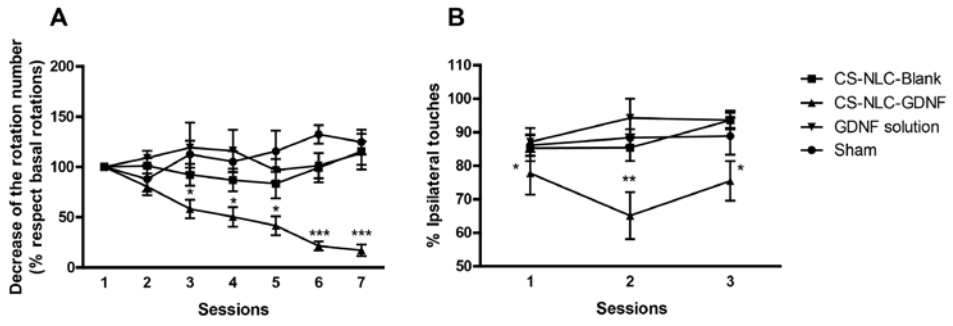

Figure 5. Graphical representation of the behavioural assessment of 6-OHDA lesioned animals. A: Amphetamine-induced rotational behaviour test. The graphic shows the percentage change in the number of ipsilateral rotations per minute, with respect to the basal rotation values obtained in the first session (100%). **B:** The graphic shows the percentage of touches performed with the ipsilateral forelimb in the cylinder test. The data are shown as the mean ± SEM (n=5), *p< 0.05, **p<0.01 and ***p< 0.001, CS-NLC-GDNF group with respect to the other three groups, Bonferroni post hoc test.

These findings were also confirmed with the histological evaluation of the brains, where a significant improvement in both the density of TH+ fibres in the striatum and the TH+ neuronal density in the SN was observed (Figure 6E and 6F).

Figures 6A-D show the photomicrographs of the TH immunostained striatums (rostral, medial and caudal). The qualitative study of the ipsilateral coronal sections of the striatum showed a different degree of neurodegeneration after the intranasal administration of different treatments. In addition, Figure 6E shows the quantitative analysis of these sections, where the percentage of TH+ fibres in the striatum of the ipsilateral or lesioned side, compared to the contralateral or non-lesioned hemisphere, was found to be significantly higher in the CS-NLC-GDNF treatment group ($F_{(1,\ 14)}$=8.96 $p<0.01$, for interaction factor, two-way ANOVA, Figure 6E). The data of the quantitative analysis of TH+ neurons in the SN confirmed these results ($F_{(1,\ 14)}$=71.37 $p<0.001$, for interaction factor, two-way ANOVA, Figure 6F). The TH+ neuronal density in the entire SN of the CS-NLC-GDNF group was significantly higher than in the other three groups, as shown in the stereological study (for statistical details, see Figure 6F).

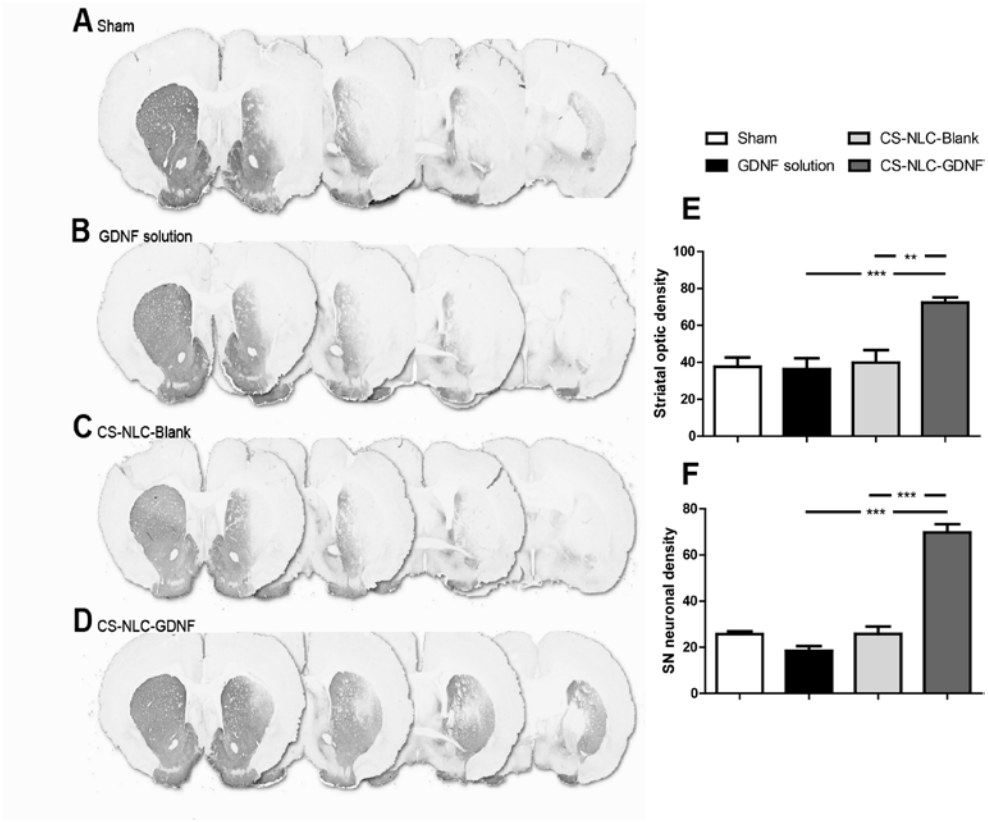

Figure 6. Histological evaluation of the striatum and SN. A-D: representative photomicrographs of the TH immunostained striatums (rostral, medial and caudal) compared with the non-lesioned side (on the left) of 6-OHDA lesioned rats, after the intranasal administration of the different treatments: **A:** Sham, **B:** GDNF solution, **C:** CS-NLC-Blank and **D:** CS-NLC-GDNF. The degeneration degree of various ipsilateral coronal sections of the striatum. **E:** The integrated optical density (IOD) of TH+ fibres of the entire striatum in the lesioned hemisphere compared to the non-lesioned hemisphere. **F:** Density of TH+ neurons in the entire SN. The results are expressed as a percentage of lesioned hemisphere compared to the intact side. The data are shown as the mean ± SEM, ***$p < 0.001$ *vs* the CS-NLC-GDNF group, Bonferroni post hoc test.

In this work, we developed for the first time a CS-coated NLC-GDNF formulation for nose-to-brain delivery and analyzed its neuroprotective ability against 6-OHDA damaged areas, as well as its potential to improve behavioural deficits in a hemiparkinsonism rat model. The results obtained from the *in vivo* studies suggested that the encapsulation of GDNF in CS-coated NLCs improves the nose-to-brain delivery of the neurotrophic factor

after i.n. administration. Furthermore, we demonstrated the neuroprotective and neurorestorative effect of CS-NLC-GDNF in a partially lesioned rat model of PD. Thus, it could be concluded that GDNF-loaded CS-NLCs administered by a non-invasive route such as the intranasal route could be a promising therapy for the treatment of PD. Despite the hopeful results obtained during this experimental work, it must bear in mind that we performed a neuroprotection study. However, diagnosis is only enabled late in the disease, when the motor symptoms reflecting the degeneration of dopaminergic neurons in the substantia nigra appear. Thus, it would be interesting for future works to investigate the neurorestorative ability of CS-NLC-GDNF in more advances stages of the disease.

Finally, in the last part of this doctoral thesis we realized about the need for an *in vitro* model of nasal mucosa, because although there are several studies on brain targeting of NPs after intranasal administration *in vivo* (Md, et al. 2013; Patel, et al. 2011; Zhang, et al. 2014), there are few studies describing NP nose-to-brain transport (Mistry, et al. 2009). Therefore, the first aim of the third work was to develop, characterize and validate *in vitro* olfactory cell monolayers that would allow the screening of different NPs intended for i.n. administration.

For this purpose, olfactory mucosa primary cells were extracted from the nasal cavity of female Wistar rats, following the protocol described by Bianco et al. (Bianco et al., 2004), and the nasal cell monolayers were developed based on previously described models such as Caco-2 and M cells *in vitro* models used to simulate the intestinal barrier (Beloqui, et al. 2013; des Rieux, et al. 2007), but taking into account the behavioral differences that exist between the different cell lines. After the extraction of the cells, the second step was to establish the optimum ratio of olfactory cells in order to form a monolayer in the inserts, and thus, to perform the transport studies. Cell monolayer integrity was assessed measuring the trans-epithelial electrical resistance (TEER) of three different cell ratios every two days during 21 days. According to the results obtained, the 500,000 cells/insert ratio and inserts with TEER values above 160 $\Omega \cdot cm^2$ at day 21 were selected to carry out the transport studies.

Once the olfactory mucosa *in vitro* cell monolayers were established, the second goal of this study was to evaluate the *in vitro* transport of CS-NLC and CPP-modified CS-NLC across them. Concretely, in this study Tat and Pen peptides were incorporated into CS-NLCs, which have been shown to increase the nasal absorption of NPs (Kamei and Takeda-Morishita 2015; Kanazawa, et al. 2011). Moreover, NLC transport was compared to that of PLGA NPs in order to evaluate whether lipid rather than polymeric NPs are better NP candidates towards brain delivery *via* the nasal route.

In this line, eight different formulations were prepared, four lipid-based NPs (NLC, CS-NLC, Tat-CS-NLC, Pen-CS-NLC) and four polymeric NPs (PLGA, PEI-PLGA, Tat-PLGA, Pen-PLGA NPs). After proving that all NLC and PLGA formulations were stable in the transport buffer and biocompatible with the olfactory mucosa cells, the ability of the different NPs to cross this monolayer was evaluated.

On the one hand, when comparing lipid nanocarriers with PLGA NPs, the transport of both, coated and uncoated NLC, resulted significantly higher than the percentage of transported PLGA NPs (***$p<0.001$, Figure 7A), suggesting that lipid-based NPs could result more appropriate than polymeric NPs for the intranasal administration. On the other hand, comparing CS-coated with uncoated NLCs, the percentage of transported NPs was significantly higher when NLCs were coated with the cationic polysaccharide CS (CS-NLC) (**$p<0.01$, Figure 7A). As known, CS NPs possess intrinsic properties that include mucoadhesion and the ability of transiently open the tight junctions (Behrens, et al. 2002; Trapani, et al. 2010). Regarding to the unalterated TEER values after the co-incubation of cells with CS-coated NLCs, we discarded the tight junction opening as an alternative mechanism of transport of these NPs across olfactory cells. CS-coated NLCs might adhere to the surface of the olfactory cells, thus increasing their interaction and transport across olfactory cells. These results justify the use of lipid NPs over polymeric and the use of CS as coating agent towards increased nasal penetration. However, further mechanistic studies need to be conducted in order to unravel this mechanism of transport.

After confirming that the coating of NLCs with CS had a significant influence in the enhancement of the transported NPs across the olfactory cells, the other aim of this work was to evaluate whether the incorporation of a CPP could improve CS-NLCs transport. Interestingly, we observed a significant increase in the percentage of transported Tat-CS-NLCs compared to CS-NLCs and NLCs ($p^* < 0.05$, Figure 7B). Although the cationic (PEI-PLGA) and CPP coated (Tat-PLGA and Pen-PLGA) NPs showed higher transport than uncoated PLGA NPs, no significant differences were observed on PLGA transport across the nasal cell monolayers whatever the formulation ($p>0.05$, Figure 7C).

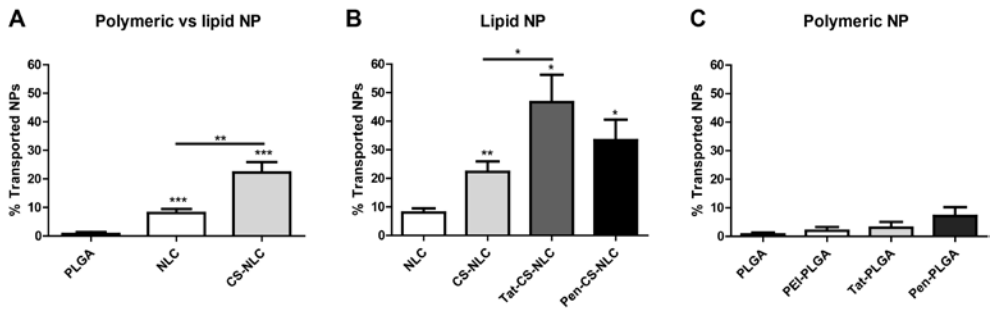

Figure 7. NP transport study across a nasal *in vitro* model. Percentage of transported NPs across olfactory mucosa cell monolayers after 2 h of co-incubation with different coated and uncoated NLC and PLGA NPs. n= 7-9, results are expressed as mean ± S.D, *p < 0.05, **p < 0.01, ***p < 0.001.

Therefore, in this last study an *in vitro* olfactory cell monolayer was validated to evaluate NP nose-to-brain delivery. This system is a valuable tool to evaluate the potential of different NPs to access the brain through the nasal route. Furthermore, our findings demonstrated the ability of lipid versus polymeric NPs to cross the nasal epithelium and, thus, reach the brain. The incorporation of a CPP to the CS-NLC formulation enhanced the *in vitro* transport of CS-NLCs across a nasal cell monolayer and points out CPP-CS-NLCs as promising nose-to-brain delivery systems to be tested in future *in vivo* studies.

In summary, considering all the results obtained during this doctoral thesis, we can conclude that we have taken another step forward in the search of new strategies to deal

with the difficulties that present most of drugs to access into the brain. During these years we have designed a safe and biocompatible nanometric formulation to be administered by the i.n. route in order to access into the brain. This CS-NLC formulation showed effective delivery to the brain after a single dose i.n. administration, and its *in vivo* efficacy was also demonstrated after being loaded with GDNF, achieving neuroprotective and neurorestorative effects in a partially lesioned rat model of PD. Moreover, with the aim of obtaining higher NP accumulation in the brain, we modify the surface of our CS-NLC formulation by incorporating CPPs, getting promising results after studying their transport across nasal *in vitro* cell monolayers developed by our research group. However, more *in vivo* studies, both biodistribution and efficacy studies are needed to verify the results obtained *in vitro*. Moreover, it would be interesting to continue working on the functionalization of these lipid-based nanocarriers to achieve the highest possible access into the brain.

References

Allen, S.J., Watson, J.J., Shoemark, D.K., Barua, N.U., Patel, N.K., 2013. GDNF, NGF and BDNF as therapeutic options for neurodegeneration. Pharmacol. Ther., 138, 155-175.

Behrens, I., Pena, A.I., Alonso, M.J., Kissel, T., 2002. Comparative uptake studies of bioadhesive and non-bioadhesive nanoparticles in human intestinal cell lines and rats: the effect of mucus on particle adsorption and transport. Pharm. Res., 19, 1185-1193.

Beloqui, A., Solinis, M.A., Gascon, A.R., del Pozo-Rodriguez, A., des Rieux, A., Preat, V., 2013. Mechanism of transport of saquinavir-loaded nanostructured lipid carriers across the intestinal barrier. J. Control. Release, 166, 115-123.

Beloqui, A., Solinís, M.Á., Rodríguez-Gascón, A., Almeida, A.J., Préat, V., 2016. Nanostructured lipid carriers: Promising drug delivery systems for future clinics. Nanomedicine: Nanotechnology, Biology and Medicine, 12, 143-161.

Bianco, J.I., Perry, C., Harkin, D.G., Mackay-Sim, A., Féron, F.. 2004. Neurotrophin 3 Promotes Purification and Proliferation of Olfactory Ensheathing Cells From Human Nose. Glia. 45(2), 111-123.

Blasi, P., Giovagnoli, S., Schoubben, A., Ricci, M., Rossi, C., 2007. Solid lipid nanoparticles for targeted brain drug delivery. Adv. Drug Deliv. Rev., 59, 454-477.

Ciesler, J., Sari, Y., 2013. Neurotrophic Peptides: Potential Drugs for Treatment of Amyotrophic Lateral Sclerosis and Alzheimer's disease. Open J. Neurosci., 3, 2.

Costantino, H.R., Illum, L., Brandt, G., Johnson, P.H., Quay, S.C., 2007. Intranasal delivery: Physicochemical and therapeutic aspects. Int. J. Pharm., 337, 1-24.

Deierborg, T., Soulet, D., Roybon, L., Hall, V., Brundin, P., 2008. Emerging restorative treatments for Parkinson's disease. Prog. Neurobiol., 85, 407-432.

des Rieux, A., Fievez, V., Théate, I., Mast, J., Préat, V., Schneider, Y., 2007. An improved in vitro model of human intestinal follicle-associated epithelium to study nanoparticle transport by M cells. Eur. J. Pharm. Sci., 30, 380-391.

Dharmala, K., Yoo, J.W., Lee, C.H., 2008. Development of Chitosan–SLN Microparticles for chemotherapy: In vitro approach through efflux-transporter modulation. J. Controlled Release, 131, 190-197.

Dhuria, S.V., Hanson, L.R., Frey, W.H.,2nd, 2010. Intranasal delivery to the central nervous system: mechanisms and experimental considerations. J. Pharm. Sci., 99, 1654-1673.

Doktorovova, S., Souto, E.B., Silva, A.M., 2014. Nanotoxicology applied to solid lipid nanoparticles and nanostructured lipid carriers - a systematic review of in vitro data. Eur. J. Pharm. Biopharm., 87, 1-18.

Foster, E.R., 2014. Themes from the special issue on neurodegenerative diseases: what have we learned, and where can we go from here?. Am J Occup Ther, 68, 6-8.

Garbayo, E., Ansorena, E., Lanciego, J.L., Blanco-Prieto, M.J., Aymerich, M.S., 2011. Long-term neuroprotection and neurorestoration by glial cell-derived neurotrophic factor microspheres for the treatment of Parkinson's disease. Mov. Disord., 26, 1943-1947.

Gartziandia, O., Herran, E., Pedraz, J.L., Carro, E., Igartua, M., Hernandez, R.M., 2015. Chitosan coated nanostructured lipid carriers for brain delivery of proteins by intranasal administration. Colloids Surf. B Biointerfaces, 134, 304-313.

Gobbi, M., Re, F., Canovi, M., Beeg, M., Gregori, M., Sesana, S., Sonnino, S., Brogioli, D., Musicanti, C., Gasco, P., Salmona, M., Masserini, M.E., 2010. Lipid-based nanoparticles with high binding affinity for amyloid-beta1-42 peptide. Biomaterials, 31, 6519-6529.

Graff, C.L., Pollack, G.M., 2005. Nasal drug administration: potential for targeted central nervous system delivery. J. Pharm. Sci., 94, 1187-1195.

Herran, E., Perez-Gonzalez, R., Igartua, M., Pedraz, J.L., Carro, E., Hernandez, R.M., 2015. Enhanced Hippocampal Neurogenesis in APP/Ps1 Mouse Model of Alzheimer's Disease After Implantation of VEGF-loaded PLGA Nanospheres. Curr. Alzheimer Res., 12, 932-940.

Herrán, E., Requejo, C., Ruiz-Ortega, J.A., Aristieta, A., Igartua, M., Bengoetxea, H., Ugedo, L., Pedraz, J.L., Lafuente, J.V., Hernández, R.M., 2014. Increased antiparkinson efficacy by the combined administration of VEGF- and GDNF-releasing nanospheres in a partial lesion model of Parkinson's disease. Int J Nanomedicine, 9, 2677-2687.

Herrán, E., Pérez-González, R., Igartua, M., Pedraz, J.L., Carro, E., Hernández, R.M., 2013a. VEGF-releasing biodegradable nanospheres administered by craniotomy: A novel therapeutic approach in the APP/Ps1 mouse model of Alzheimer's disease. J. Controlled Release, 170, 111-119.

Herrán, E., Ruiz-Ortega, J.Á., Aristieta, A., Igartua, M., Requejo, C., Lafuente, J.V., Ugedo, L., Pedraz, J.L., Hernández, R.M., 2013b. In vivo administration of VEGF- and GDNF-releasing biodegradable polymeric microspheres in a severe lesion model of Parkinson's disease. European Journal of Pharmaceutics and Biopharmaceutics, 85, 1183-1190.

Jollivet, C., Aubert-Pouessel, A., Clavreul, A., Venier-Julienne, M., Montero-Menei, C.N., Benoit, J., Menei, P., 2004. Long-term effect of intra-striatal glial cell line-derived neurotrophic factor-releasing microspheres in a partial rat model of Parkinson's disease. Neurosci. Lett., 356, 207-210.

Kamei, N., Takeda-Morishita, M., 2015. Brain delivery of insulin boosted by intranasal coadministration with cell-penetrating peptides. J. Control. Release, 197, 105-110.

Kanazawa, T., Taki, H., Tanaka, K., Takashima, Y., Okada, H., 2011. Cell-penetrating peptide-modified block copolymer micelles promote direct brain delivery via intranasal administration. Pharm. Res., 28, 2130-2139.

Kaur, I.P., Bhandari, R., Bhandari, S., Kakkar, V., 2008. Potential of solid lipid nanoparticles in brain targeting. J. Control. Release, 127, 97-109.

Kumar, M., Misra, A., Mishra, A.K., Mishra, P., Pathak, K., 2008. Mucoadhesive nanoemulsion-based intranasal drug delivery system of olanzapine for brain targeting. J. Drug Target., 16, 806-814.

Lapchak, P.A., Gash, D.M., Jiao, S., Miller, P.J., Hilt, D., 1997. Glial Cell Line-Derived Neurotrophic Factor: A Novel Therapeutic Approach to Treat Motor Dysfunction in Parkinson's Disease. Exp. Neurol., 144, 29-34.

Leonardi, A., Bucolo, C., Romano, G.L., Platania, C.B.M., Drago, F., Puglisi, G., Pignatello, R., 2014. Influence of different surfactants on the technological properties and in vivo ocular tolerability of lipid nanoparticles. Int. J. Pharm., 470, 133-140.

Levy, Y.S., Gilgun-Sherki, Y., Melamed, E., Offen, D., 2005. Therapeutic potential of neurotrophic factors in neurodegenerative diseases. BioDrugs, 19, 97-127.

Lim, S.B., Banerjee, A., Önyüksel, H., 2012. Improvement of drug safety by the use of lipid-based nanocarriers. J. Controlled Release, 163, 34-45.

Md, S., Khan, R.A., Mustafa, G., Chuttani, K., Baboota, S., Sahni, J.K., Ali, J., 2013. Bromocriptine loaded chitosan nanoparticles intended for direct nose to brain delivery: Pharmacodynamic, Pharmacokinetic and Scintigraphy study in mice model. Eur. J. Pharm. Sci., 48, 393-405.

Mistry, A., Stolnik, S., Illum, L., 2009. Nanoparticles for direct nose-to-brain delivery of drugs. Int. J. Pharm., 379, 146-157.

Patel, S., Chavhan, S., Soni, H., Babbar, A.K., Mathur, R., Mishra, A.K., Sawant, K., 2011. Brain targeting of risperidone-loaded solid lipid nanoparticles by intranasal route. J. Drug Target., 19, 468-474.

Poon, V.Y., Choi, S., Park, M., 2013. Growth factors in synaptic function. Front Synaptic Neurosci, 5.

Sandri, G., Bonferoni, M.C., Gökçe, E.H., Ferrari, F., Rossi, S., Patrini, M., Caramella, C., 2010. Chitosan-associated SLN: in vitro and ex vivo characterization of cyclosporine A loaded ophthalmic systems. J Microencapsul, 27, 735-746.

Sapsforda, R.J., Wells, C.W., Richman, P., Daviesa, R.J., 1990. Culture and comparison of human bronchial and nasal epithelial cells in vitro. Respir Med, 84, 303-3012.

Severino, P., Souto, E.B., Pinho, S.C., Santana, M.H., 2013. Hydrophilic coating of mitotane-loaded lipid nanoparticles: preliminary studies for mucosal adhesion. Pharm. Dev. Technol., 18, 577-581.

Trapani, A., Lopedota, A., Franco, M., Cioffi, N., Ieva, E., Garcia-Fuentes, M., Alonso, M.J., 2010. A comparative study of chitosan and chitosan/cyclodextrin nanoparticles as potential carriers for the oral delivery of small peptides. Eur. J. Pharm. Biopharm., 75, 26-32.

Vyas, T.K., Shahiwala, A., Marathe, S., Misra, A., 2005. Intranasal drug delivery for brain targeting. Curr Drug Deliv, 2, 165-175.

Xia, H., Gao, X., Gu, G., Liu, Z., Zeng, N., Hu, Q., Song, Q., Yao, L., Pang, Z., Jiang, X., Chen, J., Chen, H., 2011. Low molecular weight protamine-functionalized nanoparticles for drug delivery to the brain after intranasal administration. Biomaterials, 32, 9888-9898.

Zhang, C., Chen, J., Feng, C., Shao, X., Liu, Q., Zhang, Q., Pang, Z., Jiang, X., 2014. Intranasal nanoparticles of basic fibroblast growth factor for brain delivery to treat Alzheimer's disease. Int. J. Pharm., 461, 192-202.

Conclusions

On the basis of the results obtained in the experimental studies of this Doctoral Thesis, the following conclusions were derived:

1. A CS-NLC formulation has been developed using the melt-emulsification technique, with a mean particle size and a zeta potential value suitable for i.n administration, obtaining high encapsulation efficiencies when IGF -I or GDNF were encapsulated.

2. The *in vitro* and *in vivo* toxicity studies carried out in 16HBE14o- cells and in C57 mice demonstrated that the optimized CS-NLCs are safe and non-toxic nanocarriers for being intranasally administered.

3. The biodistribution study performed in nude mice using DiR fluorescence imaging (FLI) monitoring, showed that this CS-NLC formulation was biodistributed to the brain through the nose-to-brain delivery and to the lungs through the pulmonary delivery after a single dose i.n. administration.

4. The CS-NLC-GDNF achieved a behavioural improvement in hemiparkinsonian rats, as well as a significant improvement in both the density of TH+ fibres in the striatum and the TH+ neuronal density in the SN, after two weeks of daily intranasal administration.

5. An *in vitro* olfactory cell monolayer has been validated to evaluate the potential of different NPs for nose-to-brain delivery. The NP transport studies revealed the ability of lipidic *versus* polymeric NPs to cross the *in vitro* olfactory cell monolayer. Moreover, the incorporation of CPPs to the CS-NLCs surface significantly increased their transport.

6.- Although the results presented in this thesis seem promising, further modifications in the CS-NLC formulation are warranted to enhance the percentage of particles reaching the brain after their i.n. administration.

Bibliography

Acsadi G, Anguelov RA, Yang H, Toth G, Thomas R, Jani A, Wang Y, Ianakova E, Mohammad S, Lewis RA, Shy ME., 2002. Increased survival and function of SOD1 mice after glial cell-derived neurotrophic factor gene therapy. Hum Gene Ther, 13 (9), 1047-59.

Agrawal, U., Chashoo, G., Sharma, P.R., Kumar, A., Saxena, A.K., Vyas, S.P., 2015. Tailored polymer–lipid hybrid nanoparticles for the delivery of drug conjugate: Dual strategy for brain targeting. Colloids Surf. B Biointerfaces, 126, 414-425.

Alam, M.I., Baboota, S., Ahuja, A., Ali, M., Ali, J., Sahni, J.K., Bhatnagar, A., 2014. Pharmacoscintigraphic evaluation of potential of lipid nanocarriers for nose-to-brain delivery of antidepressant drug. Int. J. Pharm., 470, 99-106.

Alan E. Guttmacher, M.D., and Francis S. Collins, 2003. Alzheimer's Disease and Parkinson's Disease. N Engl J Med, 348.

Allen, S.J., Watson, J.J., Shoemark, D.K., Barua, N.U., Patel, N.K., 2013. GDNF, NGF and BDNF as therapeutic options for neurodegeneration. Pharmacol. Ther., 138, 155-175.

American Academy of Pediatrics, Committee on Drugs, 1997. Alternative routes of drug administration-advantages and disadvantages (subject review). Pediatrics, 100, 143-152.

Angelova, A., Angelov, B., Drechsler, M., Lesieur, S., 2013. Neurotrophin delivery using nanotechnology. Drug Discov. Today, 18, 1263-1271.

Azzouz, M., Ralph, GS., Storkebaum, E, Walmsley, LE., Mitrophanous, KA., Kingsman, SM., Carmeliet, P., Mazarakis, ND, 2004. VEGF delivery with retrogradely transported lentivector prolongs survival in a mouse ALS model Nature, 429, 413-417.

Barry, J.N., Vertegel, A.A., 2013. Nanomaterials for Protein Mediated Therapy and Delivery. Nano Life., 3, 1343001.

Bartus, R.T., Baumann, T.L., Siffert, J., Herzog, C.D., Alterman, R., Boulis, N., Turner, D.A., Stacy, M., Lang, A.E., Lozano, A.M., Olanow, C.W., 2013. Safety/feasibility of targeting the substantia nigra with AAV2-neurturin in Parkinson patients. Neurology, 80, 1698-1701.

Begley, D.J., 2004. Delivery of therapeutic agents to the central nervous system: the problems and the possibilities. Pharmacol. Ther., 104, 29-45.

Behrens, I., Pena, A.I., Alonso, M.J., Kissel, T., 2002. Comparative uptake studies of bioadhesive and non-bioadhesive nanoparticles in human intestinal cell lines and rats: the effect of mucus on particle adsorption and transport. Pharm. Res., 19, 1185-1193.

Beloqui, A., Solinís, M.A., Delgado, A., Évora, C., del Pozo-Rodríguez, A., Rodríguez-Gascón, A., 2013. Biodistribution of Nanostructured Lipid Carriers (NLCs) after intravenous administration to rats: Influence of technological factors. Eur J Pharm Biopharm, 84, 309-314.

Beloqui, A., Solinis, M.A., Gascon, A.R., del Pozo-Rodriguez, A., des Rieux, A., Preat, V., 2013. Mechanism of transport of saquinavir-loaded nanostructured lipid carriers across the intestinal barrier. J. Control. Release, 166, 115-123.

Beloqui, A., Solinís, M.Á., Rieux, A.d., Préat, V., Rodríguez-Gascón, A., 2014. Dextran–protamine coated nanostructured lipid carriers as mucus-penetrating nanoparticles for lipophilic drugs. Int. J. Pharm., 468, 105-111.

Beloqui, A., Solinís, M.Á., Rodríguez-Gascón, A., Almeida, A.J., Préat, V., 2016. Nanostructured lipid carriers: Promising drug delivery systems for future clinics. Nanomedicine, 12, 143-161.

Benraiss, A., Bruel-Jungerman, E., Lu, G., Economides, A.N., Davidson, B., Goldman, S.A., 2012. Sustained induction of neuronal addition to the adult rat neostriatum by AAV4-delivered noggin and BDNF. Gene Ther., 19, 483-493.

Bensimon G1, Lacomblez L, Meininger V, 1994. A controlled trial of riluzole in amyotrophic lateral sclerosis. ALS/Riluzole Study Group. N Engl J Med, 330, 585-591.

Bianco JI, Perry C, Harkin DG, Mackay-Sim A, Féron F., 2004. Neurotrophin 3 Promotes Purification and Proliferation of Olfactory Ensheathing Cells From Human Nose. Glia, 45, 111-123.

Blasco H, Mavel S, Corcia P, Gordon PH, 2014. The glutamate hypothesis in ALS: pathophysiology and drug development. Curr Med Chem, 21, 3551-3575.

Blasi, P., Giovagnoli, S., Schoubben, A., Ricci, M., Rossi, C., 2007. Solid lipid nanoparticles for targeted brain drug delivery. Adv. Drug Deliv. Rev., 59, 454-477.

Braz, L., Rodrigues, S., Fonte, P., Grenha, A., and Sarmento, B., 2011. Mechanisms of Chemical and Enzymatic Chitosan Biodegradability and its Application on Drug Delivery,

Biodegradable Polymers: Processing, Degradation and Applications. Nova Publishers, New York, USA, 325-364.

Calias, P., Banks, W.A., Begley, D., Scarpa, M., Dickson, P., 2014. Intrathecal delivery of protein therapeutics to the brain: A critical reassessment. Pharmacol. Ther., 144, 114-122.

Calvo, A.C., Moreno-Igoa, M., Mancuso, R., Manzano, R., Olivan, S., Munoz, M.J., Penas, C., Zaragoza, P., Navarro, X., Osta, R., 2011. Lack of a synergistic effect of a non-viral ALS gene therapy based on BDNF and a TTC fusion molecule. Orphanet J. Rare Dis., 6, 10-1172-6-10.

Cano-Cebrian, M.J., Zornoza, T., Granero, L., Polache, A., 2005. Intestinal absorption enhancement via the paracellular route by fatty acids, chitosans and others: a target for drug delivery. Curr. Drug Deliv., 2, 9-22.

Carmeliet, P., Storkebaum, E., 2002. Vascular and neuronal effects of VEGF in the nervous system: implications for neurological disorders. Semin. Cell Dev. Biol., 13, 39-53.

Chen, Y., Ai, Y., Slevin, J.R., Maley, B.E., Gash, D.M., 2005. Progenitor proliferation in the adult hippocampus and substantia nigra induced by glial cell line-derived neurotrophic factor. Exp. Neurol., 196, 87-95.

Ciesler, J., Sari, Y., 2013. Neurotrophic Peptides: Potential Drugs for Treatment of Amyotrophic Lateral Sclerosis and Alzheimer's disease. Open J. Neurosci., 3, 2.

Ciriza J, Moreno-Igoa M, Calvo AC, Yague G, Palacio J, Miana-Mena FJ, Muñoz MJ, Zaragoza P, Brûlet P, Osta R., 2008. A genetic fusion GDNF-C fragment of tetanus toxin prolongs survival in a symptomatic mouse ALS model. Restor Neurol Neurosci, 26 (6), 459-65.

Citron M, 2010. Alzheimer's disease: strategies for disease modification. Nat Rev Drug Discov, 9, 387-398.

Cook AM, Mieure KD, Owen RD, Pesaturo AB, Hatton J, 2009. Intracerebroventricular administration of drugs. Pharmacotherapy, 29, 832-845.

Coppola, V., Kucera, J., Palko, M.E., Martinez-De Velasco, J., Lyons, W.E., Fritzsch, B., Tessarollo, L., 2001. Dissection of NT3 functions in vivo by gene replacement strategy. Development, 128, 4315-4327.

Costantino, H.R., Illum, L., Brandt, G., Johnson, P.H., Quay, S.C., 2007. Intranasal delivery: physicochemical and therapeutic aspects. Int. J. Pharm., 337, 1-24.

De Luca, M.A., Lai, F., Corrias, F., Caboni, P., Bimpisidis, Z., Maccioni, E., Fadda, A.M., Di Chiara, G., 2015. Lactoferrin- and antitransferrin-modified liposomes for brain targeting of the NK3 receptor agonist senktide: Preparation and in vivo evaluation. Int. J. Pharm., 479, 129-137.

Deierborg, T., Soulet, D., Roybon, L., Hall, V., Brundin, P., 2008. Emerging restorative treatments for Parkinson's disease. Prog. Neurobiol., 85, 407-432.

des Rieux, A., Fievez, V., Théate, I., Mast, J., Préat, V., Schneider, Y., 2007. An improved in vitro model of human intestinal follicle-associated epithelium to study nanoparticle transport by M cells. Eur J Pharm Sci, 30, 380-391.

Desai AK, G.G., 2005. Diagnosis and treatment of Alzheimer's disease. Neurology, 64, 34-39.

Devkar, T.B., Tekade, A.R., Khandelwal, K.R., 2014. Surface engineered nanostructured lipid carriers for efficient nose to brain delivery of ondansetron HCl using Delonix regia gum as a natural mucoadhesive polymer. Colloids Surf. B Biointerfaces, 122, 143-150.

Dharmala, K., Yoo, J.W., Lee, C.H., 2008. Development of Chitosan–SLN Microparticles for chemotherapy: In vitro approach through efflux-transporter modulation. J. Control Release, 131, 190-197.

Dhuria, S.V., Hanson, L.R., Frey, W.H.,2nd, 2010. Intranasal delivery to the central nervous system: mechanisms and experimental considerations. J. Pharm. Sci., 99, 1654-1673.

Djupesland, P.G., Messina, J.C., Mahmoud, R.A., 2014. The nasal approach to delivering treatment for brain diseases: an anatomic, physiologic, and delivery technology overview. Ther. Deliv., 5, 709-733.

Dodane, V., Amin Khan, M., Merwin, J.R., 1999. Effect of chitosan on epithelial permeability and structure. Int. J. Pharm., 182, 21-32.

Dodge, J.C., Treleaven, C.M., Fidler, J.A., Hester, M., Haidet, A., Handy, C., Rao, M., Eagle, A., Matthews, J.C., Taksir, T.V., Cheng, S.H., Shihabuddin, L.S., Kaspar, B.K., 2010. AAV4-mediated expression of IGF-1 and VEGF within cellular components of the

ventricular system improves survival outcome in familial ALS mice. Mol. Ther., 18, 2075-2084.

Doktorovova, S., Souto, E.B., Silva, A.M., 2014. Nanotoxicology applied to solid lipid nanoparticles and nanostructured lipid carriers - a systematic review of in vitro data. Eur. J. Pharm. Biopharm., 87, 1-18.

Drin, G., Cottin, S., Blanc, E., Rees, A.R., Temsamani, J., 2003. Studies on the internalization mechanism of cationic cell-penetrating peptides. J. Biol. Chem., 278, 31192-31201.

Eberling JL, Kells AP, Pivirotto P, Beyer J, Bringas J, Federoff HJ, Forsayeth J, Bankiewicz KS, 2009. Functional effects of AAV2-GDNF on the dopaminergic nigrostriatal pathway in parkinsonian rhesus monkeys. Hum Gene Ther., 20, 511-8.

Egusquiaguirre, S.P., Beziere, N., Pedraz, J.L., Hernandez, R.M., Ntziachristos, V., Igartua, M., 2015. Optoacoustic imaging enabled biodistribution study of cationic polymeric biodegradable nanoparticles. Contrast Media Mol. Imaging.

Egusquiaguirre, S.P., Manguán-García, C., Pintado-Berninches, L., Iarriccio, L., Carbajo, D., Albericio, F., Royo, M., Pedraz, J.L., Hernández, R.M., Perona, R., Igartua, M., 2015. Development of surface modified biodegradable polymeric nanoparticles to deliver GSE24.2 peptide to cells: A promising approach for the treatment of defective telomerase disorders. Eur J Pharm Biopharm, 91, 91-102.

Ellison, SM., Trabalza, A., Tisato, V., Pazarentzos, E., Lee, S., Papadaki, V., Goniotaki, D., Morgan, S., Mirzaei, N., Mazarakis, ND., 2013. Dose-dependent Neuroprotection of VEGF165 in Huntington's Disease Striatum. Mol Ther, 21, 1862-1875.

Eslamboli, A., Georgievska, B., Ridley, R.M., Baker, H.F., Muzyczka, N., Burger, C., Mandel, R.J., Annett, L., Kirik, D., 2005. Continuous low-level glial cell line-derived neurotrophic factor delivery using recombinant adeno-associated viral vectors provides neuroprotection and induces behavioral recovery in a primate model of Parkinson's disease. J. Neurosci, 25, 769-777.

Foster ER, 2014. Themes from the special issue on neurodegenerative diseases: what have we learned, and where can we go from here?. Am J Occup Ther, 68, 6-8.

Foust KD, Flotte TR, Reier PJ, Mandel RJ., 2008. Recombinant adeno-associated virus-mediated global anterograde delivery of glial cell line-derived neurotrophic factor to the

spinal cord: comparison of rubrospinal and corticospinal tracts in the rat.. Hum Gene Ther, 19 (1), 71-82.

Gainza, G., Pastor, M., Aguirre, J.J., Villullas, S., Pedraz, J.L., Hernandez, R.M., Igartua, M., 2014. A novel strategy for the treatment of chronic wounds based on the topical administration of rhEGF-loaded lipid nanoparticles: In vitro bioactivity and in vivo effectiveness in healing-impaired db/db mice. J. Control Release, 185, 51-61.

Garbayo, E., Ansorena, E., Blanco-Prieto, M.J., 2013. Drug development in Parkinson's disease: From emerging molecules to innovative drug delivery systems. Maturitas, 76, 272-278.

Garbayo, E., Ansorena, E., Lanciego, J.L., Blanco-Prieto, M.J., Aymerich, M.S., 2011. Long-term neuroprotection and neurorestoration by glial cell-derived neurotrophic factor microspheres for the treatment of Parkinson's disease. Mov. Disord., 26, 1943-1947.

Garcia-Fuentes, M., Torres, D., Alonso, M.J., 2005. New surface-modified lipid nanoparticles as delivery vehicles for salmon calcitonin. Int. J. Pharm., 296, 122-132.

Garinot, M., Fiévez, V., Pourcelle, V., Stoffelbach, F., des Rieux, A., Plapied, L., Theate, I., Freichels, H., Jérôme, C., Marchand-Brynaert, J., Schneider, Y., Préat, V., 2007. PEGylated PLGA-based nanoparticles targeting M cells for oral vaccination. J. Control Release, 120, 195-204.

Gartziandia, O., Herran, E., Pedraz, J.L., Carro, E., Igartua, M., Hernandez, R.M., 2015. Chitosan coated nanostructured lipid carriers for brain delivery of proteins by intranasal administration. Colloids Surf. B Biointerfaces, 134, 304-313.

Gastaldi, L., Battaglia, L., Peira, E., Chirio, D., Muntoni, E., Solazzi, I., Gallarate, M., Dosio, F., 2014. Solid lipid nanoparticles as vehicles of drugs to the brain: Current state of the art. Eur J Pharm Biopharm, 87, 433-444.

George J. Siegela , Neelima B. Chauhanb, 2000. Neurotrophic factors in Alzheimer’s and Parkinson’s disease brain. Brain Res Rev, 33.

Géral, C., Angelova, A., Angelov, B., Nicolas, V., Lesieur, S., 2012. Multicompartment Lipid Nanocarriers for Targeting of Cells Expressing Brain Receptors. Self-Assembled Supramolecular ArchitecturesJohn Wiley & Sons, Inc, 319-355.

Gobbi, M., Re, F., Canovi, M., Beeg, M., Gregori, M., Sesana, S., Sonnino, S., Brogioli, D., Musicanti, C., Gasco, P., Salmona, M., Masserini, M.E., 2010. Lipid-based nanoparticles with high binding affinity for amyloid-beta1-42 peptide. Biomaterials, 31, 6519-6529.

Gonzalez-Barrios, J.A., Lindahl, M., Bannon, M.J., Anaya-Martinez, V., Flores, G., Navarro-Quiroga, I., Trudeau, L.E., Aceves, J., Martinez-Arguelles, D.B., Garcia-Villegas, R., Jimenez, I., Segovia, J., Martinez-Fong, D., 2006. Neurotensin polyplex as an efficient carrier for delivering the human GDNF gene into nigral dopamine neurons of hemiparkinsonian rats. Mol. Ther., 14, 857-865.

Gordon, P.H., 2013. Amyotrophic Lateral Sclerosis: An update for 2013 Clinical Features, Pathophysiology, Management and Therapeutic Trials. Aging Dis., 4, 295-310.

Graff, C.L., Pollack, G.M., 2005. Nasal drug administration: potential for targeted central nervous system delivery. J. Pharm. Sci., 94, 1187-1195.

Grandoso, L., Ponce, S., Manuel, I., Arrúe, A., Ruiz-Ortega, J.A., Ulibarri, I., Orive, G., Hernández, R.M., Rodríguez, A., Rodríguez-Puertas, R., Zumárraga, M., Linazasoro, G., Pedraz, J.L., Ugedo, L., 2007. Long-term survival of encapsulated GDNF secreting cells implanted within the striatum of parkinsonized rats. Int. J. Pharm., 343, 69-78.

Guillot, S., Azzouz, M., Deglon, N., Zurn, A., Aebischer, P., 2004. Local GDNF expression mediated by lentiviral vector protects facial nerve motoneurons but not spinal motoneurons in SOD1(G93A) transgenic mice. Neurobiol. Dis., 16, 139-149.

Gullberg, E., Leonard, M., Karlsson, J., Hopkins, A.M., Brayden, D., Baird, A.W., Artursson, P., 2000. Expression of Specific Markers and Particle Transport in a New Human Intestinal M-Cell Model. Biochem. Biophys. Res. Commun., 279, 808-813.

Gusella JF, MacDonald ME, Ambrose CM, Duyao MP, 1993. Molecular genetics of huntington´s disease. Arch Neurol, 50, 1157-1163.

Hájos, N., Mody, I., 2009. Establishing a physiological environment for visualized in vitro brain slice recordings by increasing oxygen supply and modifying aCSF content. J. Neurosci. Methods, 183, 107-113.

Hanson, L.R., Frey, W.H.,2nd, 2008. Intranasal delivery bypasses the blood-brain barrier to target therapeutic agents to the central nervous system and treat neurodegenerative disease. BMC Neurosci., 9 Suppl 3, S5-2202-9-S3-S5.

Hardy J, C.K., 2006. Amyloid at the blood vessel wall. Nat Med, 12, 756-757.

Herrán E, Requejo C, Ruiz-Ortega JA, Aristieta A, Igartua M, Bengoetxea H, Ugedo L, Pedraz JL, Lafuente JV, Hernández RM, 2014. Increased antiparkinson efficacy by the combined administration of VEGF- and GDNF-releasing nanospheres in a partial lesion model of Parkinson's disease. Int J Nanomedicine, 9.

Herran, E., Perez-Gonzalez, R., Igartua, M., Pedraz, J.L., Carro, E., Hernandez, R.M., 2015. Enhanced Hippocampal Neurogenesis in APP/Ps1 Mouse Model of Alzheimer's Disease After Implantation of VEGF-loaded PLGA Nanospheres. Curr. Alzheimer Res., 12, 932-940.

Herrán, E., Pérez-González, R., Igartua, M., Pedraz, J.L., Carro, E., Hernández, R.M., 2013. VEGF-releasing biodegradable nanospheres administered by craniotomy: A novel therapeutic approach in the APP/Ps1 mouse model of Alzheimer's disease. J. Control Release, 170, 111-119.

Herrán, E., Ruiz-Ortega, J.Á., Aristieta, A., Igartua, M., Requejo, C., Lafuente, J.V., Ugedo, L., Pedraz, J.L., Hernández, R.M., 2013. In vivo administration of VEGF- and GDNF-releasing biodegradable polymeric microspheres in a severe lesion model of Parkinson's disease. Eur J Pharm Biopharm, 85, 1183-1190.

Hottinger, A.F., Azzouz, M., Deglon, N., Aebischer, P., Zurn, A.D., 2000. Complete and long-term rescue of lesioned adult motoneurons by lentiviral-mediated expression of glial cell line-derived neurotrophic factor in the facial nucleus. J. Neurosci., 20, 5587-5593.

Huang, R., Ke, W., Liu, Y., Wu, D., Feng, L., Jiang, C., Pei, Y., 2010. Gene therapy using lactoferrin-modified nanoparticles in a rotenone-induced chronic Parkinson model. J. Neurol. Sci., 290, 123-130.

Huwyler, J., Wu, D., Pardridge, W.M., 1996. Brain drug delivery of small molecules using immunoliposomes. Proc. Natl. Acad. Sci. U. S. A., 93, 14164-14169.

Illum, L., 2000. Transport of drugs from the nasal cavity to the central nervous system. Eur J Pharm Sci, 11, 1-18.

Jain, R.A., 2000. The manufacturing techniques of various drug loaded biodegradable poly(lactide-co-glycolide) (PLGA) devices. Biomaterials, 21, 2475-2490.

Jollivet, C., Aubert-Pouessel, A., Clavreul, A., Venier-Julienne, M., Remy, S., Montero-Menei, C.N., Benoit, J., Menei, P., 2004. Striatal implantation of GDNF releasing biodegradable microspheres promotes recovery of motor function in a partial model of Parkinson's disease. Biomaterials., 25, 933-942.

Jollivet, C., Aubert-Pouessel, A., Clavreul, A., Venier-Julienne, M., Montero-Menei, C.N., Benoit, J., Menei, P., 2004. Long-term effect of intra-striatal glial cell line-derived neurotrophic factor-releasing microspheres in a partial rat model of Parkinson's disease. Neurosci. Lett., 356, 207-210.

Kabanov, A.V., Batrakova, E.V., 2004. New technologies for drug delivery across the blood brain barrier. Curr. Pharm. Des., 10, 1355-1363.

Kamei, N., Takeda-Morishita, M., 2015. Brain delivery of insulin boosted by intranasal coadministration with cell-penetrating peptides. J. Control. Release, 197, 105-110.

Kanazawa, T., Taki, H., Tanaka, K., Takashima, Y., Okada, H., 2011. Cell-penetrating peptide-modified block copolymer micelles promote direct brain delivery via intranasal administration. Pharm. Res., 28, 2130-2139.

Kaspar, BK., Lladó, J., Sherkat, N., Rothstein, JD., Gage, FH., 2003. Retrograde Viral Delivery of IGF-1 Prolongs Survival in a Mouse ALS Model. Science, 301, 839-842.

Kaur, I.P., Bhandari, R., Bhandari, S., Kakkar, V., 2008. Potential of solid lipid nanoparticles in brain targeting. J. Control. Release, 127, 97-109.

Kaur, P., Garg, T., Vaidya, B., Prakash, A., Rath, G., Goyal, A.K., 2015. Brain delivery of intranasal in situ gel of nanoparticulated polymeric carriers containing antidepressant drug: behavioral and biochemical assessment. J. Drug Target., 23, 275-286.

Keir SD, Xiao X, Li J, Kennedy PG, 2001. Adeno-associated virus-mediated delivery of glial cell line-derived neurotrophic factor protects motor neuron-like cells from apoptosis. J Neurovirol, 7 (5), 437-36.

Kells, AP., Fong, DM., Dragunow, M., During, MJ., Young, D., Connor, B., 2004. AAV-Mediated Gene Delivery of BDNF or GDNF Is Neuroprotective in a Model of Huntington Disease. Mol Ther, 9, 682-688.

Killoran, A., Biglan, K.M., 2014. Current therapeutic options for Huntington's disease: good clinical practice versus evidence-based approaches? Mov. Disord., 29, 1404-1413.

Kliem MA, Heeke BL, Franz CK, Radovitskiy I, Raore B, Barrow E, Snyder BR, Federici T, Kaye Spratt S, Boulis NM., 2011. Intramuscular administration of a VEGF zinc finger transcription factor activator (VEGF-ZFP-TF) improves functional outcomes in SOD1 rats. Amyotroph Lateral Scler, 12 (5), 331-9.

Koennings, S., Sapin, A., Blunk, T., Menei, P., Goepferich, A., 2007. Towards controlled release of BDNF--manufacturing strategies for protein-loaded lipid implants and biocompatibility evaluation in the brain. J. Control. Release, 119, 163-172.

Kordower, J.H., Palfi, S., Chen, E.Y., Ma, S.Y., Sendera, T., Cochran, E.J., Cochran, E.J., Mufson, E.J., Penn, R., Goetz, C.G., Comella, C.D., 1999. Clinicopathological findings following intraventricular glial-derived neurotrophic factor treatment in a patient with Parkinson's disease. Ann. Neurol, 46, 419-424.

Kordower, J.H., Emborg, M.E., Bloch, J., Ma, S.Y., Chu, Y., Leventhal, L., McBride, J., Chen, E.Y., Palfi, S., Roitberg, B.Z., Brown, W.D., Holden, J.E., Pyzalski, R., Taylor, M.D., Carvey, P., Ling, Z., Trono, D., Hantraye, P., Deglon, N., Aebischer, P., 2000. Neurodegeneration prevented by lentiviral vector delivery of GDNF in primate models of Parkinson's disease. Science, 290, 767-773.

Kordower, J.H., Herzog, C.D., Dass, B., Bakay, R.A., Stansell, J.,3rd, Gasmi, M., Bartus, R.T., 2006. Delivery of neurturin by AAV2 (CERE-120)-mediated gene transfer provides structural and functional neuroprotection and neurorestoration in MPTP-treated monkeys. Ann. Neurol., 60, 706-715.

Kreuter, J., 2014. Drug delivery to the central nervous system by polymeric nanoparticles: What do we know? Adv. Drug Deliv. Rev., 71, 2-14.

Kumar, M., Misra, A., Mishra, A.K., Mishra, P., Pathak, K., 2008. Mucoadhesive nanoemulsion-based intranasal drug delivery system of olanzapine for brain targeting. J. Drug Target., 16, 806-814.

Kuo, A., Smith, M.T., 2014. Theoretical and practical applications of the intracerebroventricular route for CSF sampling and drug administration in CNS drug discovery research: A mini review. J. Neurosci. Methods, 233, 166-171.

Kurakhmaeva KB, Voronina TA, Kapica IG, Kreuter J, Nerobkova LN, Seredenin SB, Balabanian VY, Alyautdin RN, 2008. Antiparkinsonian effect of nerve growth factor adsorbed on polybutylcyanoacrylate nanoparticles coated with polysorbate-80. Bull Exp Biol Med, 145, 259-262.

Kurakhmaeva, K.B., Djindjikhashvili, I.A., Petrov, V.E., Balabanyan, V.U., Voronina, T.A., Trofimov, S.S., Kreuter, J., Gelperina, S., Begley, D., Alyautdin, R.N., 2009. Brain targeting of nerve growth factor using poly(butyl cyanoacrylate) nanoparticles. J. Drug Target., 17, 564-574.

Kurosaki, T., Kitahara, T., Fumoto, S., Nishida, K., Yamamoto, K., Nakagawa, H., Kodama, Y., Higuchi, N., Nakamura, T., Sasaki, H., 2010. Chondroitin sulfate capsule system for efficient and secure gene delivery. J. Pharm. Pharm. Sci., 13, 351-361.

Lacomblez L, Bensimon G, Leigh PN, Guillet P, Meininger V, 1996. Dose-ranging study of riluzole in amyotrophic lateral sclerosis. Amyotrophic Lateral Sclerosis/Riluzole Study Group II. Lancet, 347, 1425-1431.

Lang, A.E., Gill, S., Patel, N.K., Lozano, A., Nutt, J.G., Penn, R., Brooks, D.J., Hotton, G., Moro, E., Heywood, P., Brodsky, M.A., Burchiel, K., Kelly, P., Dalvi, A., Scott, B., Stacy, M., Turner, D., Wooten, V.G., Elias, W.J., Laws, E.R., Dhawan, V., Stoessl, A.J., Matcham, J., Coffey, R.J., Traub, M., 2006. Randomized controlled trial of intraputamenal glial cell line-derived neurotrophic factor infusion in Parkinson disease. Ann. Neurol, 59, 459-466.

Lapchak, P.A., Gash, D.M., Jiao, S., Miller, P.J., Hilt, D., 1997. Glial Cell Line-Derived Neurotrophic Factor: A Novel Therapeutic Approach to Treat Motor Dysfunction in Parkinson's Disease. Exp. Neurol., 144, 29-34.

Larsen, K.E., Benn, S.C., Ay, I., Chian, R.J., Celia, S.A., Remington, M.P., Bejarano, M., Liu, M., Ross, J., Carmillo, P., Sah, D., Phillips, K.A., Sulzer, D., Pepinsky, R.B., Fishman, P.S., Brown, R.H.,Jr, Francis, J.W., 2006. A glial cell line-derived neurotrophic factor (GDNF):tetanus toxin fragment C protein conjugate improves delivery of GDNF to spinal cord motor neurons in mice. Brain Res., 1120, 1-12.

Layek B, S.J., 2013. Cell penetrating peptide conjugated polymeric micelles as a high performance versatile nonviral gene carrier. Biomacromolecules., 14, 4071-4081.

Leonardi, A., Bucolo, C., Romano, G.L., Platania, C.B.M., Drago, F., Puglisi, G., Pignatello, R., 2014. Influence of different surfactants on the technological properties and in vivo ocular tolerability of lipid nanoparticles. Int. J. Pharm., 470, 133-140.

Levy YS, Gilgun-Sherki Y, Melamed E, Offen D, 2005. Therapeutic potential of neurotrophic factors in neurodegenerative diseases. BioDrugs, 19, 97-127.

Lim, S.B., Banerjee, A., Önyüksel, H., 2012. Improvement of drug safety by the use of lipid-based nanocarriers. J. Control Release, 163, 34-45.

Linazasoro, G., 2009. A global view of Parkinson's disease pathogenesis: Implications for natural history and neuroprotection. Parkinsonism Relat. Disord., 15, 401-405.

Liu, X., Fawcett, J.R., Thorne, R.G., DeFor, T.A., Frey II, W.H., 2001. Intranasal administration of insulin-like growth factor-I bypasses the blood–brain barrier and protects against focal cerebral ischemic damage. J. Neurol. Sci., 187, 91-97.

Lochhead, J.J., Thorne, R.G., 2012. Intranasal delivery of biologics to the central nervous system. Adv. Drug Deliv. Rev., 64, 614-628.

Lu, Y.Y., Wang, L.J., Muramatsu, S., Ikeguchi, K., Fujimoto, K., Okada, T., Mizukami, H., Matsushita, T., Hanazono, Y., Kume, A., Nagatsu, T., Ozawa, K., Nakano, I., 2003. Intramuscular injection of AAV-GDNF results in sustained expression of transgenic GDNF, and its delivery to spinal motoneurons by retrograde transport. Neurosci. Res., 45, 33-40.

Madane, R.G., Mahajan, H.S., 2015. Curcumin-loaded nanostructured lipid carriers (NLCs) for nasal administration: design, characterization, and in vivo study. Drug Deliv., 1-9.

Madane, R.G., Mahajan, H.S., 2014. Curcumin-loaded nanostructured lipid carriers (NLCs) for nasal administration: design, characterization, and in vivo study. Drug Deliv., 1-9.

Mahapatro, A., Singh, D.K., 2011. Biodegradable nanoparticles are excellent vehicle for site directed in-vivo delivery of drugs and vaccines. J. Nanobiotechnology, 9, 55-3155-9-55.

Marks Jr, W.J., Bartus, R.T., Siffert, J., Davis, C.S., Lozano, A., Boulis, N., Vitek, J., Stacy, M., Turner, D., Verhagen, L., Bakay, R., Watts, R., Guthrie, B., Jankovic, J., Simpson, R., Tagliati, M., Alterman, R., Stern, M., Baltuch, G., Starr, P.A., Larson, P.S., Ostrem, J.L., Nutt, J., Kieburtz, K., Kordower, J.H., Olanow, C.W., 2010. Gene delivery of AAV2-neurturin for Parkinson's disease: a double-blind, randomised, controlled trial. Lancet Neurol, 9, 1164-1172.

Marks Jr, W.J., Ostrem, J.L., Verhagen, L., Starr, P.A., Larson, P.S., Bakay, R.A., Taylor, R., Cahn-Weiner, D.A., Stoessl, A.J., Olanow, C.W., Bartus, R.T., 2008. Safety and tolerability of intraputaminal delivery of CERE-120 (adeno-associated virus serotype 2–neurturin) to patients with idiopathic Parkinson's disease: an open-label, phase I trial. Lancet Neurol, 7, 400-408.

Mathias, N.R., Hussain, M.A., 2010. Non-invasive systemic drug delivery: developability considerations for alternate routes of administration. J. Pharm. Sci., 99, 1-20.

Mathot, F., des Rieux, A., Ariën, A., Schneider, Y., Brewster, M., Préat, V., 2007. Transport mechanisms of mmePEG750P(CL-co-TMC) polymeric micelles across the intestinal barrier. J. Control Release, 124, 134-143.

McBride, JL., Ramaswamy, S., Gasmi, M., Bartus, RT., Herzog, CD., Brandon, EP., Zhou, L., Pitzer, MR., Berry-Kravis, EM., Kordower, JH., 2006. Viral delivery of glial cell line-derived neurotrophic factor improves behavior and protects striatal neurons in a mouse model of Huntington's disease. PNAS, 103, 9345-9350.

McBride, J.L., During, M.J., Wuu, J., Chen, E., Leurgans, S.E., Kordower, J.H., 2003. Structural and functional neuroprotection in a rat model of Huntington's disease by viral gene transfer of GDNF. Exp. Neurol., 181, 213-223.

Md, S., Khan, R.A., Mustafa, G., Chuttani, K., Baboota, S., Sahni, J.K., Ali, J., 2013. Bromocriptine loaded chitosan nanoparticles intended for direct nose to brain delivery: Pharmacodynamic, Pharmacokinetic and Scintigraphy study in mice model. Eur J Pharm Sci, 48, 393-405.

Md, S., Khan, R.A., Mustafa, G., Chuttani, K., Baboota, S., Sahni, J.K., Ali, J., 2013. Bromocriptine loaded chitosan nanoparticles intended for direct nose to brain delivery: Pharmacodynamic, Pharmacokinetic and Scintigraphy study in mice model. Eur J Pharm Sci, 48, 393-405.

Migliore, M.M., Ortiz, R., Dye, S., Campbell, R.B., Amiji, M.M., Waszczak, B.L., 2014. Neurotrophic and neuroprotective efficacy of intranasal GDNF in a rat model of Parkinson's disease. Neuroscience, 274, 11-23.

Miguelez, C., Aristieta, A., Cenci, M.A., Ugedo, L., 2011. The locus coeruleus is directly implicated in L-DOPA-induced dyskinesia in parkinsonian rats: an electrophysiological and behavioural study. PLoS One, 6, e24679.

Mistry, A., Stolnik, S., Illum, L., 2015. Nose-to-Brain Delivery: Investigation of the Transport of Nanoparticles with Different Surface Characteristics and Sizes in Excised Porcine Olfactory Epithelium. Mol. Pharm., 12, 2755-2766.

Mistry, A., Stolnik, S., Illum, L., 2009. Nanoparticles for direct nose-to-brain delivery of drugs. Int. J. Pharm., 379, 146-157.

Mittal, D., Ali, A., Md, S., Baboota, S., Sahni, J.K., Ali, J., 2014. Insights into direct nose to brain delivery: current status and future perspective. Drug Deliv., 21, 75-86.

Mittoux V1, Ouary S, Monville C, Lisovoski F, Poyot T, Conde F, Escartin C, Robichon R, Brouillet E, Peschanski M, Hantraye P., 2002. Corticostriatopallidal Neuroprotection by Adenovirus-Mediate Ciliary Neurotrophic Factor Gene Transfer in a Rat Model of Progressive Striatal Degeneration. J Neurosci, 22 (11), 4478-86.

Mochly-Rosen, D., Disatnik, M.H., Qi, X., 2014. The challenge in translating basic research discoveries to treatment of Huntington disease. Rare Dis., 2, e28637.

Moreno-Igoa M, Calvo AC, Ciriza J, Muñoz MJ, Zaragoza P, Osta R., 2012. Non-viral gene delivery of the GDNF, either alone or fused to the C-fragment of tetanus toxin protein, prolongs survival in a mouse ALS model. Restor Neurol Neurosci, 30 (1), 69-80.

Muller, R.H., Radtke, M., Wissing, S.A., 2002. Nanostructured lipid matrices for improved microencapsulation of drugs. Int. J. Pharm., 242, 121-128.

Murlidharan, G., Samulski, R.J., Asokan, A., 2014. Biology of adeno-associated viral vectors in the central nervous system. Front. Mol. Neurosci., 7, 76.

Musumeci, T., Pellitteri, R., Spatuzza, M., Puglisi, G., 2014. Nose-to-brain delivery: evaluation of polymeric nanoparticles on olfactory ensheathing cells uptake. J. Pharm. Sci., 103, 628-635.

Nutt, J.G., Burchiel, K.J., Comella, C.L., Jankovic, J., Lang, A.E., Laws, E.R.,Jr, Lozano, A.M., Penn, R.D., Simpson, R.K.,Jr, Stacy, M., Wooten, G.F., 2003. Implanted intracerebroventricular. Glial cell line-derived neurotrophic factor Randomized, double-blind trial of glial cell line-derived neurotrophic factor (GDNF) in PD. Neurology, 60, 69-73.

O'Mahony, A.M., Godinho, B.M., Cryan, J.F., O'Driscoll, C.M., 2013. Non-viral nanosystems for gene and small interfering RNA delivery to the central nervous system: formulating the solution. J. Pharm. Sci., 102, 3469-3484.

Pardridge, W.M., 2005. The blood-brain barrier: bottleneck in brain drug development. NeuroRx, 2, 3-14.

Patel, S., Chavhan, S., Soni, H., Babbar, A.K., Mathur, R., Mishra, A.K., Sawant, K., 2011. Brain targeting of risperidone-loaded solid lipid nanoparticles by intranasal route. J. Drug Target., 19, 468-474.

Poon VY, Choi S, Park M, 2013. Growth factors in synaptic function. Front Synaptic Neurosci, 5.

Popovic, N., Maingay, M., Kirik, D., Brundin, P., 2005. Lentiviral gene delivery of GDNF into the striatum of R6/2 Huntington mice fails to attenuate behavioral and neuropathological changes. Exp. Neurol., 193, 65-74.

Prego, C., Garcia, M., Torres, D., Alonso, M.J., 2005. Transmucosal macromolecular drug delivery. J. Control. Release, 101, 151-162.

Ramaswamy, S., McBride, J.L., Han, I., Berry-Kravis, E.M., Zhou, L., Herzog, C.D., Gasmi, M., Bartus, R.T., Kordower, J.H., 2009. Intrastriatal CERE-120 (AAV-Neurturin) protects striatal and cortical neurons and delays motor deficits in a transgenic mouse model of Huntington's disease. Neurobiol. Dis., 34, 40-50.

Ramos-Cabrer, P., Campos, F., 2013. Liposomes and nanotechnology in drug development: focus on neurological targets. Int. J. Nanomedicine, 8, 951-960.

Rassu, G., Soddu, E., Cossu, M., Gavini, E., Giunchedi, P., Dalpiaz, A., Particulate formulations based on chitosan for nose-to-brain delivery of drugs. A review. J Drug Deliv Sci Technol.

Reger, M.A., Watson, G.S., Frey, W.H.,2nd, Baker, L.D., Cholerton, B., Keeling, M.L., Belongia, D.A., Fishel, M.A., Plymate, S.R., Schellenberg, G.D., Cherrier, M.M., Craft, S., 2006. Effects of intranasal insulin on cognition in memory-impaired older adults: modulation by APOE genotype. Neurobiol. Aging, 27, 451-458.

Requejo C, Ruiz-Ortega JA, Bengoetxea H, Garcia-Blanco A, Herrán E, Aristieta A, Igartua M, Ugedo L, Pedraz JL, Hernández RM, Lafuente JV., 2015. Topographical Distribution of Morphological Changes in a Partial Model of Parkinson's Disease--Effects of Nanoencapsulated Neurotrophic Factors Administration.. Mol Neurobiol., 52, 846-858.

Rieux, A.d., Ragnarsson, E.G.E., Gullberg, E., Préat, V., Schneider, Y., Artursson, P., 2005. Transport of nanoparticles across an in vitro model of the human intestinal follicle associated epithelium. Eur J Pharm Sci, 25, 455-465.

Rosen DR, Siddique T, Patterson D, Figlewicz DA, Sapp P, Hentati A, Donaldson D, Goto J, O'Regan JP, Deng HX, et al, 1993. Mutations in Cu/Zn superoxide dismutase gene are associated with familial amyotrophic lateral sclerosis. Nature, 362, 59-62.

Rowland LP, S.N., 2001. Amyotrophic lateral sclerosis. N Engl J Med, 344, 1688-1700.

Sandri G, Bonferoni MC, Gökçe EH, Ferrari F, Rossi S, Patrini M, Caramella C, 2010. Chitosan-associated SLN: in vitro and ex vivo characterization of cyclosporine A loaded ophthalmic systems. J Microencapsul, 27, 735-746.

Sapsforda RJ, Wells CW, Richman P, Daviesa RJ, 1990. Culture and comparison of human bronchial and nasal epithelial cells in vitro. . Respir Med, 84, 303-3012.

Schallert, T., Fleming, S.M., Leasure, J.L., Tillerson, J.L., Bland, S.T., 2000. CNS plasticity and assessment of forelimb sensorimotor outcome in unilateral rat models of stroke, cortical ablation, parkinsonism and spinal cord injury. Neuropharmacology, 39, 777-787.

Schlachetzki, F., Zhang, Y., Boado, R.J., Pardridge, W.M., 2004. Gene therapy of the brain: the trans-vascular approach. Neurology, 62, 1275-1281.

Seju, U., Kumar, A., Sawant, K.K., 2011. Development and evaluation of olanzapine-loaded PLGA nanoparticles for nose-to-brain delivery: In vitro and in vivo studies. Acta Biomaterialia, 7, 4169-4176.

Sendtner M, Carroll P, Holtmann B, Hughes RA, Thoenen H, 1994. Ciliary neurotrophic factor. J Neurobiol, 25, 1436-1453.

Severino, P., Souto, E.B., Pinho, S.C., Santana, M.H., 2013. Hydrophilic coating of mitotane-loaded lipid nanoparticles: preliminary studies for mucosal adhesion. Pharm. Dev. Technol., 18, 577-581.

Sharma, D., Maheshwari, D., Philip, G., Rana, R., Bhatia, S., Singh, M., Gabrani, R., Sharma, S.K., Ali, J., Sharma, R.K., Dang, S., 2014. Formulation and optimization of polymeric nanoparticles for intranasal delivery of lorazepam using Box-Behnken design: in vitro and in vivo evaluation. Biomed. Res. Int., 2014, 156010.

Sharma, D., Maheshwari, D., Philip, G., Rana, R., Bhatia, S., Singh, M., Gabrani, R., Sharma, S.K., Ali, J., Sharma, R.K., Dang, S., 2014. Formulation and optimization of polymeric nanoparticles for intranasal delivery of lorazepam using Box-Behnken design: in vitro and in vivo evaluation. Biomed. Res. Int., 2014, 156010.

Sharma, D., Sharma, R.K., Sharma, N., Gabrani, R., Sharma, S.K., Ali, J., Dang, S., 2015. Nose-To-Brain Delivery of PLGA-Diazepam Nanoparticles. AAPS PharmSciTech.

Slevin, J.T., Gash, D.M., Smith, C.D., Gerhardt, G.A., Kryscio, R., Chebrolu, H., Walton, A., Wagner, R., Young, A.B., 2006. Unilateral intraputaminal glial cell line-derived

neurotrophic factor in patients with Parkinson disease: response to 1 year each of treatment and withdrawal. Neurosurg. Focus, 20.

Sofroniew, M.V., Howe, C.L., Mobley, W.C., 2001. Nerve growth factor signaling, neuroprotection, and neural repair. Annu. Rev. Neurosci., 24, 1217-1281.

Stockwell, J., Abdi, N., Lu, X., Maheshwari, O., Taghibiglou, C., 2014. Novel central nervous system drug delivery systems. Chem. Biol. Drug Des., 83, 507-520.

Stoessl AJ., 2014. Gene therapy for Parkinson's disease: a step closer?. Lancet, 383, 1107-1109.

Storkebaum, E., Lambrechts, D., Carmeliet, P., 2004. VEGF: once regarded as a specific angiogenic factor, now implicated in neuroprotection. Bioessays, 26, 943-954.

Tajes, M., Ramos-Fernandez, E., Weng-Jiang, X., Bosch-Morato, M., Guivernau, B., Eraso-Pichot, A., Salvador, B., Fernandez-Busquets, X., Roquer, J., Munoz, F.J., 2014. The blood-brain barrier: structure, function and therapeutic approaches to cross it. Mol. Membr. Biol., 31, 152-167.

Tan J, Wang Y, Yip X, Glynn F, Shepherd RK, Caruso F, 2012. Nanoporous peptide particles for encapsulating and releasing neurotrophic factors in an animal model of neurodegeneration. Adv Mater, 24, 3362-3366.

Trabulo, S., Cardoso, A.L., Mano, M., MCP, D.L., 2010. Cell-penetratingpeptides—mechanisms of cellular uptake and generation of delivery systems. Pharmaceuticals, 3, 961-993.

Trapani, A., De Giglio, E., Cafagna, D., Denora, N., Agrimi, G., Cassano, T., Gaetani, S., Cuomo, V., Trapani, G., 2011. Characterization and evaluation of chitosan nanoparticles for dopamine brain delivery. Int. J. Pharm., 419, 296-307.

Trapani, A., Lopedota, A., Franco, M., Cioffi, N., Ieva, E., Garcia-Fuentes, M., Alonso, M.J., 2010. A comparative study of chitosan and chitosan/cyclodextrin nanoparticles as potential carriers for the oral delivery of small peptides. Eur J Pharm Biopharm, 75, 26-32.

Ventriglia, M., Zanardini, R., Bonomini, C., Zanetti, O., Volpe, D., Pasqualetti, P., Gennarelli, M., Bocchio-Chiavetto, L., 2013. Serum brain-derived neurotrophic factor levels in different neurological diseases. Biomed. Res. Int., 2013, 1-7.

Vila, A., Sanchez, A., Tobio, M., Calvo, P., Alonso, M.J., 2002. Design of biodegradable particles for protein delivery. J. Control. Release, 78, 15-24.

Vyas TK, Shahiwala A, Marathe S, Misra A, 2005. Intranasal drug delivery for brain targeting. Curr Drug Deliv, 2, 165-175.

Wang, LJ., Lu, YY., Muramatsu, S., Ikeguchi, K., Fujimoto, K., Okada, T., Mizukami, H., Matsushita, T., Hanazono, Y., Kume, A., Nagatsu, T., Ozawa, K., Nakano, I., 2002. Neuroprotective Effects of Glial Cell Line-Derived Neurotrophic Factor Mediated by an Adeno-Associated Virus Vector in a Transgenic Animal Model of Amyotrophic Lateral Sclerosis. J. Neurosci., 22, 6920-6928.

Wohlfart, S., Gelperina, S., Kreuter, J., 2012. Transport of drugs across the blood–brain barrier by nanoparticles. J. Control Release, 161, 264-273.

Wong, H.L., Wu, X.Y., Bendayan, R., 2012. Nanotechnological advances for the delivery of CNS therapeutics. Adv. Drug Deliv. Rev., 64, 686-700.

Wu, H., Hu, K., Jiang, X., 2008. From nose to brain: understanding transport capacity and transport rate of drugs. Expert Opin. Drug Deliv., 5, 1159-1168.

Xia, H., Gao, X., Gu, G., Liu, Z., Zeng, N., Hu, Q., Song, Q., Yao, L., Pang, Z., Jiang, X., Chen, J., Chen, H., 2011. Low molecular weight protamine-functionalized nanoparticles for drug delivery to the brain after intranasal administration. Biomaterials, 32, 9888-9898.

Xie, Y., Ye, L., Zhang, X., Cui, W., Lou, J., Nagai, T., Hou, X., 2005. Transport of nerve growth factor encapsulated into liposomes across the blood–brain barrier: In vitro and in vivo studies. J. Control Release, 105, 106-119.

Xing, B., Xin, T., Zhao, L., Hunter, R.L., Chen, Y., Bing, G., 2010. Glial cell line-derived neurotrophic factor protects midbrain dopaminergic neurons against lipopolysaccharide neurotoxicity. J. Neuroimmunol., 225, 43-51.

Yadav, S.C., Kumari, A., Yadav, R., 2011. Development of peptide and protein nanotherapeutics by nanoencapsulation and nanobioconjugation. Peptides, 32, 173-187.

Yasir, M., Sara, U.V.S., 2014. Solid lipid nanoparticles for nose to brain delivery of haloperidol: in vitro drug release and pharmacokinetics evaluation. Acta Pharm Sin B, 4, 454-463.

Yi, X., Manickam, D.S., Brynskikh, A., Kabanov, A.V., 2014. Agile delivery of protein therapeutics to CNS. J. Control Release, 190, 637-663.

Yue, X., Hariri, D.J., Caballero, B., Zhang, S., Bartlett, M.J., Kaut, O., Mount, D.W., Wüllner, U., Sherman, S.J., Falk, T., 2014. Comparative study of the neurotrophic effects elicited by VEGF-B and GDNF in preclinical in vivo models of Parkinson's disease. Neuroscience, 258, 385-400.

Yunus, M.H., Siang, K.C., Hashim, N.I., Zhi, N.P., Zamani, N.F., Sabri, P.P., Busra, M.F., Chowdhury, S.R., Idrus, R.B., 2014. The effects of human serum to the morphology, proliferation and gene expression level of the respiratory epithelium in vitro. Tissue Cell, 46, 233-240.

Yusuf M, Khan M, Khan RA, Ahmed B, 2012. Preparation, characterization, in vivo and biochemical evaluation of brain targeted Piperine solid lipid nanoparticles in an experimentally induced Alzheimer's disease model. J Drug Target, 21 (3), 300-311.

Zavalishin IA, Bochkov NP, Suslina ZA, Zakharova MN, Tarantul VZ, Naroditskiy BS, Suponeva NA, Illarioshkin SN, Shmarov MM, Logunov DY, Tutyhina IL, Verkhovskaya LV, Sedova ES, Vasiliev AV, Brylev LV, Ginzburg AL, 2008. Gene therapy of amyotrophic lateral sclerosis. Bull Exp Biol Med, 145 (4), 483-6.

Zeng X, Chen J, Deng X, et al., 2006. An in vitro model of human dopaminergic neurons derived from embryonic stem cells: MPP+ toxicity. Neuropsychopharmacology, 31, 2708-2715.

Zhang, C., Chen, J., Feng, C., Shao, X., Liu, Q., Zhang, Q., Pang, Z., Jiang, X., 2014. Intranasal nanoparticles of basic fibroblast growth factor for brain delivery to treat Alzheimer's disease. Int. J. Pharm., 461, 192-202.

Zhao, Y.Z., Li, X., Lu, C.T., Lin, M., Chen, L.J., Xiang, Q., Zhang, M., Jin, R.R., Jiang, X., Shen, X.T., Li, X.K., Cai, J., 2014. Gelatin nanostructured lipid carriers-mediated intranasal delivery of basic fibroblast growth factor enhances functional recovery in hemiparkinsonian rats. Nanomedicine, 10, 755-764.

Zielonka, D., Piotrowska, I., Marcinkowski, J.T., Mielcarek, M., 2014. Skeletal muscle pathology in Huntington's disease. Front. Physiol., 5, 380.

Zorko, M., Langel, Ü., 2005. Cell-penetrating peptides: mechanism and kinetics of cargo delivery. Adv. Drug Deliv. Rev., 57, 529-545.